Distribution Category:
LMFBR Reactor Plant Systems
(UC-79i)

ANL-76-74

ARGONNE NATIONAL LABORATORY
9700 South Cass Avenue
Argonne, Illinois 60439

GERMANIUM-LITHIUM ARGON SCANNING SYSTEM (GLASS): DESIGN AND EXPERIENCE THROUGH 1974

by

G. S. Brunson

EBR-II Project

July 1976

TABLE OF CONTENTS

TABLE OF CONTENTS

LIST OF FIGURES

LIST OF FIGURES

LIST OF FIGURES

LIST OF TABLES

GERMANIUM-LITHIUM ARGON SCANNING SYSTEM (GLASS): DESIGN AND EXPERIENCE THROUGH 1974

by

G. S. Brunson

ABSTRACT

The germanium-lithium argon scanning system (GLASS) was installed in EBR-II to monitor and analyze the gamma activity of the reactor cover gas and the reactor building air. GLASS has the capability to identify and meacure 20 or more gamma peaks. Applied to the reactor cover gas, this capability has proven useful in identifying the sources of fission-gas leakage from fuel elements. The gamma-peak data can clearly distinguish a carbide-fuel source from an oxide-fuel source and can often help distinguish an oxide-fuel source from a metallic-fuel source.

This report summarizes the experience with GLASS in 1971-1974 and explains in detail the operation of the system.

I. INTRODUCTION

The germanium-lithium argon scanning system (GLASS) is an advanced gamma-analysis system for detecting, identifying, and measuring specific fission products in the cover gas of EBR-II.[1] In principle, it is similar to the reactor-cover-gas monitor (RCGM);[2] the difference lies in their resolution. The RCGM can identify (and measure very poorly) only four or five gamma peaks in the cover-gas gamma spectrum. GLASS, with about 20 times better energy resolution, can identify (and measure very well) 20 or more gamma peaks. The improved detail provided by GLASS is of great help in identifying leakers. GLASS additionally has another detector associated with an air-sampling system that monitors the air in the reactor building.

Physically, GLASS is located in several places. The cover-gas monitor with associated equipment (Fig. 1) is located in the "depressed area" of the reactor building. The experimental air monitor is located on the north side of the operating floor. The analytical equipment (Fig. 2) is in the experimental engineering laboratory (EEL) in the power plant. Certain signal outputs are provided to the EBR-II data-acquisition system and the reactor control room as well as being locally available in the EEL.

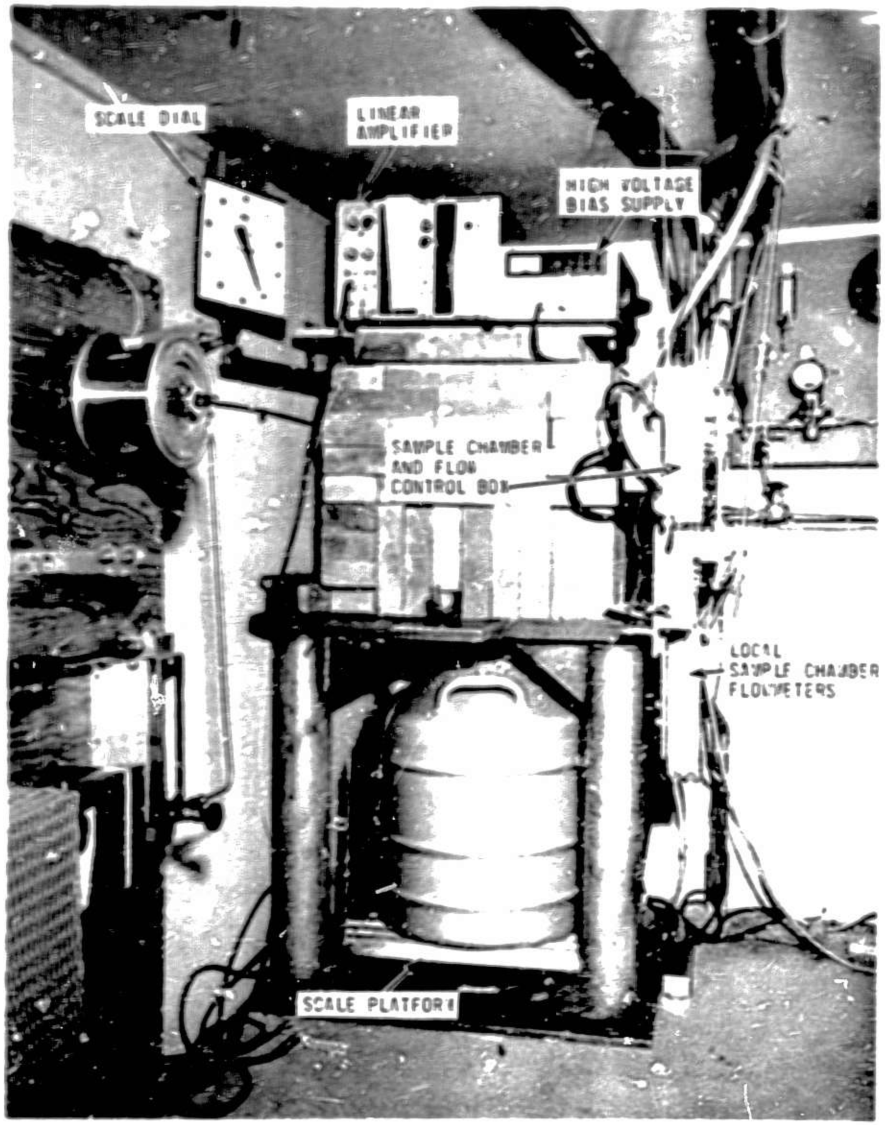

Fig. 1. GLASS Cover-gas-detector Equipment. ANL Neg. No. 103-R5966.

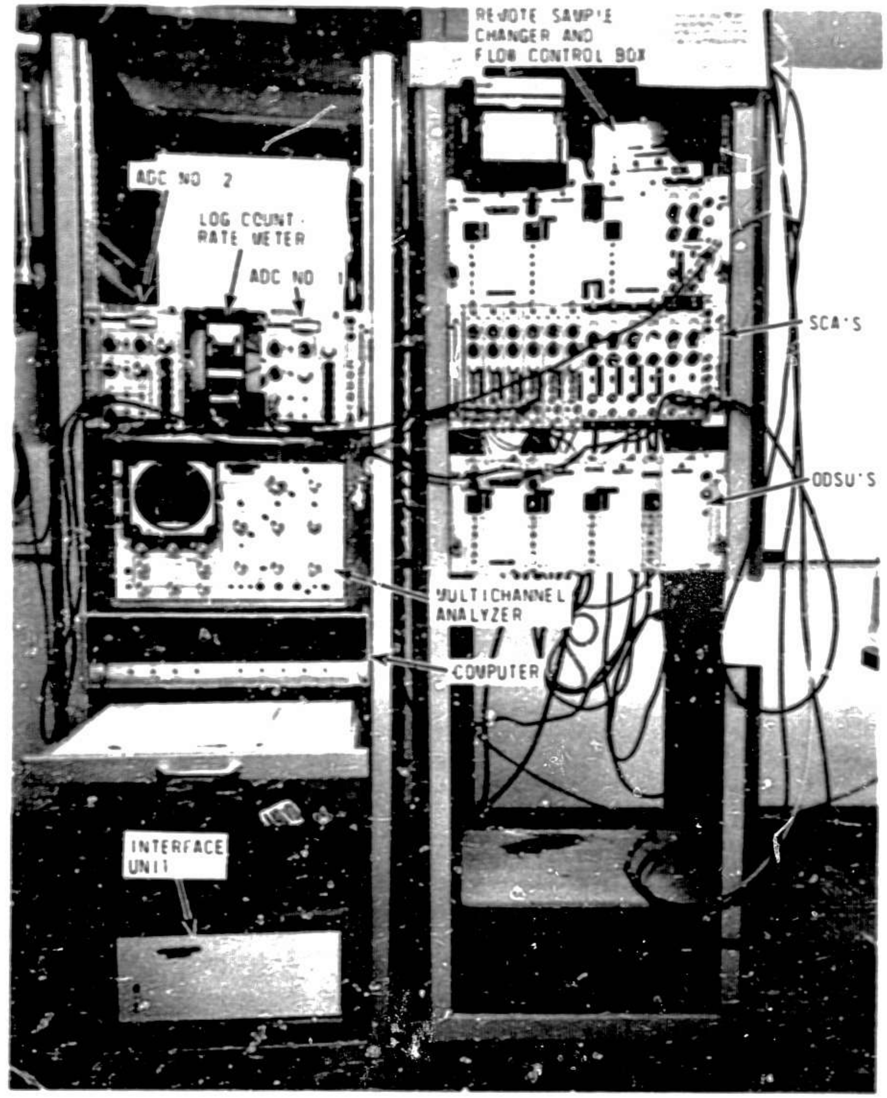

Fig. 2. GLASS Analytical Electronics in Experimental Engineering Laboratory. ANL Neg. No. 103-R5963.

The first experimental operation of GLASS was in mid-1971. Since then, a number of changes have been made in technique and equipment. As experience accumulates in the application of GLASS to actual reactor operation, further changes may be made. However, some attempt must be made to describe the equipment and experience to date. Therefore, this is a status report to cover development and experience to the end of 1974.

II. GENERAL DESCRIPTION OF EQUIPMENT IN REACTOR BUILDING

Following is a general description of GLASS by components (see also Fig. 3).

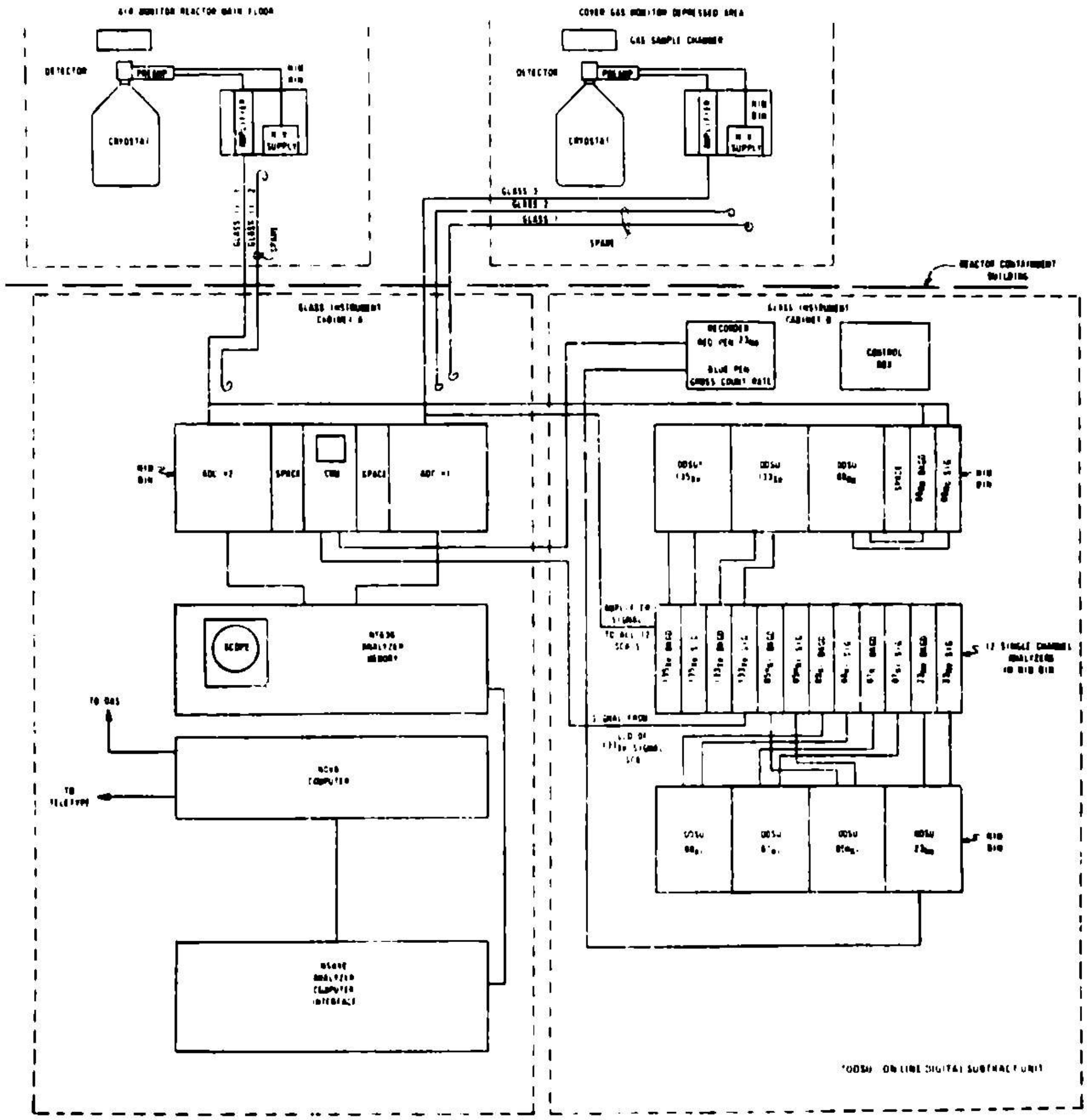

Fig. 3. Schematic of GLASS, Including Experimental Air Monitor. ANL Neg. No. 103-R5987.

A. Detector for Cover-gas Monitor

The detector is a lithium-drifted germanium crystal in the form of a cylinder about 44 mm in diameter by 44 mm high. The crystal is mounted in a thin metal can on the upper end of a large copper rod ("dipstick"), which extends down into a 30-liter (L) Dewar of liquid nitrogen (as shown in Fig. 4). The dipstick is surrounded by a stainless steel tube; the space between crystal and can, and between dipstick and outer tube, is maintained under vacuum to inhibit the inflow of heat. This permits the crystal to be kept cold by means of the heat conducted by the copper rod to the liquid nitrogen. The crystal must be kept cold to prevent the out-diffusion of lithium. If the crystal does warm up, it will have to be returned to the manufacturer for reprocessing, which is both expensive and time-consuming. There are three of these detectors, one being a spare. The nominal resolution of the detectors is about 2.3 keV as measured in a laboratory; actual resolution as installed at EBR-II is about 4 keV. Nominal detector efficiency is about 6.5%.

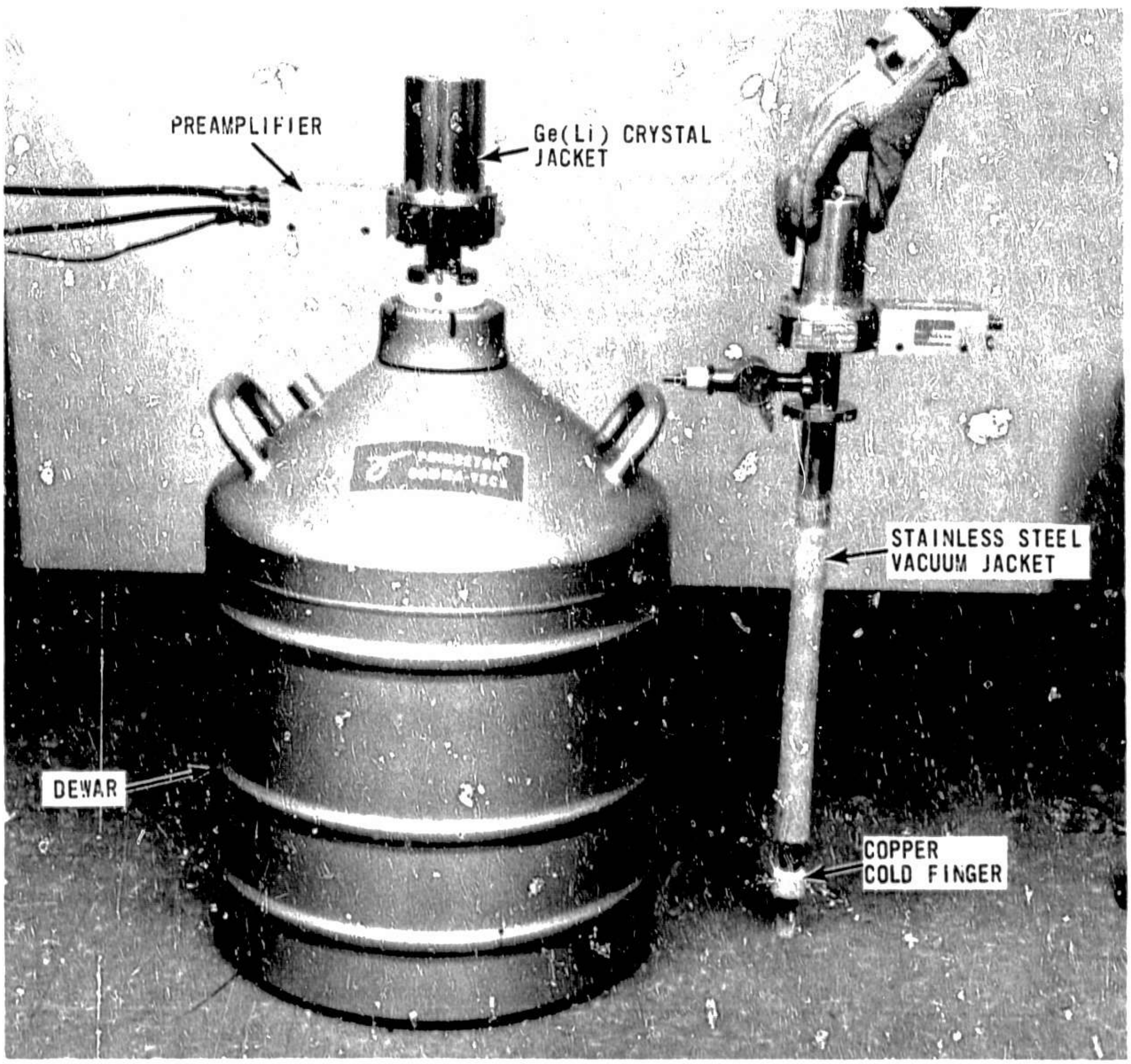

Fig. 4. Lithium-drifted Germanium Detector with Associated Dewar to Hold Liquid Nitrogen. ANL Neg. No. 103-S5580.

Two of these detectors were manufactured by Princeton Gamma-Tech, and the third by Nuclear Diodes. When the detectors are connected, it is essential that they be connected for proper polarity of the high-voltage detector bias. The practices of the two manufacturers differ, as covered in detail in the operating instructions in Appendix A.

B. Gas-sample System

The cover-gas stream counted by GLASS is drawn from the sample-gas manifold through valve V-322A and returned to the exhaust manifold through valve V-322R (see Fig. 5). The object at the bottom of Fig. 5 is a delay line to allow additional decay of ^{23}Ne. Under normal conditions, gas flows through the sample chamber (immediately above the detector) at a rate of about 57 L/hr. This chamber is 34 mm in diameter and 25 mm deep. The volume is about 23.5 mL. Under high-count-rate conditions such as are encountered when a leaker occurs in the core, the sample chamber can be contracted to an effective volume of about 1 mL. This results in a reduction of count rate by a factor of about 30 due to an additional geometric effect. Under conditions of extremely high cover-gas activity, the sensitivity can be further reduced by dilution. This is accomplished with solenoid valves, which bleed an aliquot of sample into the clean argon at about 1 part in 28. The volume reduction and dilution, when combined, reduce the sensitivity by a factor of about 500. The effect of these reductions in detector sensitivity is covered in detail in Sec. VI.D.

For collateral measurements, operation of the bypass alone permits observation of the decay of stagnant gas in the sample chamber. In addition, operation of the bypass and purge permits the observation of solid daughters deposited in the sample chamber.

C. Shield

The detector and gas-sample chamber are surrounded by a shield of leak bricks stacked to an effective thickness of about 4 in. (102 mm). This shield is necessary to allow the detector to "see" the gas sample with a minimum of interference from the general background (see Fig. 1).

The shield is supported by a steel table that permits access to the Dewar. Associated with the shield is a suspended platform on which the Dewar sits. This platform is connected by means of a lever arrangement to a suspended dial-indicating scale to the left of the shield. The lever gives a scale factor of 10 so that a reading of 4 on the scale represents a mass of 40 lb (18 kg). The mass of the Dewar has been counterbalanced so the 40 lb would be the net mass of nitrogen in the Dewar. When full, the Dewar contains 50 lb (23 kg). It is scheduled for service once a week, and the weekly consumption is about 20 lb (9 kg). Any substantially higher rate of consumption must be investigated to see if the cryostat has been damaged through loss of the insulating vacuum.

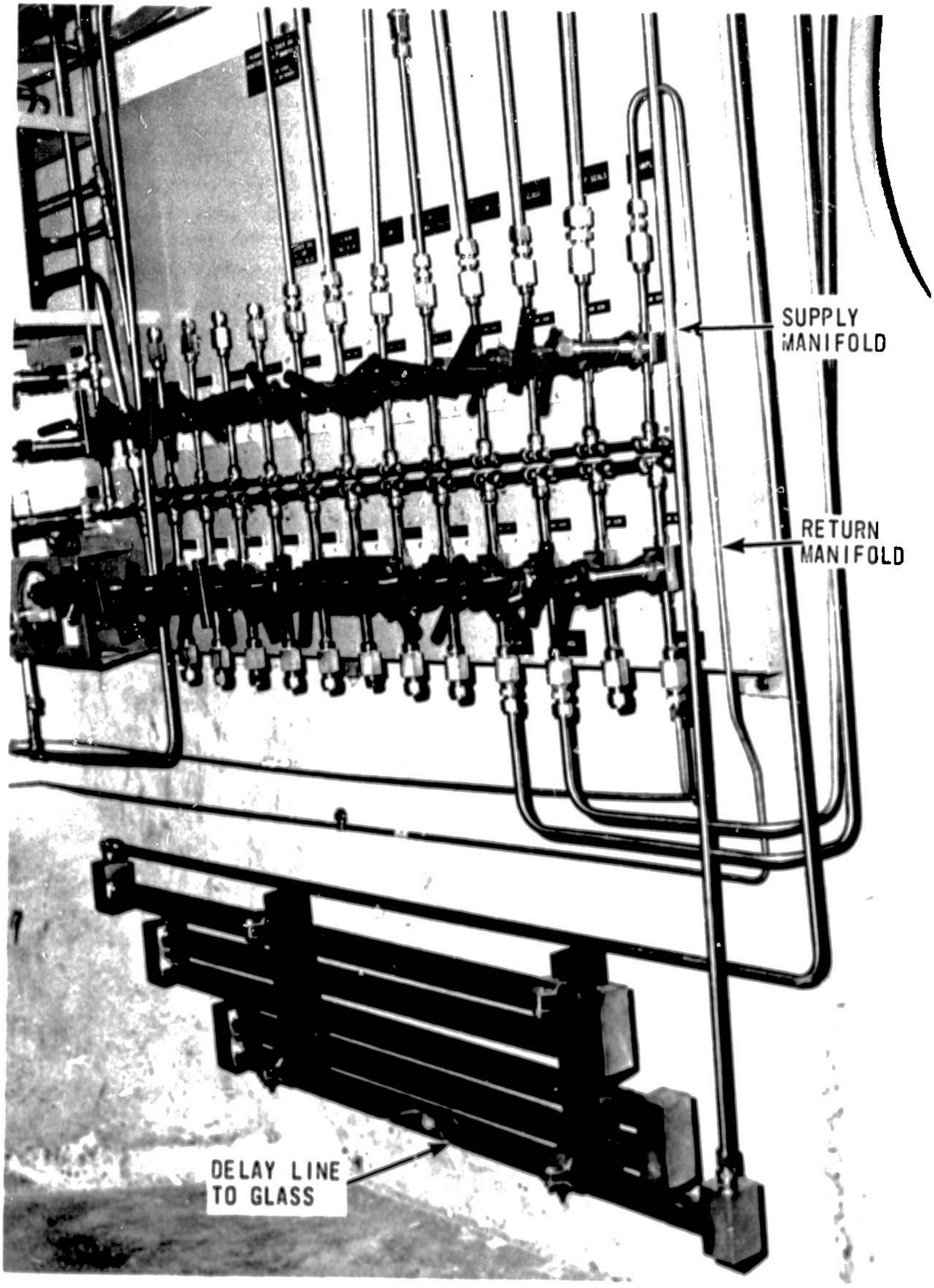

Fig. [illegible] Manifolds, Valving and Delay Line for [illegible]

D. Electronics in the Depressed Area

The electronics in the depressed area include (a) a preamplifier attached directly to the detector assembly, (b) an amplifier, (c) a high-voltage power supply, and (d) a nuclear-instrument-module (NIM) bin to provide the standard dc voltages to the amplifier and preamplifier. Three coaxial signal cables, labeled GLASS I, GLASS 2, and GLASS 3, have been provided to communicate with the analyzer equipment. In addition, three seven-conductor cables provide control and indication functions between the depressed area and the analyzer. Power for the equipment in the depressed area comes from breaker No. 8 in power panel RB-7 near the FERD system.

E. Air Monitor

An air-monitoring system is installed on the main reactor-operating floor. This monitor is similar to the system described for the depressed area; it has approximately the same shield, detector, Dewar, and electronics. However, instead of the gas-sample chamber, there is an air-sampling system. This consists of a constant-duty blower with suction hose and filter head, attached to the detector shield. The blower draws about 283 L/min of room air through a standard 100-mm Whatman paper filter, which the filter head maintains about 6 mm above the detector. Normally the only isotope of interest detected by this system is ^{88}Rb, which is the daughter of fission product ^{88}Kr, some of which leaks from the reactor in the cover gas. (The air monitor was modified in July 1974 to detect ^{133}Xe and ^{135}Xe. The effect of this modification is discussed in Sec. VI.H.)

Two coaxial signal cables are used for communication with the analyzer equipment. They are marked GLASS II 1 and GLASS II 2.

III. DESCRIPTION OF SIGNALS TO BE ANALYZED

The signals coming to the analysis equipment from either detector consist of a series of electrical pulses of positive polarity. Typically they are about 6 μs wide and range from 0 to 8 V in amplitude. The purpose of the analysis equipment is to sort these pulses by size; this provides data that can be interpreted to indicate the species and concentration of fission-product gases in the cover gas. The signals are presented simultaneously to both the on-line analog system and the high-resolution digital equipment; the two techniques are covered separately below.

The operation of the GLASS system is complicated by its location. Space limitations require that the analysis equipment be separated from the detector. This complicates system checkout and calibration. In addition, the 60 m or more of signal cable pass through a relatively hostile environment in terms of electronic noise (from pumps, heaters, etc.), resulting in some loss of resolution.

A point should also be made about the choice of amplifier. Figure 3 shows that the amplifier signals, especially in the case of the cover-gas channel, are supplied to a number of different units. The combination of a long signal cable with multiple inputs places an unusual requirement on the amplifier's line-driving capability, i.e., its output impedence. We have selected Canberra amplifiers (Models 1417B or 1413), and no other amplifier should be used unless the line-driving capacity is known to be adequate.

Figure 6 shows a typical cover-gas spectrum observed from essentially saturated "tramp" activity. (See Sec. VI for a discussion of "tramp" activity.) It is this spectrum that is processed by the equipment discussed in the following sections. Table I lists the isotopes of interest in this application. (In November 1974, a cadmium filter was interposed between the detector and the sample chamber. This strongly suppresses ^{133}Xe and leaves the rest of the spectrum largely unchanged. This is explained in detail in Sec. VI.E.)

TABLE I. Principal Isotopes of Interest in GLASS

Isotope	Half-life	Energy, keV	Stored at Channel	Remarks
^{133}Xe	5.30 days	81.0	162	
			2210	From air monitor
^{135}Xe	9.14 hr	249.7	499	
			2547	From air monitor
^{85m}Kr	4.48 hr	149.5	299	
^{88}Kr	2.80 hr	196.3	392	
^{87}Kr	76.4 min	402.6	806	
^{138}Xe	14.2 min	258.0	516	
^{135m}Xe	15.6 min	526.6	1053	
^{88}Rb	17.8 min	898.0	1844	From air monitor
			12048 + (2 x 898)	
^{23}Ne	37.6 s	440.0	880	
^{41}Ar	1.83 hr	1293.1		Observed in cover gas, but not stored
^{137}Cs	30 yr	661.6	1323	^{137}Cs calibration source permanently installed at each detector
			3371	From air monitor

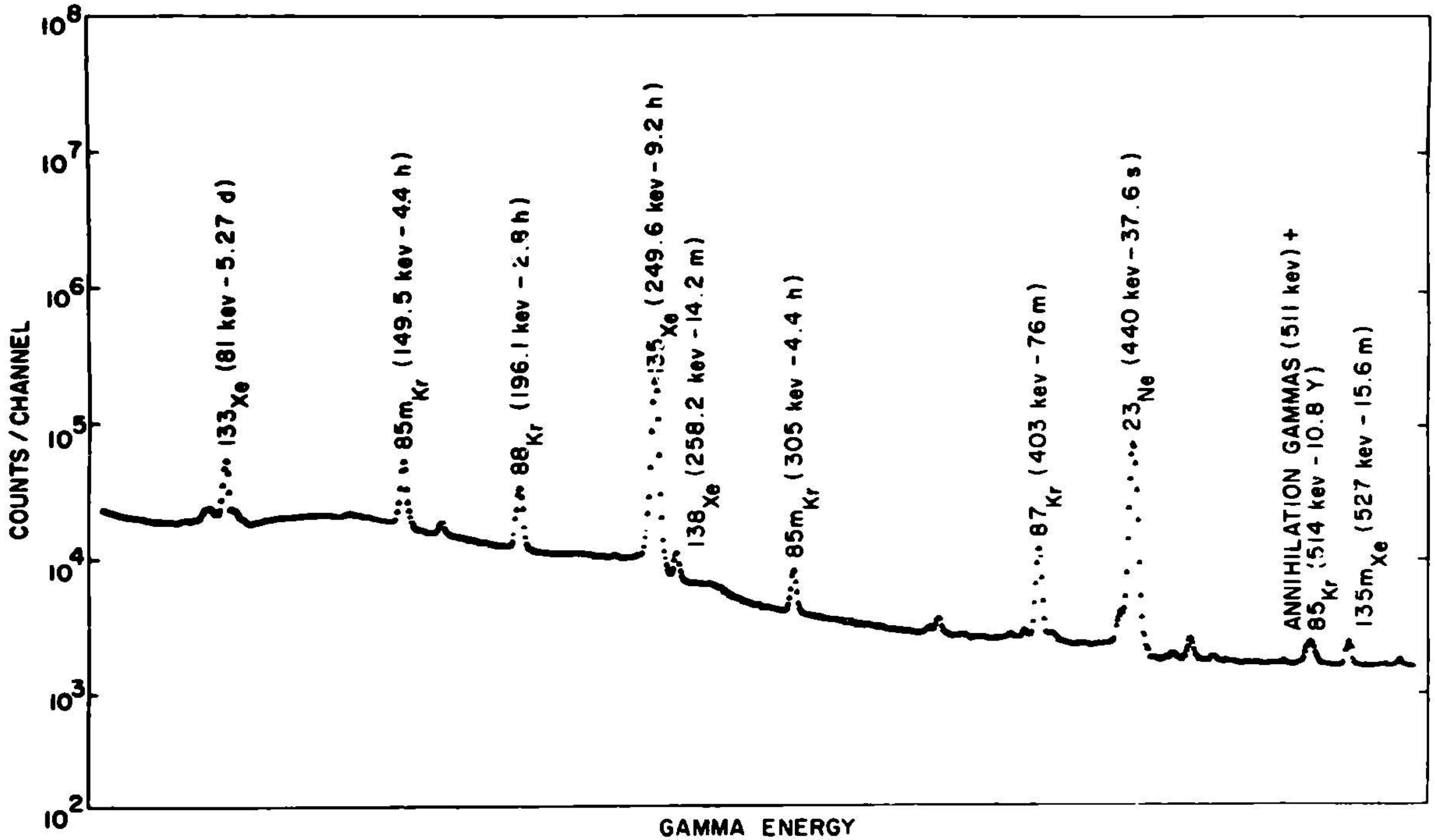

Fig. 6. Typical Gamma Spectrum of Tramp Background in the Cover Gas. ANL Neg. No. 103-R5659 Rev. 1.

IV. DESCRIPTION OF ANALYSIS EQUIPMENT

The signals from the two detectors described above are brought by coaxial cable to the experimental engineering laboratory (EEL) on the ground floor of the power plant. The analytical equipment there is arranged in two instrument cabinets. The on-line fast-response equipment (analog output) is in the right-hand cabinet. The high-resolution digital analyzer and associated equipment are in the left-hand cabinet (see Figs. 2 and 3).

A. On-line Analog System

The on-line analog system is based on the technique illustrated in Fig. 7. For each gamma peak to be analyzed, there are two single-channel analyzers (SCA's). One SCA is set directly on the gamma peak in question; the second is set with the same channel width (ΔE) at a place in the spectrum where area C is a good approximation of area B. The on-line digital subtract units (ODSU's)[3] in Fig. 7 subtract the pulse train originating in area ΔE_2 from that originating in ΔE_1. The result is a signal that represents the peak count rate very well despite drastic change in the level of the Compton continuum.

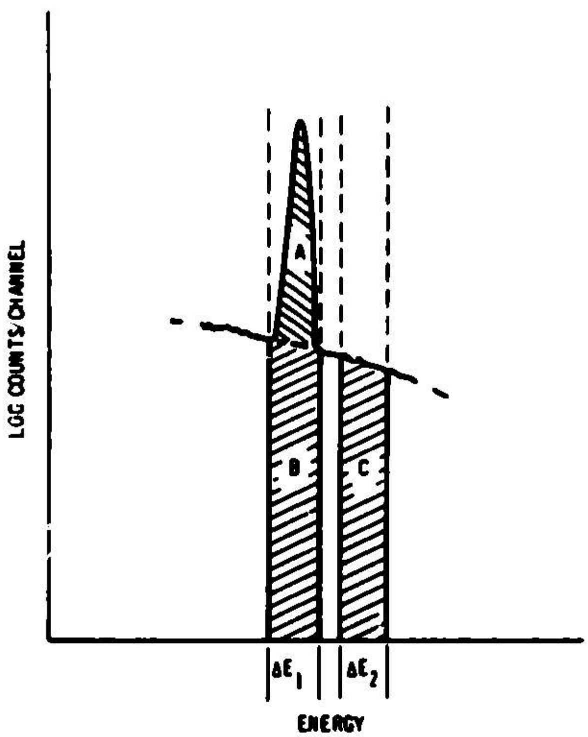

Fig. 7. Adjustment of Single-channel-analyzer Windows to Feed an On-line Digital Subtract Unit (ODSU). ANL Neg. No. 103-P5908.

There are 12 SCA's feeding six ODSU's in the right-hand cabinet; this portion of the system provides for the counting of six different gammas in the cover gas. In addition, one pair of SCA's and one ODSU serve the reactor-building air monitor.

The number of modules drawing signals from the cover-gas signal bus needs some discussion. Together these modules represent a near-maximum load on the amplifier. If one SCA is disconnected from the signal bus, all the rest see an increase in effective amplifier gain, which means that all the previously set channels are in error. Thus it is essential, when removing a module from the signal bus, to either replace it with an equivalent unit or carefully readjust the amplifier gain.

Two types of SCA's are in use: CANBERRA 1431 and ORTEC 406A. They are essentially equivalent in operation, but may not be substituted for each other without readjusting the amplifier gain, since they differ markedly in loading effect on the amplifier. The CANBERRA is preferred because it represents a much smaller load.

The SCA's and the ODSU's are mounted in and powered by standard NIM bins, which provide ±12 and ±24 V to each module. In addition, the ODSU's require ±6 V. This is supplied by auxiliary supplies, which are connected to supply that voltage through each of the NIM connectors for those bins holding ODSU's.

Each ODSU consists of two modules, a timer in a single-width NIM module and a double-width analog unit. The two modules interconnect in the rear. Each timer has a two-digit switch to adjust the counting time. Depending on the count rate for a particular gamma line, the timer is set to count a specified time (1-99 s). Say the switch is set to 10. The ODSU will then accumulate counts (the difference between ΔE_1 and ΔE_2) for 10 s. At the end of 10 s, this count is transferred to a second register (a "latch"). A digital-to-analog converter (DAC) converts the latch reading to an analog voltage, which is further converted to a logarithmic signal. This signal, representing three decades (10 to 10^4), is available in two forms (0-10 V or 0-1 mA). Thus, each 10 s a new value appears at the output representing the count obtained during the preceding 10 s. This is termed a "sample and hold" technique. The sampling time is chosen to give reasonable statistics for the gamma peak concerned. The 0-1-mA output is used by the small three-pen recorders in the control room. The 0-10-V outputs are read and logged (with suitable conversion factor) by the EBR-II data-acquisition system (DAS).

B. Digital Analysis Equipment

1. Description

The digital analysis equipment consists of the following six separate units (see Figs. 2 and 3):

- Analog-to-digital converter (ADC No. 1).
- Analog-to-digital converter (ADC No. 2).
- Northern Scientific Memory Unit Model 636.
- Northern Scientific Interface Unit Model 440 N.
- NOVA minicomputer.
- ASR 35 teletype.

The two ADC's are contained in and powered by a NIM bin. An ADC is a highly sophisticated electronic device that accepts an incoming pulse from the linear amplifier, measures the height very accurately, and outputs a digital signal corresponding to that pulse height. The effective input range is 0 to +8 V. Based on operating experience with cover gas GLASS uses 2048 channels to cover the full range of pulse-height values; this appears to be a reasonable tradeoff between resolution and time required for analysis. One of these ADC's analyses pulses from the cover-gas system; the other serves the reactor-building air monitor.

The Model 636 memory unit stores the numbers generated by the two ADC's. Assume that ADC No. 1 receives a pulse about 4 V high and measures that height as 1027 (on a scale of 2048). The number 1027 is signaled to the memory unit, which goes to memory location 1027 (termed channel 1027) and adds one to whatever number is already there. Thus, after many pulses have been analyzed, channels 1-2048 will contain numbers representing the number of times a pulse of each of the 2048 different sizes was detected. The multiplex capability makes it possible for signals from ADC No. 2 to be stored without confusion. This is accomplished in the memory unit by adding the number 2048 to whatever number is transmitted by ADC No. 2. For example, suppose ADC No. 2 receives a pulse of ~6 V, which it measures as 1537 (on a scale of 2048). On receipt in the memory unit, this number is augmented by 2048 (1537 + 2048 = 3583) and the number at address (channel) 3583 will be increased by 1. Thus, the channels from 2049 to 4096 will contain the spectrum corresponding to the pulse range 0-8 V going into ADC No. 2. Since the capability of the memory is 8192, this arrangement means that the spectrum from the cover-gas detector coming through ADC No. 1 will occupy the first quadrant of the memory and the spectrum from the air monitor coming through ADC No. 2 will occupy the second quadrant.

2. Application

The practice is to set the cover-gas amplifier gain and baseline adjustment so that a gamma ray (measured in keV) is recorded in the channel whose number is 2 x keV; for example, the 661.6-keV gamma from the calibration source will fall in channel 2 x 661.6 ≈ 1323. Thus, the full range of 2048 channels corresponds to about 1 meV (1000 keV), which is adequate for the activities of interest in the cover gas.

The amplifier on the air monitor is also adjusted so that there is a 2:1 correspondence between channel number (corrected for the 2048-channel offset) and the energy in keV; that is, the 661.6-keV (line falls in channel 3371 (2 x 661.6 + 2048).

The Model 636 memory unit includes an oscilloscope display, which permits the visual inspection of any portion of the memory. Figure 6 shows the spectrum obtained from the cover gas with the important energies indicated. Some of the important data on the isotopes of interest are summarized in Table I. Gamma-emitting isotopes frequently emit more than one gamma energy; the energies shown in Table I pertain only to the most prominent and hence most easily measurable gamma peak for each isotope.

A large number of channels is required to properly utilize the exceptional resolution obtained from the germanium-lithium detector. On the other hand, this presents us with a large array of numbers that must be handled in order to extract useful information from the data collected. This is beyond our capacity to do in any feasible way by hand; for example, if we simply typed out the information on the teletype, it would require about half an hour, and the result would be a solid block of numbers spread across the page from margin to margin and more than 5 ft (1.5 m) long.

The answer to this problem is to use a computer to "predigest" the data and give a few usable numbers. In this application, the NOVA mini-computer is employed full time to control the data-taking cycle as well as to compress the data. The Northern Scientific Interface provides intercommunication between the memory unit and the NOVA. Communication is in both directions; the computer sends signals that control the collection of data, and in turn receives data at the end of an accumulation cycle. The teletype enables the operator to control the system by commands sent to the computer and provides the means for the computer to output the results of its data analysis.

3. Summary of Analysis Cycle

The automatic data-collection program has a number of steps, which are outlined below. The normal data cycle is 30 min, although it can be easily changed by keyboard command. The interval timing is carefully programmed so that, no matter what the exact output time is, each data-collection period ends exactly 30 min (to the tenth of a second) after the end of the preceding data-collection period. This means that the data-collection cycle remains in phase "with the clock on the wall" day after day.

For the purposes of this description, assume that a data-taking period has ended at some time T_1 and analysis begins. We will skip discussion of analysis and output until the end of the following cycle. At T_1, an internal clock in the computer was reset and started.

a. At the end of the output period, the computer clears the analyzer memory, starts the collection of a fresh batch of data, and types out from the internal time-of-day clock the time at which data collection started. When data collection begins, the analyzer starts a separate internal live-time clock (actually in channel 0), which measures the length of the data-collection period corrected for dead time.

b. At exactly T_1 + 30 min, the computer halts data collection (and stops the clock in the analyzer) and begins the analysis and output. First, it gets reactor power from the EBR-II DAS and types that out at the head of the block of data.

c. Analysis of individual gamma peaks then begins. Take the first (lowest energy) as an example. The line associated with ^{133}Xe falls at channel 162 (81 keV x 2 channels/keV). Because of the finite resolution of the detector, the gamma peak will actually be spread over a few channels. In this case, the program sums the contents of the nine channels 158-166. Call this sum S_1. It then sums nine more channels 170-178 as a sample of Compton background, call this S_2. It then subtracts S_2 from S_1 to obtain an estimate of the net counts in the peak. This remainder is then divided by the time (in seconds) recorded in the live-time clock (channel 0) to obtain the net rate in counts per second due to the 81-keV gamma grom ^{133}Xe. This is typed out by the teletype labeled as XE133, and the process is repeated for each of the other isotopes. Table 1 lists the isotopes of interest, their pertinent parameters, and the channels at which their peaks are located.

d. At the end of data analysis and output, the memory is again cleared, the live-time clock reset and restarted, data collection initiated, and the date and time typed out.

4. Options and Other Considerations

The foregoing has been described with specific numbers to show how the equipment is usually operated. The actual program permits, by keyboard command, a good deal of flexibility. For example, the data-taking cycle can be any integral number of minutes from 1 to 100.

The output labeled CS137 represents a fixed source of ^{137}Cs used to observe the stability of the pulse-handling channel of the cover-gas detector. There is a small, permanently mounted source of ^{137}Cs (half-life, 30 years), which yields a net photopeak count rate of about 3 counts/s.

Although the same programming is used for this peak as for the others, the "signal" region and "background" region are carefully chosen to constitute an extremely sensitive test for a change of gain relative to the analyzer energy scale. The "signal" count is obtained from a block of channels on the left shoulder of the peak. The "background" count is taken from a symmetrically located block on the right shoulder of the peak. When these two counts are subtracted and the result divided (as the program automatically does) by the count time, the result should be a count rate very close to zero. Should the gain decrease so that the peak drifts down in the signal block of channels, the count rate will increase until it finally reaches the entire 3 counts/s attributable to the source. Conversely, if the gain increases enough to bring the peak into the "background" region, the indicated count rate will approach -3 counts/s. The source strength of the calibration source on the cover-gas detector is such that an indication of ±1 count/s corresponds closely with a gain change of ±1 channel at the ^{137}Cs peak (equivalent to a gain change of ±0.07%). Within the narrow actual range of variation, this relationship is, conveniently, very nearly linear.

5. Data Presentation

Digital data in counts per second for each of the specified isotopes are transferred to the EBR-II DAS as part of each 30-min data cycle. In addition, the minicomputer each minute takes data "on the fly" for ^{133}Xe and ^{135}Xe; this information is transmitted to the DAS without interfering with data acquisition.

Analog data from the single-channel analog array are presented on two three-pen recorders in the reactor control room, as shown in Fig. 8. These data are also presented continuously to the DAS. Data from either source, if logged in the DAS, are available through the normal DAS display scopes.

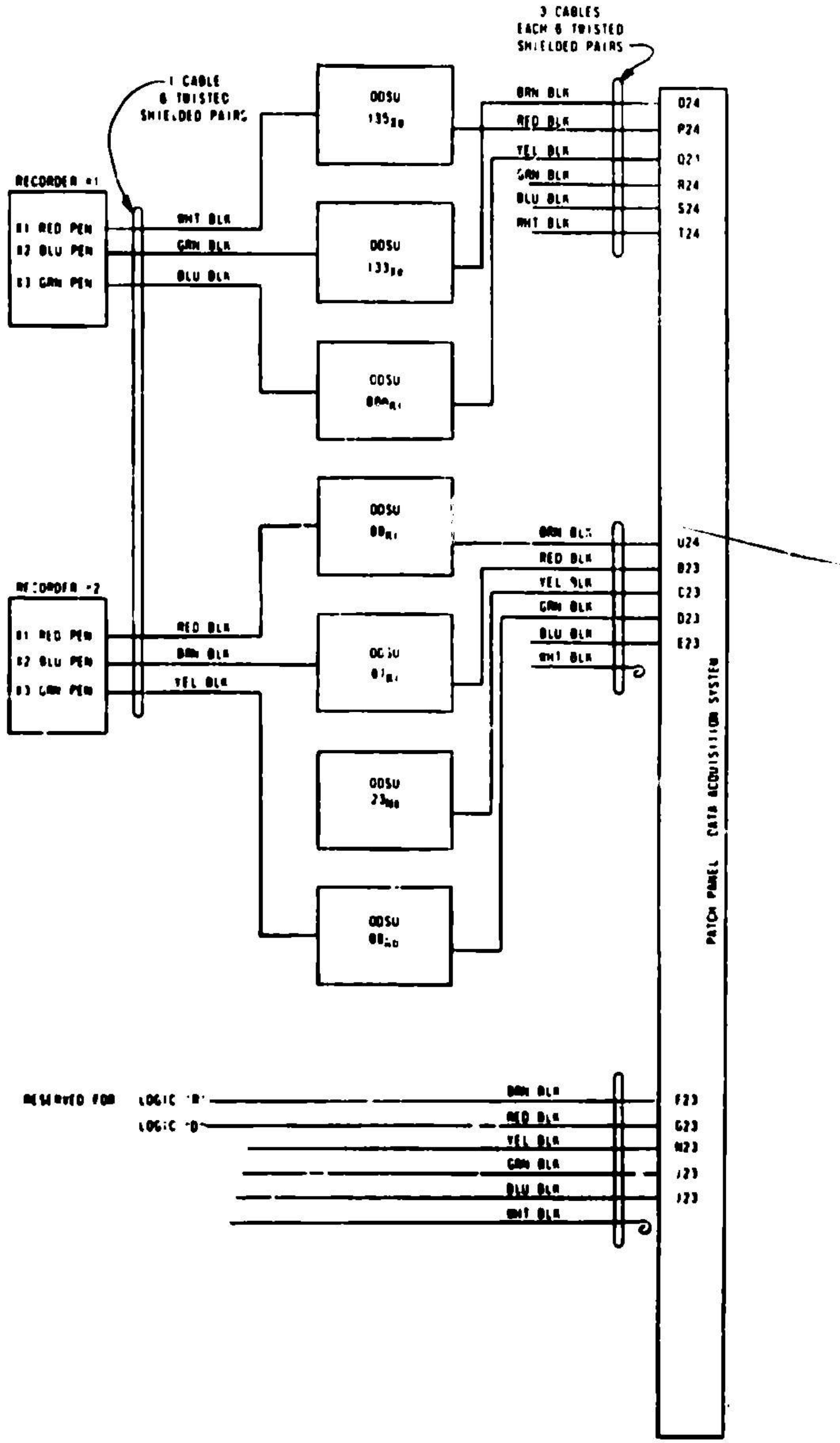

Fig. 8. Cable Connections for GLASS Output to the Data-acquisition System and to the Control Room. ANL Neg. No. 103-S5002.

V. SENSITIVITY CONTROL

The excellent resolution of the detector on which successful operation depends is degraded at high count rates. Whenever the gross count rate exceeds ~30,000 counts/s, the sensitivity of the system must be reduced by reducing the sample-chamber volume. If the count rate again exceeds ~30,000 counts/s, the sensitivity is further reduced by diluting the sample gas. The gross count rate is determined as shown in Fig. 3 by a count-rate meter attached to the lower-level discriminator (LLD) of the SCA set for ^{133}Xe. This is the lowest signal threshold available without installing additional equipment.

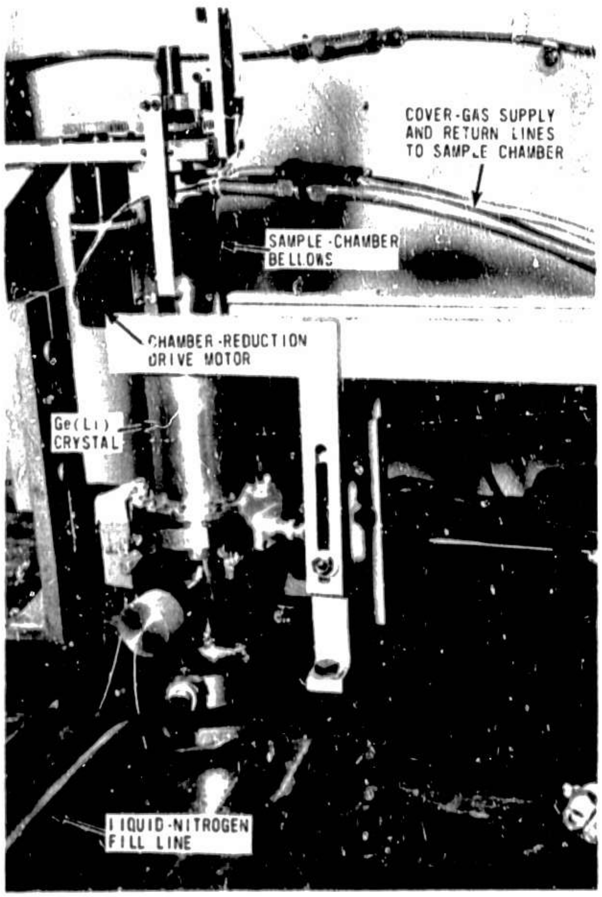

Fig. 9. Variable-volume Sample Chamber. ANL Neg. No. 103-P5698.

A. Volume Reduction

The sample chamber with the volume-reduction device is shown in Fig. 9 as it appeared before being enclosed in the lead shield. Basically, the chamber consists of a stainless steel can, which slides on a stationary piston to create a varying volume between the end of the piston and the end of the can. A metal bellows attaches to a flange on the piston and to the edge of the can so that the sliding joint is gastight. Also shown is the gear motor that reduces the volume. The sample chamber is operated only in the fully open and fully closed positions.

B. Gas Dilution

The sensitivity, if not adequately reduced by the volume reduction, may be further reduced by dilution of the sample gas. To accomplish this (see Fig. 10), a set of solenoid valves (a) bypasses the main sample stream around the sample chamber (valves V1 and V2), (b) flows clean argon through the sample chamber (valves V3 and V4), and (c) bleeds an aliquot of sample gas through valve V5 into the clean argon stream in a ratio of ~1:28. Because of the high ambient field existing under such circumstances, this results in a sensitivity reduction of only about 15 times.

The metal bellows on the variable-volume sample chamber is rated at 48 kPa. This limitation is harmless under almost any condition, because the system is operated with valve V-322R on the return manifold wide open.

This effectively maintains the maximum differential at 1 kPa or less. Moreover, the supply pressure at the supply manifold is only 34 kPa. The only source of risk is the triple contingency of turning on the high-pressure clean-argon supply while (a) valve V-322R is inadvertently closed, (b) having a simultaneous malfunction of valve V4, and (c) having a further malfunction of the relief valve in parallel with V4.

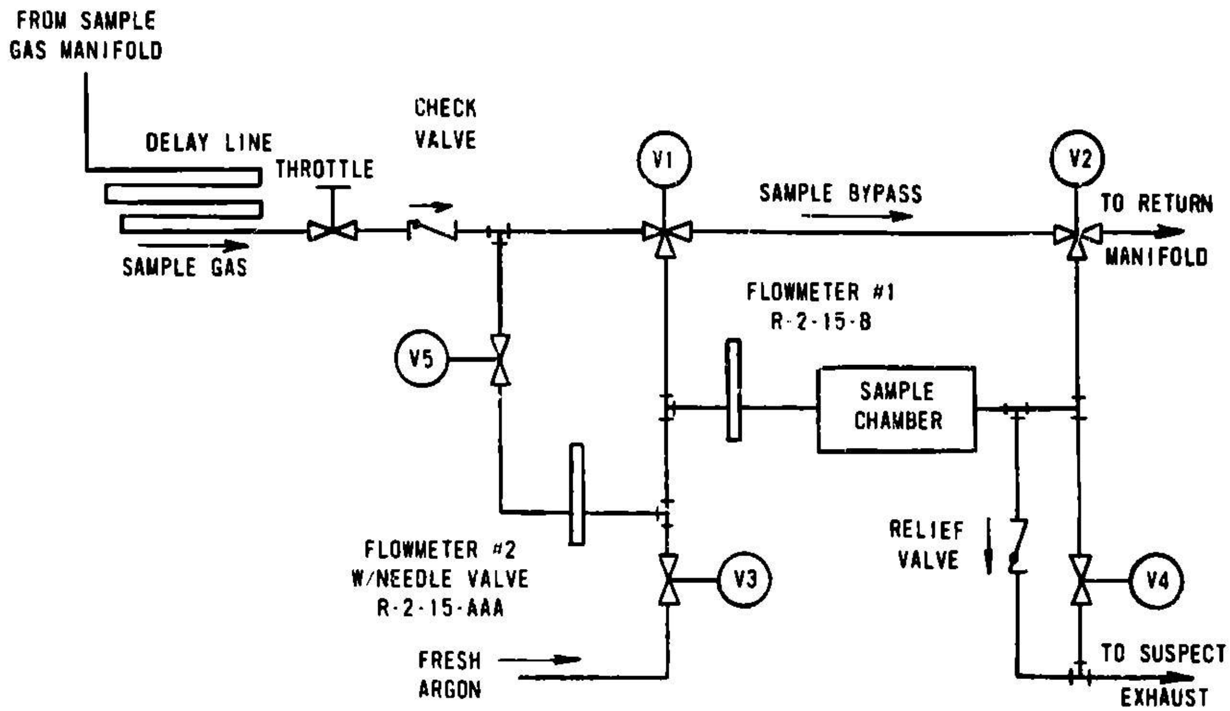

Fig. 10. Schematic of Gas-sample Flow in GLASS. ANL Neg. No. 103-R5990.

C. Operation of Sensitivity Control

The sensitivity control box appears in the upper-right-hand cabinet in Figs. 2 and 3. Figure 11 is a schematic of the control system for the variable-volume sample chamber. Figure 12 is a schematic for dilution control. The control box is shown in the schematics by dotted lines. Parallel controls are available in the depressed area for system checkout.

Arbitrarily, volume reduction always precedes dilution in reducing sensitivity. The actual reduction in sensitivity is a function of gamma energy, due to the varying effectiveness of streaming from emitter nuclei in tubing at some distance from the detector. Figure 13 shows the energy-dependent scale factors for sensitivity for volume reduction alone, and also those for volume reduction and gas dilution combined.

So far, there have been few occasions that required both means of sensitivity reduction. Leaker X084A, which occurred in March 1973, resulted in ^{133}Xe levels of the order of 10^4 above background. The ^{135}Xe was $>10^3$ above background. Leaker X213 exhibited similar levels in December 1974. It is anticipated that there will be numerous such high-burnup oxide leakers in the future.

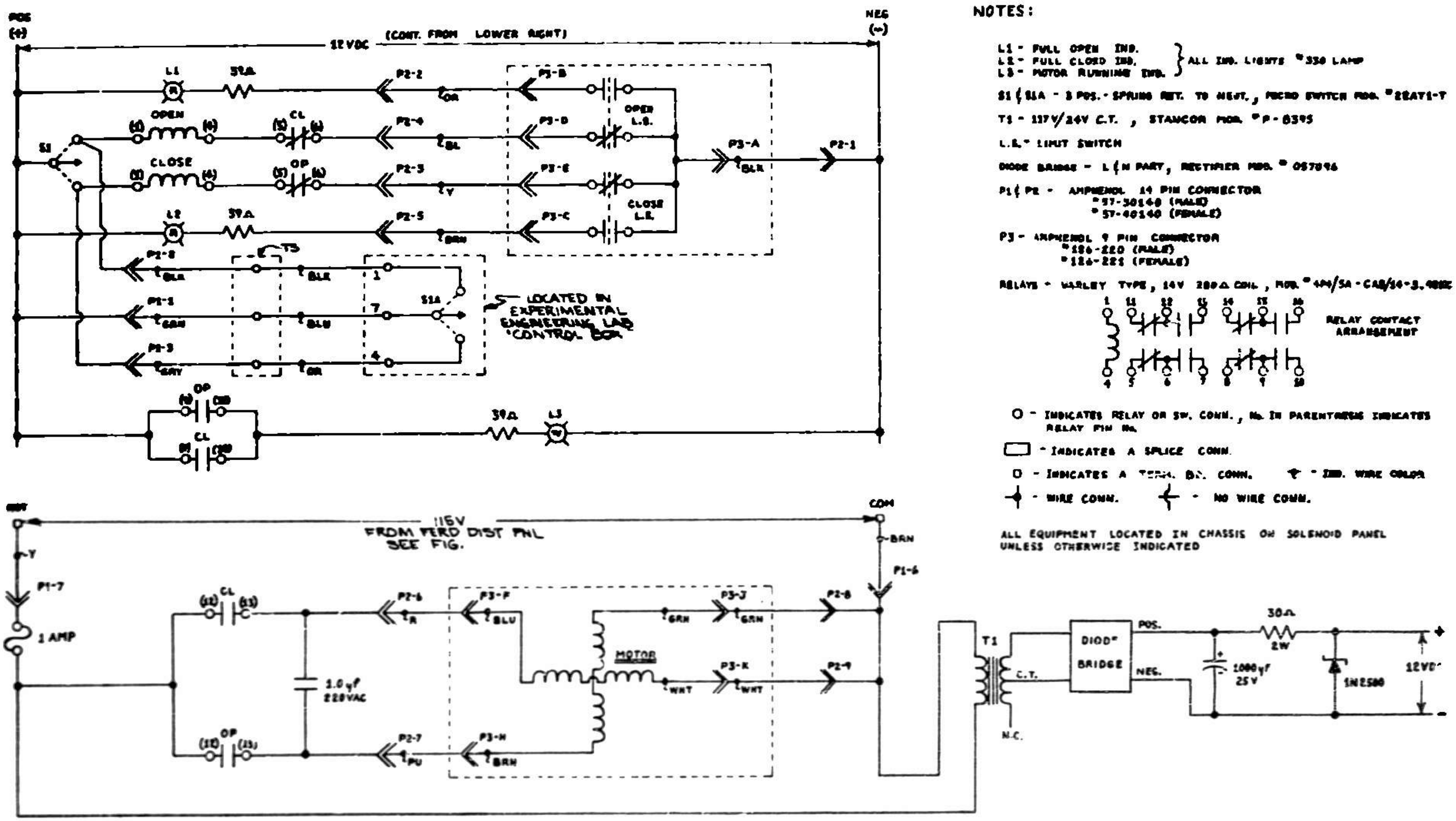

Fig. 11. Schematic of Controls for Variable-volume Sample Chamber. ANL Neg. No. 103-R5995

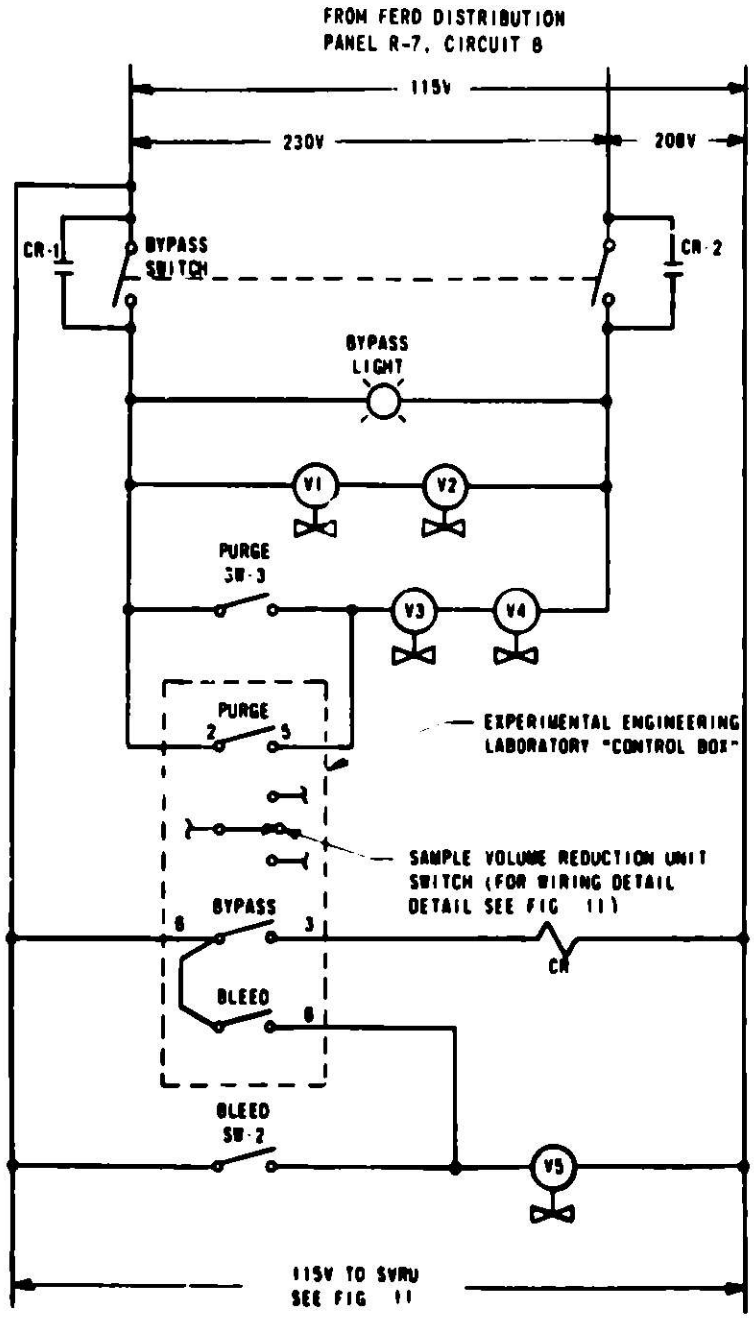

Fig. 12

Schematic of Sample-gas Dilution Control. ANL Neg. No. 103-R5992.

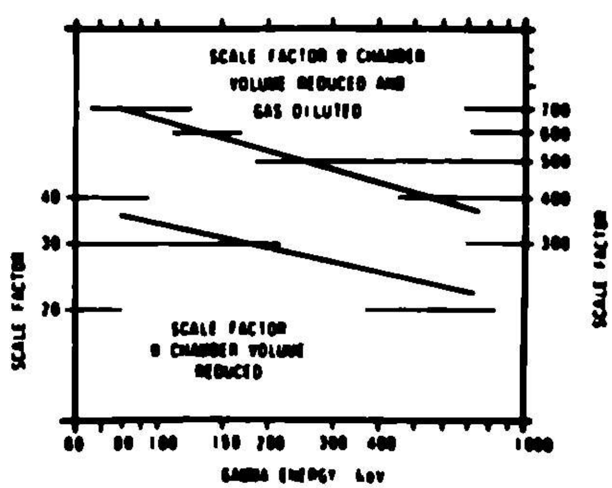

Fig. 13

GLASS Count-rate Scale Factors for Conditions of Reduced Sensitivity. ANL Neg. No. 103-R5980.

VI. SYSTEM PERFORMANCE UNDER NORMAL CONDITIONS

The EBR-II primary system contains a small, and apparently irreducible, trace of fissionable material in the core external to the fuel cladding. This material produces fission products at a rate equivalent to that which would be expected from the exposure of about 3 mg of ^{235}U. Because of the still unconfirmed assumption that this material is actually contamination on the surface of the fuel cladding, it is termed "tramp" uranium, and the associated background is termed "tramp" activity. In actual practice, this activity constitutes a useful calibration source for the operation of fission-product-monitoring equipment.

A. Stability

As mentioned earlier, GLASS (both the detector and the analysis equipment) is located in a hostile environment. This is particularly true of the cover-gas detector, which is located in an essentially unventilated cell in which the temperature normally fluctuates between 87 and 97°F (31 and 36°C). This has been alleviated slightly by placing an ordinary fan to blow into the cell; this results in a somewhat more stable temperature in the vicinity of 90°F (32°C). The analysis equipment is located in the experimental engineering laboratory (EEL), where unstable air conditioning results in temperatures varying generally between 72 and 86°F (22 and 30°C).

The preamplifier, amplifier, and analog-to-digital converter are specified as having temperature stability of 100 ppm/°C (55 ppm/°F). Hence, if the temperatures happened to vary 10°F (5.5°C) in additive directions it would be possible to get an extreme gain shift of ~0.2% (550 ppm in the preamplifier, 550 ppm in the amplifier, and 550 ppm in the analog-to-digital converter). Actual observation over a period of time suggests that the foregoing is a reasonable outside limit on gain changes, which have rarely exceeded 0.14% peak-to-peak. While this gain variation is tolerable in the present application, it is nevertheless desirable to improve the environment for this instrumentation. The permanently installed calibration source has turned out to be very effective in correcting for the gain variation.

B. Background Fission-product Data

The cover-gas spectrum normally observed is shown in Fig. 6. Typical background concentrations measured from this spectrum are given in Table II. Because of the "poor" geometry in the cover-gas detector (a large source volume near a detector of similar volume), it is not possible to do a convincing calculation of the geometric efficiency. Hence, the absolute concentrations in the table have been obtained by normalization to an independent measurement of ^{135}Xe concentration that is routinely performed on a discrete sample in the analytical laboratory. The photopeak efficiencies are taken from the experimental curve given in Fig. 14.

TABLE II. Typical EBR-II Cover-gas Activities as Determined by GLASS
(Data from 0500 hours, June 23, 1973)

Isotope	Gamma Peak, keV	Half-life	Photopeak Efficiency	Branching Ratio	Count Rate, s^{-1}	Concentration,[a] nCi/ml	Total Gas Activity, dis/s	Fission Yield, %	Production Rate,[b] atoms/s	Release/Birth
^{85m}Kr	151.2	4.48 hr	0.70	0.75	18.0	0.32	1.06×10^8	1.5	3×10^8	0.35
^{87}Kr	402.6	76.4 min	0.25	0.84	3.58	0.16	0.53×10^8	2.7	5.4×10^8	0.10
^{88}Kr	196.3	2.80 hr	0.50	0.35	10.27	0.55	1.83×10^8	3.6	7.2×10^8	0.25
^{133}Xe	81.0	5.30 days	0.63[c]	0.37	20.0	0.8[d]	2.66×10^8	6.7	13.4×10^8	0.20
^{135}Xe	249.7	9.14 hr	0.39	0.91	85.1	0.25[d]	7.49×10^8	6.5	13.0×10^8	0.58
^{135m}Xe	526.6	15.65 min	0.20	0.80	0.604	0.035	0.12×10^8	2.2	4.4×10^8	0.027
^{138}Xe	258.6	14.2 min	0.37	0.40	1.60	0.10	0.33×10^8	6.6	13.2×10^8	0.025
^{23}Ne	440.0	37.6 s	0.23	0.33	60	1.4[e]	5.7×10^{10}		1×10^{15}[f]	5.7×10^{-5}

[a]Nanocuries per milliliter of gas at 12.2 psia (84.1 kPa) and 70°F (21°C).
[b]Assumes 2×10^{10} fissions/s in tramp material, corresponding to 2.5 mg of free uranium.
[c]This effective photopeak efficiency has been inferred from Ebersole's data. It is entirely consistent with what would be estimated by taking into account absorption of this soft gamma in the window of the sample chamber and the envelope of the detector.
[d]The concentrations of ^{133}Xe and ^{135}Xe were obtained from E. Ebersole, who routinely reports these values measured on discrete samples under laboratory conditions. The value for ^{135}Xe has been used to normalize all other activities except ^{133}Xe.
[e]Estimated actual ^{23}Ne activity in reactor correcting for travel time to detector is 170 nCi/ml.
[f]The calculation of this is described in Ref. 2. The number has been adjusted to reflect an increase in power and an effective increase in core size.

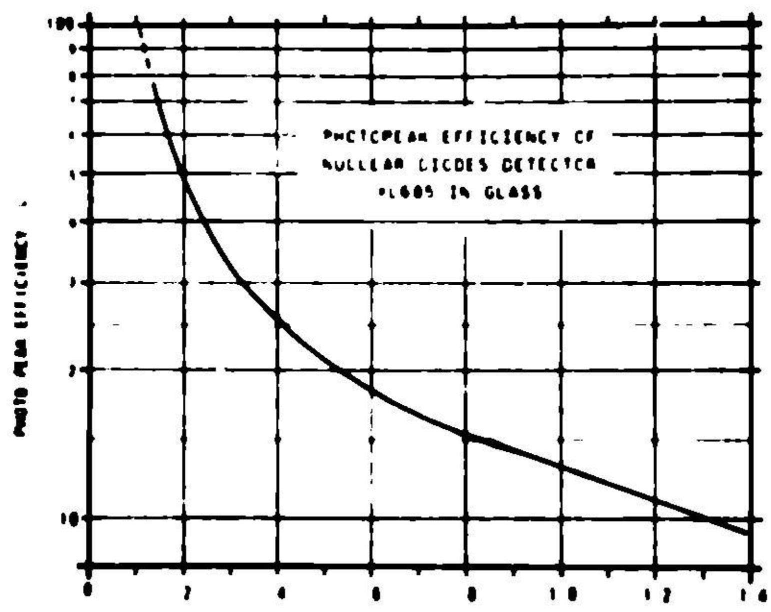

Fig. 14. Photopeak Efficiency of GLASS Detector.
ANL Neg. No. 103-R5997.

The photopeak efficiencies given are those actually measured in the present shield, which has a relatively small cavity. Scattering from the cavity walls contributes to the Compton background. In addition, the interior surface of the lead shield under gamma irradiation emits X-rays at 75 and 85 keV, and these interfere with the precise counting of ^{133}Xe at low levels. The GLASS detector system will eventually be moved to a more adequate location. At that time the shield will be rebuilt with a much larger cavity and lined with sheet steel. The steel liner will suppress the lead X rays, and the larger cavity will ameliorate the backscatter effects. The photopeak efficiencies (see Fig. 14) will have to be remeasured for the new configuration.

The count-rate data in Table II were taken at about 0500 hours on June 23, 1973. All isotopes are essentially at equilibrium concentration, except ^{133}Xe (5.3-days half-life). The behavior of this isotope is complicated by leakage from the cover gas. The leakage "half-life" fluctuates in the vicinity of 4 days, but is visibly and erratically affected by the irregularly scheduled fuel transfers into and out of the reactor vessel. In addition, there is a "cold trap" (designed to remove oxygen from the sodium coolant), which depresses the concentration of ^{133}Xe (and to a lesser extent ^{135}Xe) by removing their iodine precursors from the sodium. Because of a number of competing effects, the contribution of the cold trap is difficult to measure confidently, but is of the order of 10%. For the six or seven years that ^{133}Xe and ^{135}Xe have been analyzed in cover-gas samples, the level of tramp activity has remained remarkably constant. This very stability raises some doubt as to whether the tramp uranium could actually be incidental contamination. If this were the case, the tramp level might reasonably be expected to fluctuate, depending on the cleanliness with which the most recent batch of fuel was fabricated.

In July 1973, the concentration of ^{133}Xe in the cover gas was 1.6×10^{-3} μCi/mL after something more than 10 days of full-power operation. It is estimated that ultimately equilibrium would be $\sim 1.7 \times 10^{-3}$ μCi/mL.* The equation for the equilibrium population in the sodium is

$$Y_{133}FR = \lambda_R N_S + \lambda_D N_S \tag{1}$$

or

$$N_S = \frac{Y_{133}FR}{\lambda_R + \lambda_D}, \tag{2}$$

where

FR = fission rate in tramp,

Y_{133} = fractional yield per fission of ^{133}Xe,

N_S = number of ^{133}Xe atoms in the sodium,

λ_R = the radioactive decay constant,

λ_D = the fractional diffusion rate to the cover gas,

*It may appear superficial or incorrect to estimate the 5.2-days ^{133}Xe so close to saturation in only 10 days. However, due to leakage from the reactor, which is estimated to have an effective time constant of 0.16 day^{-1}, the combined effect causes the ^{133}Xe to approach saturation with an effective time constant of 0.16 + 0.13 = 0.29 day^{-1}. Thus, 10 days corresponds to ~4.2 half-lives or ~95% of saturation.

and the equilibrium population in the cover gas is governed by

$$\lambda_D N_S = \lambda_R N_G + \lambda_\ell N_G \tag{3}$$

or

$$N_G = \frac{\lambda_D N_S}{\lambda_R + \lambda_\ell}, \tag{4}$$

where

N_G = number of ^{133}Xe atoms in cover gas

and

λ_ℓ = leakage constant from the cover gas.

From Eq. 2, the net input from the sodium to the cover gas is

$$\lambda_D N_S = Y_{133} FR \frac{\lambda_D}{\lambda_R + \lambda_D}. \tag{5}$$

Similarly, from Eq. 4, the total equilibrium decay rate in the cover gas is

$$\lambda_R N_G = \lambda_D N_S \frac{\lambda_R}{\lambda_R + \lambda_\ell}. \tag{6}$$

Thus the total decay rate in the cover gas is

$$\lambda_R N_G = Y_{133} FR \frac{\lambda_D}{\lambda_R + \lambda_D} \frac{\lambda_R}{\lambda_R + \lambda_\ell}, \tag{7}$$

where

$$\lambda_R = \frac{0.693}{\text{half-life}} = 0.131\ \text{day}^{-1}.$$

The argon-cover-gas volume is estimated at 9000 L at operating temperature and pressure. The leakage, although erratic, averages an estimated 1 L/min or 1440 L/day; λ_ℓ = 1440/9000 = 0.16 day^{-1}. Thus the value of the second fraction in Eq. 7 that corrects for leakage is 0.450. As is discussed later, there is a sensible "holdup" in the sodium as specified by λ_D. In this case, with small error, λ_D can be estimated as 3 day^{-1}. The value of the first fraction becomes 0.96.

We can now use Eq. 7 and the measured decay rate in the cover gas to solve for FR. The measured total decay rate is $\lambda_R N_G$ = concentration in cover gas (1.7×10^{-3} µCi/cm^3) times decay rate per µCi (3.7×10^4 dis/s per µCi) times volume of cover gas (9×10^6 cm^3) = 5.66×10^8 dis/s. We then obtain

$$FR = \frac{5.66 \times 10^8}{(0.45)(0.96)(6.7 \times 10^{-2})} = 1.95 \times 10^{10}\ s^{-1},$$

where the last term in the denominator is the yield of ^{133}Xe.

Taking into account the ~10% loss of ^{133}I in the cold trap mentioned above, we obtain the final estimate of the fission rate as ~2×10^{10} s^{-1} (± 30%). This corresponds to what would be produced by roughly 2.5 mg of ^{235}U in some average flux in the core, both fission fragments are assumed to be free to recoil into the sodium.

Table II includes the estimated production rate for each isotope, based on the ~2×10^{10} fissions/s derived above. The last column of the table gives the ratio of total disintegrations in the cover gas to the estimated product rate (release/birth). This ratio is highly dependent on decay constant, as shown in Fig. 15.

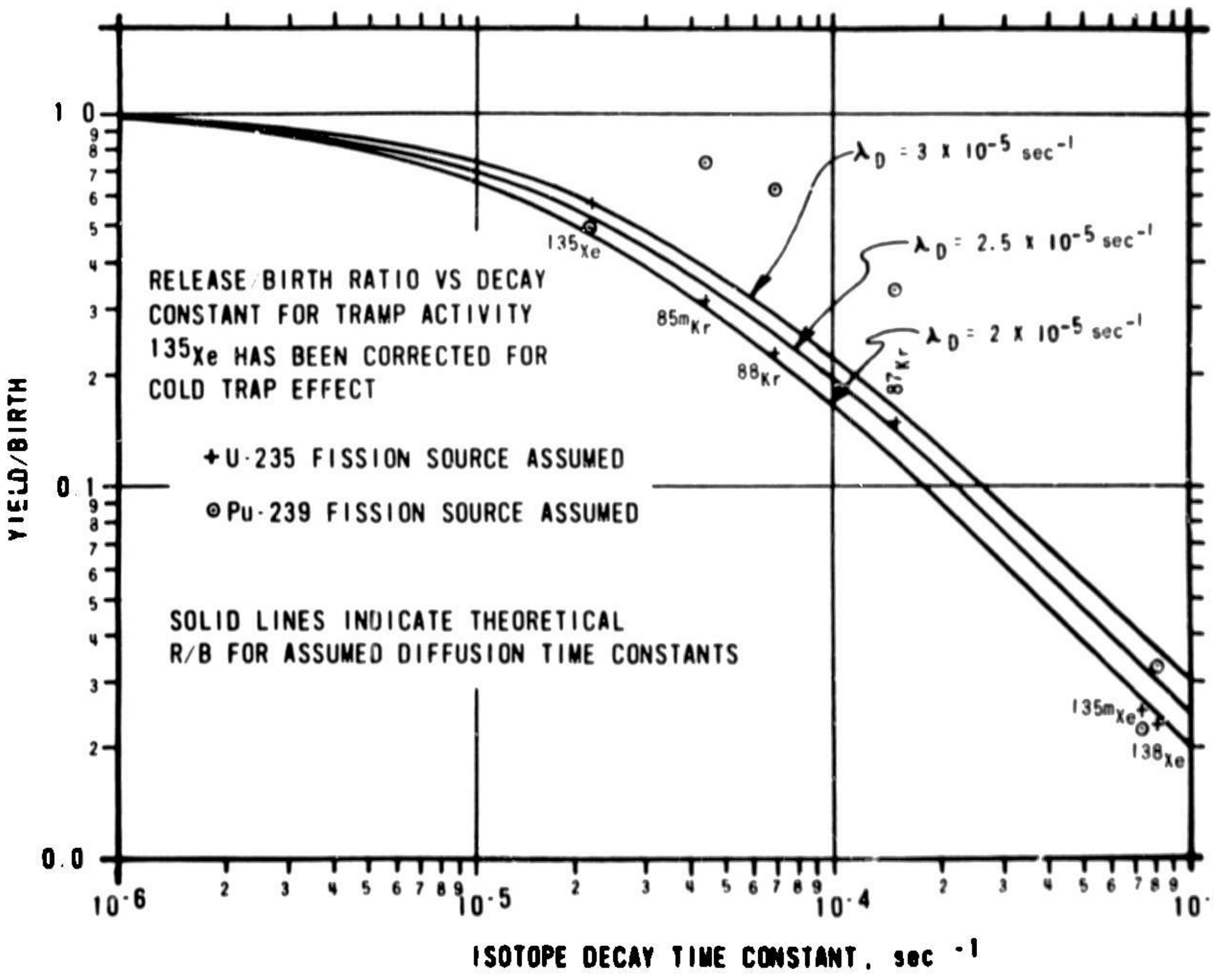

Fig. 15. Release-to-Birth Ratio for Tramp Activity. ANL Neg. No. 103-R5986.

The three curves plotted in Fig. 15 are based on the assumption that the diffusion from the sodium to the cover gas can be represented by a simple time constant λ_{DIFF}. Under this assumption, the yield/birth ratio is

$$\frac{\lambda_D}{\lambda_D + \lambda_R}.$$

The three curves correspond to $\lambda_D = 2 \times 10^{-5}$, 2.5×10^{-5}, and 3×10^{-5} s^{-1}. It appears that 2.5×10^{-5} s^{-1} (corresponding to ~7.7-hr "half-life") gives the most reasonable fit to the data, assuming ^{235}U as the fission source (plotted as crosses). These estimates are subject to wide uncertainty because of the complexity of the primary system, and they also depend on the unsubstantiated assumption that λ_D is the same for both krypton and xenon.

Incidentally, $\lambda_D/(\lambda_D + \lambda_R)$ estimates a yield/birth ratio of ~1.3×10^{-3} for ^{23}Ne versus an observed value (from Table II) of 5.7×10^{-5}. This factor-of-18 discrepancy is not particularly surprising when it is noted that the crucial assumption of good mixing in the reactor tank is not valid on the time scale of ^{23}Ne decay (37.6-s half-life).

Another estimate of the diffusion time constant in the primary sodium is available from measurements during scrams and startups. Assume, before a scram, that a noble-gas species is in equilibrium. If there is no holdup in the sodium, then the activity will immediately decay according to the half-life with (in the cases of the kryptons and ^{138}Xe) an imperceptible perturbation due to the very short precursors. In actual fact, the decay of these isotopes clearly lags the anticipated decay by reason of the "reservoir" held in the sodium. Similarly, the increase in activity during a startup lags because of the atoms going to refill the "reservoir." This effect is clearly shown in Figs. 16 and 17,

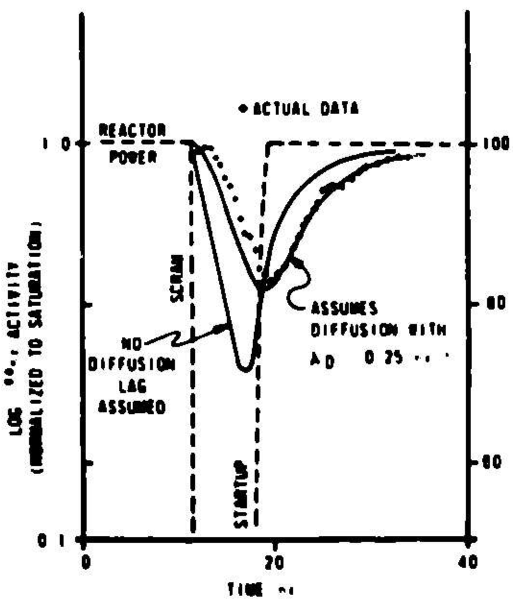

Fig. 16. Transient Behavior of ^{88}Kr Activity during Scram and Restart. ANL Neg. No. 103-R5982.

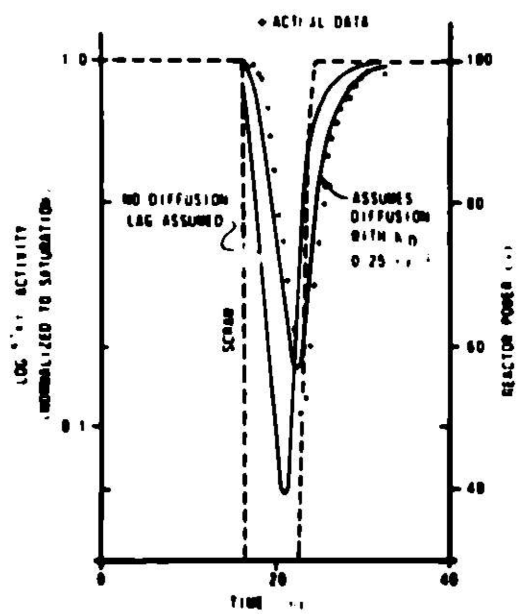

Fig. 17. Transient Behavior of ^{87}Kr Activity during Scram and Restart. ANL Neg. No. 103-R5984.

which show data taken during a scram and startup sequence on March 16, 1972. This segment of data was more suitable for analysis than usual because the downtime was relatively short, followed by a rapid return to full power. The primary pumps were left on. The sodium turbulence caused by the pumps has a substantial effect on diffusion from the sodium to the cover gas, and the gas data would have been perturbed if the pumps had been turned off.

These figures are typical of a number of attempts to fit data to a diffusion model for the transport of noble gases from the sodium to the cover gas. The values for λ_D obtained thus are consistently larger than those estimated above from the equilibrium ^{133}Xe data. The holdup "half-life" obtained from this type of observation is on the order of

$$\frac{\ln 2}{\lambda_D} = \frac{0.693}{0.25} = 2.8 \text{ hr}.$$

This differs by a factor of ~3 from the 7.7 hr inferred from equilibrium measurements; such a discrepancy is not surprising in view of the complexity of the system and the simplicity of the model described by the single diffusion time constant λ_D. Moreover, the difference may simply be due to the fact that the temperature regime during shutdown is different from that at power. The important point is that both static and kinetic measurements agree in indicating a holdup "half-life" of a few hours in the sodium; such a delay has a widely varying effect on the different isotopes, depending on their respective half-lives.

C. Nonfission Background Activity

The purpose of this section is to discuss the counting problems introduced in the system by activation products and by noble-gas daughters deposited in the sample chamber.

It is important to evaluate these extraneous activities in terms of the total counting load they add to the system. As shown in Fig. 14, the photopeak efficiency is low, especially at high energy. As an example, the identifiable photopeak count rate of 0.3 counts/s for the ^{24}Na gamma at 1369 keV implies a total pulse input to the system of ~6 counts/s, when the ^{24}Na gamma at 2754 keV is also taken into account.

The gas-sampling system is carefully designed to prevent the carryover of sodium vapor, which would condense in the cooler areas and clog the system. Equilibrium ^{24}Na activity as a measurement of sodium carryover to the GLASS detector indicates that at the highest flow rate [~50 cfh (1.4 m^3/hr)] the gross count rate due to ^{24}Na was ~6 counts/s. It was noted that the signal from ^{24}Na was associated with the gas and essentially disappeared when the sample chamber was purged. Some sodium vapor had been expected to condense in the sample chamber, but it apparently did not to any significant extent.

The question of fission-product fallout in the sample chamber turned out to be much less significant than had been expected. Of the various daughters of the noble gases, only ^{88}Rb appeared in measurable quantity, and that amounted to about 20 counts/s gross.

Argon-41 presents a much more serious problem. For convenience in measuring the fission products, the energy scale of the analyzer is adjusted to span 0 to ~1000 keV. This range misses the ^{41}A gamma at 1293.6 keV. However, discrete sample measurements by Ebersole give an equilibrium concentration of 3.2 nCi/mL. The ^{41}A is produced by simple neutron activation of the cover gas and to a lesser extent by the $^{41}K(n,p)^{41}A$ reaction on a small potassium fraction in the sodium coolant. Although the ^{41}A peak is not analyzed, the ^{41}A at saturation contributes about 350 counts/s to the pulse-handling load of the amplifier and analyzer.

Neon-23 (37.6-s half-life) is produced by the $^{23}Na(n,p)^{23}Ne$ reaction on the sodium coolant and has been discussed in Ref. 2. Since that paper was written, an increase in reactor power and certain changes in core geometry have increased the estimate of the production rate to roughly 1×10^{15} atoms/s.

Compared to the ^{23}Ne half-life, the sample transit time is relatively long, and an effort was made to evaluate the effect of sample-gas pumping rate on the count rate at the detector. Varying the nominal flow from 283 to 850 L/hr can increase the gross counting load due to ^{23}Ne from ~25 to ~800 counts/s. Hence, from the standpoint of conserving the count-rate capacity of the channel, it is desirable to operate the gas system at the lower flow rates. Subsequent to the measurement on ^{23}Ne just mentioned, a delay line with a volume of ~2 L was installed to reduce the effect of ^{23}Ne at the detector. The calculated delay (at a nominal flow rate of 2 cfh) is ~130 s, which reduces the ^{23}Ne count rate by a factor of ~11. Figure 5 shows the delay line positioned below the supply and return manifolds that service the several devices monitoring cover gas.

Another important point can be made in connection with ^{23}Ne. In Table II, note that the release of ^{23}Ne to the cover gas is ~50 ppm of the total production, the remainder decaying (37.6-s half-life) in the sodium. As was discussed in Ref. 2, the concentration of ^{23}Ne in the cover gas is extremely sensitive to relatively small changes in the bulk-sodium temperature. In March 1973, an experiment was performed to better measure the effect of bulk-sodium temperature on ^{23}Ne activity in the cover gas.

The experiment consisted of observing ^{23}Ne with GLASS while varying the bulk-sodium temperature. The bulk-sodium temperature was controlled by varying the flow rate in the secondary system, which governs the rate of heat removal from the primary system. The time constants of the system are long, and precise control is very difficult. However, so far as possible the system was stabilized at 690°F (365.5°C), then raised as quickly as permitted (0.33°F/min, or 0.18°C/min) to 700°F (371°C), where it was stabilized for

~30-40 min before being returned to 690°F (365.5°C), again moving as quickly as permissible. The results of this experiment are plotted in Fig. 18, in which the temperatures are plotted as a continuous line. The ^{23}Ne activity levels fluctuate wildly, even though the ΔT of 10°F (5.5°C) must be considered a small perturbation at a nominal operating temperature of 700°F (371°C). Note that the ^{23}Ne activity levels bear a rate-dependent relationship to the temperature, the highest (and lowest) levels coinciding with the steepest slopes in the temperature profile.

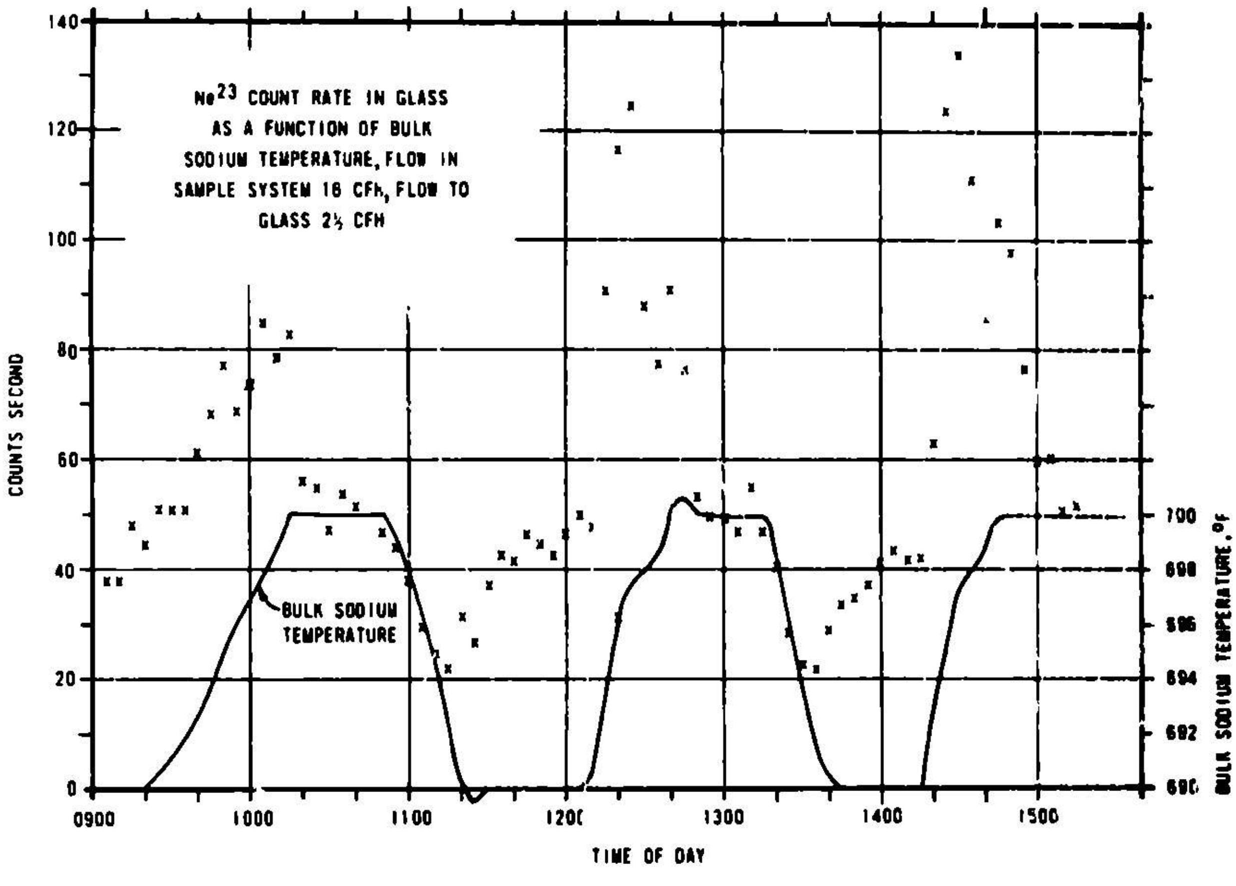

Fig. 18. Effect of Changing Bulk-sodium Temperature on the ^{23}Ne Activity. ANL Neg. No. 103-S5003.

D. Necessity for Reduction in Sensitivity

It was apparent soon after experimentation began with GLASS that it would be necessary to effect drastic changes in sensitivity in order to span the range of activities occurring in the cover gas. The chamber and detector were sized so as to obtain, during normal operation, photopeak count rates ranging from ~100 s^{-1} for ^{135}Xe down to ~0.5 s^{-1} for ^{135m}Xe. These conditions result in a gross count rate of ~1000 s^{-1}, which is the measure of how "busy" the amplifier channel is. This situation represents a compromise. If the sensitivity were much less, the data for ^{135m}Xe and ^{138}Xe would be statistically unusable. On the other hand, a higher sensitivity would mean that the amplifier channel would be fairly well loaded, even at background level, and would not have much range left to follow an excursion. It is undesirable to allow the gross count rate to exceed, say, 40,000 s^{-1}.

Two methods are available for changing sensitivity. First, by means of a bellows, the sample chamber is collapsed from a volume of ~23.5 to ~1 mL, resulting in a sensitivity reduction of about 30. The actual change in sensitivity varies with energy and is shown in Table III. This variation with energy is due to the fact that, after the chamber is collapsed, the tubes leading to and from the chamber have a considerable volume relative to that of the chamber itself. The higher-energy gammas have a greater probability of reaching the detector through intervening material; this effect reduces the ratio of the sensitivities with increasing gamma energy.

TABLE III. Scale Factors for Various Isotopes during Reduction in Sensitivity

Isotope	Normal Operation Factor A	Sample Chamber Reduced Factor B (± 3%)	Sample Chamber Reduced + Dilution Factor C (± 10%)	Conversion Factor D, counts/s to nCi/mL: Before 11/06/74	11/06/74 to 2/26/75	After 2/26/75	Typical Count Rate[a] at Saturated Background, counts/s
^{85m}Kr	1	30.8	585	0.018	0.033 (± 8%)	0.040 (± 8%)	11
^{87}Kr	1	25	440	0.045	0.052 (± 8%)	0.061 (± 8%)	3
^{88}Kr	1	29.3	540	0.054	0.077 (± 8%)	0.094 (± 8%)	6.5
^{133}Xe	1	36	700	0.080	0.60 (± 9%)	0.82 (± 9%)	1.5
^{135}Xe	1	28	500	0.026	0.033 (± 6%)	0.041 (± 6%)	60
^{135m}Xe	1	23.6	410	0.058	0.065 (± 8%)	0.079 (± 8%)	0.25
^{138}Xe	1	27.7	500	0.062	0.078 (± 8%)	0.098 (± 8%)	1.0

[a]Raw count rate × (A, B, or C) = adjusted count rate. (The EBR-II DAS performs this adjustment for its output.) Adjusted count rate × D = concentration in nCi/mL of cover gas at 84.1 kPa absolute pressure and ~70°F (21°C).

In the normal operation of EBR-II as an irradiation facility, fission-product releases can result in cover-gas activity levels 1000 or more times as high as normal background. Simply reducing the GLASS sample volume does not decrease the sensitivity enough to encompass a severe rise in activity. Additional range is obtained by bypassing the main sample stream and diluting a very small amount of sample gas with clean argon for counting. (See the piping diagram in Fig. 10.) Dilution is accomplished by operation of valves V1-V5.

The approximate dilution ratio is 28:1, which, superficially, would appear to reduce the sensitivity by a factor of ~30. The actual effect of dilution as determined by experience is energy dependent, but averages about 18. The results are also tabulated in Table III. The standard procedure is always to compress the chamber before diluting.

The decision to reduce sensitivity is based on the count-rate meter (Fig. 3) connected to the lower-level discriminator of the "signal" SCA for ^{133}Xe. This low-threshold discriminator effectively gives the gross count rate for the entire system. This count-rate signal is displayed by the blue pen of the recorder shown at the top of Fig. 2. In general, the sensitivity rate is reduced when the gross count rate exceeds ~30,000 counts/s. There may be some discretion in this. For example, if it is known that a large part of the count is due to ^{133}Xe at low energy, then a somewhat higher count rate (say ~40,000) may be tolerated.

Normally, the sensitivity is increased when the count rate falls below ~1000 counts/s gross; however, some discretion is necessary here because of the widely varied circumstances that might ensue after the fission-product release that required the original reduction in sensitivity.

E. Modification of GLASS on November 6, 1974

On November 6, 1974, a cadmium absorber with a density of 0.80 g/cm^2 was installed between the gas sample chamber and the detector. The absorber preferentially reduces the count rate of ^{133}Xe because of the low energy of that gamma ray. This effectively increases the dynamic range of GLASS by largely suppressing the extreme excursions in the count rate for ^{133}Xe that occur when a high-burnup element leaks. Similarly, it means that GLASS can operate with a much larger ^{133}Xe inventory at a subsequent startup. This increased tolerance to high ^{133}Xe levels will make it possible to reduce purging by ~3.5 hr.

Table III gives the former (before cadmium) and current conversion factors for determining absolute concentrations from raw count rates.

F. Possible Inferences from Cover-gas Data

Figure 19 illustrates an interesting and potentially useful point. As fissionable species increase in mass, the additional mass tends to appear in the lighter of the two fission fragments. Complete distributions are plotted for ^{235}U and ^{239}Pu (fission spectrum) with data from Ref. 4. In addition, yields are plotted for the production of the most significant noble-gas species from ^{233}U, ^{238}U, and ^{232}Th. (Note: 133 and 135 were not plotted for ^{238}U, since these points effectively coincide with those for ^{235}U.)

Table IV presents the relevant yields and their ratios. Xenon-133 was omitted, since its yield does not differ markedly from ^{135}Xe. From the table, it would appear relatively easy to determine if a certain fission-gas source were ^{235}U or ^{239}Pu, since yield ratios for these two isotopes differ so widely. However, there are a few hours of diffusion time in the sodium, which confuses the matter, since the various half-lives also vary widely.

To this point, we have assumed that the tramp activity originates in ^{235}U. This is reasonable, because approximately this same level of tramp activity was present long before there was any plutonium in the reactor. However, as a matter of interest, Fig. 15 includes (plotted as circles) those yield/birth ratios that result when it is assumed that the fission source is plutonium. Their departure from any consistent trend is of itself a strong qualitative argument that the source is not plutonium, apart from the historical consideration mentioned above.

Two isotopes, ^{131m}Xe and ^{85}Kr, not normally monitored, may, under unusual circumstances, be of considerable significance. Xenon-131m has a 12-day half-life and a low branching ratio. These combine to give a very low

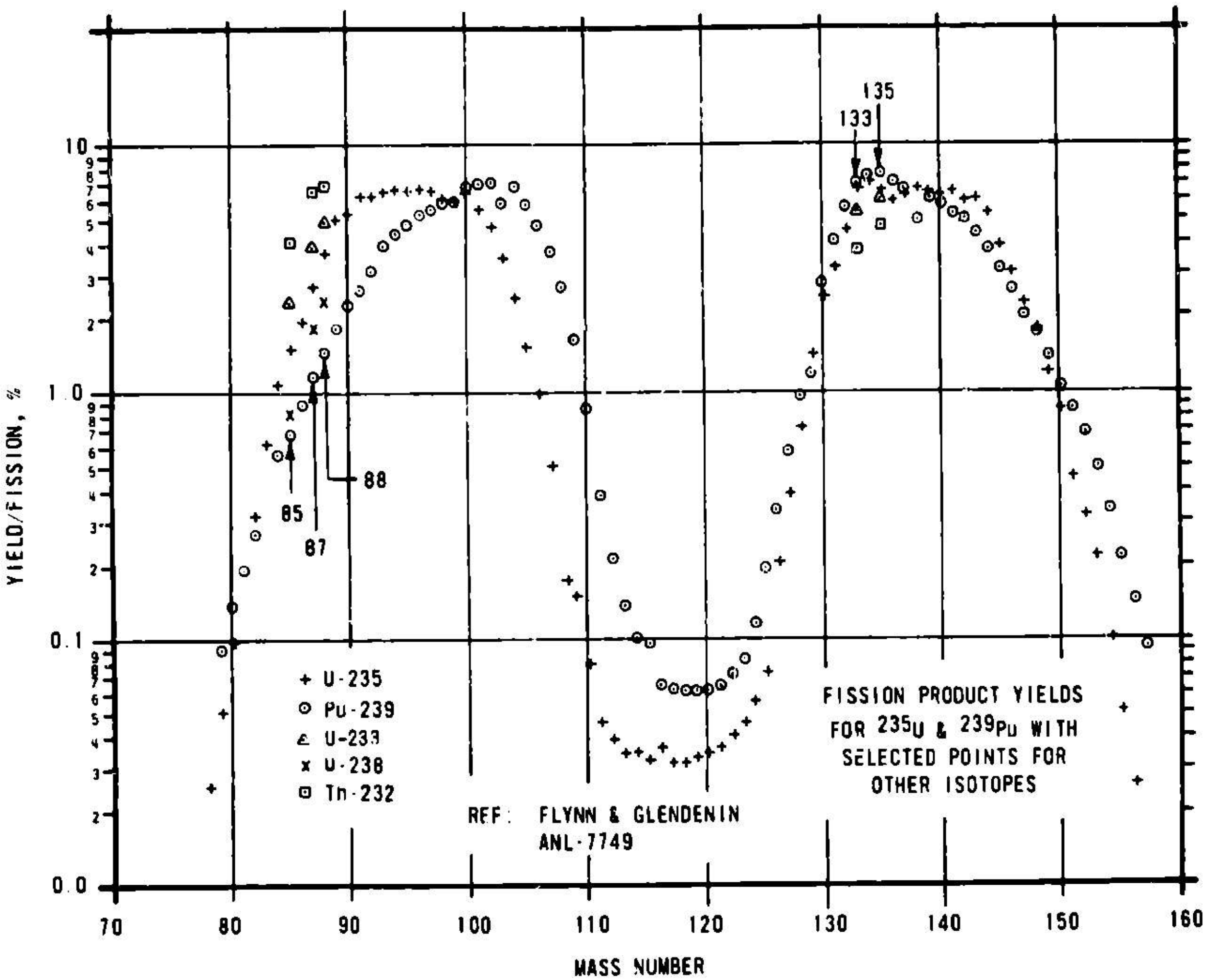

Fig. 19. Fission-product Yields for ^{235}U and ^{239}Pu with Selected Points for Other Isotopes. ANL Neg. No. 103-R5983.

TABLE IV. Fission-product Yields and Ratios of Yields for Certain Noble-gas Species

	Yields, %				
Mass No.	^{232}Th	^{233}U	^{235}U	^{238}U	^{239}Pu
85	4.01	2.35	1.49	0.83	0.67
87	6.57	3.95	2.66	1.93	1.16
88	6.92	4.95	3.63	2.36	1.44
135	4.66	6.1	6.54	6.23	7.54
138	6.85	6.3	6.71	6.1	5.9
Ratios					
85/135	0.86	0.39	0.23	0.13	0.09
87/135	1.41	0.65	0.41	0.31	0.15
88/135	1.48	0.81	0.55	0.38	0.19
88/138	1.01	0.79	0.54	0.39	0.24

count rate under usual conditions. The gamma is 164 keV and is normally obscured by other competing activities with similar energies. However, the abundance of this isotope relative to ^{133}Xe might, under some circumstances, serve to distinguish between a leaker that had been last irradiated three weeks past from one that had been last irradiated, say, one week past. If this possibility exists, it is advisable to inspect the actual spectrum from anomalous levels of ^{131m}Xe.

To an even greater extent, ^{85}Kr normally cannot be monitored. It has an even lower specific activity (10.8-yr half-life) and a very low branching ratio, and the gamma energy (514 keV) is effectively obscured by the positron annihilation gamma at 511 keV. Krypton-85 might, nevertheless, be significant if a high-burnup fuel element leaked soon after it was returned to the reactor in a reconstituted subassembly. Krypton-85 would be the only radioactive noble-gas fission product that would survive the long "rest period" while the subassembly was being reconstituted. Thus, the abundance of ^{85}Kr relative to ^{133}Xe would signal an old element recently returned to the core. So far, neither of these cases has arisen, but they represent possibilities of which we should be aware.

G. Air Monitor

Of the several noble-gas fission products that have been identified in the EBR-II cover gas, the ^{88}Kr-^{88}Rb chain is the only one having the proper combination of yield and half-lives to be detected as particulate in reactor-building air during normal "clean" operation. The ^{88}Rb is born in the air from escaping ^{88}Kr and is captured on the filter, where it is detected by a characteristic 898-keV gamma ray (branching ratio, 0.14).

Under normal operating conditions, the reactor-building air monitor has a low ^{88}Rb count rate, which fluctuates in the neighborhood of 0.05 counts/s. Working backward, we can use this number to estimate the leakage from the reactor cover gas to the air in the building. The measured photopeak efficiency of the germanium-lithium detector is 7×10^{-3}. Thus, there are

$$\frac{\text{counts/s}}{\text{(branching ratio)(eff)}} = \frac{0.050}{(0.14)(0.007)} = 50 \text{ dis/s}$$

on the filter. The airflow through the filter is 5 L/s.

Assuming 100% filter efficiency for the ^{88}Rb (which probably attaches to dust particles while still ionized), this means that there are about ten ^{88}Rb atoms per liter. The es ated volume of air in the reactor building is 1.4×10^7 L, giving ~14 x atoms in the building air volume. The reactor building has a throughpu 1.9×10^5 L of air per minute. Thus the dilution time constant is

$$\lambda_D = \frac{1.9 \times 10^5}{1.4 \times 10^7} = 1.35 \times 10^{-2} \text{ min}^{-1} = 0.81 \text{ hr}^{-1}.$$

Balancing ^{88}Rb input against loss, we have

$$\lambda_{Kr}N_{Kr} = N_{Rb}(\lambda_D + \lambda_{Rb}) = 14 \times 10^7(0.81 + 2.33) \approx 4.4 \times 10^8 \text{ atoms/hr},$$

where N_{Kr} and N_{Rb} are the number of atoms in the reactor-building air of ^{88}Kr and ^{88}Rb, respectively. The value of N_{Kr} is

$$N_{Kr} = \frac{4.4 \times 10^8}{\lambda_{Kr}} = \frac{4.4 \times 10^8}{0.247} = 18 \times 10^8 \text{ atoms}.$$

Balancing ^{88}Kr input against loss, we obtain

$$LN = N_{Kr}(\lambda_D + \lambda_{Kr}) = 18 \times 10^8(0.81 + 0.247) \approx 19 \times 10^8 \text{ atoms/hr},$$

where L is the leak rate from the tank to the building air in L/hr and N is the number of atoms of ^{88}Kr per liter of cover gas.

To obtain L, we first evaluate N. From Table II, the equilibrium concentration of ^{88}Kr in the cover gas is 0.55 nCi/mL = 0.55 μCi/L. Since 0.55 μCi = 0.55 x 3.7 x 10^4 = 2.0 x 10^4 dis/s,

$$\text{number of atoms/L} = \frac{2.0 \times 10^4}{6.87 \times 10^{-5}} = 2.9 \times 10^8 = N$$

and, by substitution, we obtain

$$L = \frac{19 \times 10^8}{2.9 \times 10^8} \approx 6.5 \text{ L/hr}.$$

In an earlier section dealing with the dilution of cover gas, the makeup flow of fresh argon was estimated at 1 L/min. These two numbers are not necessarily contradictory, for two reasons:

1. The larger part of the input replaces cover gas that is supplied to the following instrumentation and discharged to the stack:

   a. Hanford charged-tape monitor ≈ 36 L/hr.

   b. Argonne charged-wire monitor (FGM) ≈ 5 L/hr.

   c. Gas chromatograph ≈ 2 L/hr.

2. The 6.5-L/hr leak rate is based on data obtained while no fuel was being transferred into or out of the tank.

When fuel is transferred, there is evidence of minor leakage of cover gas to the building air. The count rate on the air monitor usually rises to between 0.15 and 0.3 counts/s in the hour or two after a transfer has been completed. Because of the transitory nature of the event and the several time constants involved, it is difficult to make a quantitative estimate. Clearly, however, only a few liters are leaked in a transfer.

The great sensitivity of this system, derived from high-volume sampling in conjunction with high-resolution gamma analysis, is apparent when the count rates are interpreted in terms of the maximum permissible concentrations (MPC's) listed in Ref. 5. For both ^{88}Kr and ^{88}Rb, the MPC's are given as 1 pCi/mL.

Taking the above estimate of 10 atoms/L of ^{88}Rb, we see that the disintegration rate is $10\lambda_{Rb} = 10 \times 6.5 \times 10^{-4} = 6.5 \times 10^{-3}\ s^{-1}/L$, which is $(6.5 \times 10^{-3})/(3.7 \times 10^{-2}) \approx 0.2$ pCi per liter. (Compare with the MPC of 1 pCi per milliliter.)

Thus the system is capable of detecting ^{88}Rb and ^{88}Kr at a concentration almost four orders of magnitude below the MPC. In addition, the high-resolution counting of a specific gamma makes the system essentially free of the effects of inversions or other meteorological conditions, which perturb the usual gross air-monitoring systems.

In December 1972, a leaking gasket allowed an abnormal quantity of cover gas into the reactor building, and the ^{88}Rb count rate rose to about 100 min^{-1}, corresponding to substantially less than 1% of an MPC. The leak was quickly repaired, and the good data derived from the die-away of the concentration substantially confirmed the assumptions of good mixing in the building and the effect of nuclear dilution, as mentioned above.

II. Modified Air Monitor

Although the above system was very successful in detecting the ^{88}Kr-^{88}Rb chain, it did nothing toward detecting abnormal levels of fission-product gas in the room air after the mass-88 chain had decayed. It could not detect high levels of ^{133}Xe and ^{135}Xe, which sometimes result from transferring a leaking subassembly. In July 1974, the lead shield on the air monitor was enlarged to about 0.40 x 0.40 x 0.45 m in internal dimensions, and the blower was used only to move room air through the shield. Thus, in the modified system, the sample is simply the approximately 70 L of room air within the lead shield. The air moves through this space at the rate of one sample volume in ~15 s.

On November 8, 1974, when leaker X180 was removed from the reactor, a substantial amount of ^{133}Xe was released to the air in the reactor building. This was "old" gas from the leaker itself, and the shorter-lived isotopes including ^{135}Xe had largely decayed. Two large grab samples of reactor-building air were taken and counted in the radiochemistry laboratory. The simultaneous count rates on the GLASS air monitor could then be correlated with absolute concentrations of ^{133}Xe. It was found that 1.6 counts/s in the ^{133}Xe peak corresponds to 1 pCi/mL. This conversion factor was confirmed on November 25 and again on December 2, when there were subsequent releases of ^{133}Xe to the building.

On November 22, there was a substantial release of ^{135}Xe, which permitted a firm calibration of the detector sensitivity for that isotope. The results of these correlations are shown in the following table.

Isotope	Detector counts/s for 1 pCi/mL	Maximum Permissible Concentration, pCi/mL	Detector counts/s for 1 MPC	Normal Background, counts/s	Minimum Detectable Fraction of MPC, %
^{133}Xe	1.6	10	16	0.2	<1
^{135}Xe	2.3	4	9	0.1	<1

As the results show, this is a very effective system in detecting the most prevalent noble-gas fission products in the reactor-building air. In addition, it still has the advantage of being insensitive to variations in the natural background resulting from changing meteorological conditions.

So far, this system has been operated as an experiment, but now that utility has been demonstrated, permanent operation is proposed. This will include installing a steel liner in the lead shield; such a liner will reduce the effect of lead X rays which now contribute somewhat to the background level of ^{133}Xe.

VII. RESULTS OBTAINED DURING FISSION-PRODUCT RELEASE

Since GLASS came into effective operation, there have been 11 leakers in EBR-II. They are summarized in Table V. Note that, for each release (and for each of the seven isotopes analyzed), there is estimated and tabulated a "normalized excursion amplitude" (signal + tramp background)/(tramp background). These seven ratios are an important part of the leaker's "fingerprint." It should be emphasized that the various isotopes peak at different times; the excursion amplitudes are rough estimates scaled from the graphs.

A. Subassembly X083A (September 25, 1972)[6]

Fuel element No. 38 of X083A contained a normal Mark-IA driver-fuel pin of 52%-enriched uranium metal. This fuel was being irradiated experimentally well beyond the normal burnup limit. Subsequent examination revealed that a microscopic leak had occurred about 4 in. (102 mm) below the top of the fuel pin. At this burnup, the fuel had swelled into contact with the cladding, restricting the leak. From the relatively small release of fission products (~1% based on ^{133}Xe), it appears that only the material near the hole was leaked, despite an estimated 2000-psi (13.8 MPa) pressure in the plenum.

The data obtained during this release are shown in Fig. 20. The curves for the shorter-lived isotopes (^{135m}Xe, ^{138}Xe, and ^{87}Kr) show that after the first release, there were several small bubbles. The humps on these curves are confirmed by inflections in the curves for the longer-lived species. After the reactor was shut down, there was some further growth in ^{133}Xe activity, probably because of continued diffusion from the sodium to the cover gas.

The behavior of ^{135m}Xe is of considerable significance. In contrast to all other isotopes involved, its half-life (~15 min) is much shorter than the half-life (6.7 hr) of the precursor (^{135}I). After each bubble, the ^{135m}Xe died away relatively rapidly; this indicates that at least some of it had leaked from the element as the gas and not as the iodine precursor. However, the presence of extraneous ^{135}I in the sodium was verified after the reactor was shut down. About 1630 hours on September 25, the primary pumps were shut off. The ^{135m}Xe died away rapidly until the pumps were restarted, whereupon it rose quickly by a factor of ~3, indicating an in-growth of ^{135m}Xe while the pumps were shut down. This could only occur if there was extra ^{135}I in the sodium (i.e., over and above that due to tramp fissions). On the other hand, there was no surge in ^{135}Xe activity as would have occurred if the pump shutdown had stimulated extrusion of more bond sodium. This off-on pump operation has in the past been used to diagnose "bottom leakers."

Subsequently, the loss of bond sodium was confirmed by radiochemical analysis, which found a small amount of anomalous ^{131}I in the bulk-sodium sample. Also, the postirradiation examination of the failed pin showed measurable bond loss.

TABLE V. Summary of Leakers for Which GLASS Data Were Recorded

Date	Reactor Run	Subassembly Number	Type of Fuel	Approximate Peak Burnup, %	Normalized Excursion Amplitude (NEA)[a] ^{133}Xe	^{135}Xe	^{85m}Kr	^{88}Kr	^{87}Kr	^{138}Xe	^{135m}Xe	Remarks
9/25/72	58A	X083A	Mark-IA metal driver, Na-bonded, 52% enriched.	3.3	350	85	45	30	30	15	60	Leak located 102 mm below top of fuel, limited Na loss due to swollen fuel.
3/13/73	62A	X084A	Mixed-oxide experiment, 20% PuO_2-80% UO_2, U 93% enriched.	18	20 10^4	10 1,000	5.5 350	3.3 150	4 130	3 50?	10 200	Burped first. Leak suspected 51 mm below top of fuel; 2-g weight loss.
9/16/73 10/23/73	65A 66F	X168A	Mark-IA metal driver, Na-bonded, 52% enriched.	2.6	250	60	45	35	30	15	25	Leak located 102 mm below top of fuel, limited Na loss due to swollen fuel.
9/19/73	65C	X114	Mixed-oxide experiment, 25% PuO_2-75% UO_2, U 93% enriched.	14	200 1,200	40 350	30 220	20 130	25 200	20 200	80 1,000	Two separate signals, a small initial leak followed by a large one requiring shutdown; 1.3-g weight loss. No indication to date of leak location.
10/03/73	66B				10	6	30	24	27	20	15	
11/26/73	67A	X186	Mixed-oxide experiment, 25% PuO_2-75% UO_2, U 93% enriched.	4.1	4 1,000	3 350	3 200	2.2 130	2.5 170	5 120	20 600	Burped first. Leak suspected 51 mm below top of fuel, 0.3-g weight loss.
12/13/73	67B	X191	Mixed-oxide experiment, 25% PuO_2-75% UO_2, U 93% enriched.	4.6	9 1,000	6 600	5 450	4 300	6 500	6 500	35 2,500	Burped first. Leak suspected at top of fuel 0.4-g weight loss.
12/21/73	68A	X193	Mixed-oxide experiment, 25% PuO_2-75% UO_2, U 65% enriched.	6.8	1,000	800	500	300	400	300	1,200	No indication of leak location to date, 0.5-g weight loss.
12/28/73	68D	X156	Mixed-carbide experiment, 15% PuC-85% U, U 93% enriched Na-bonded.	3.4	10	6	1.5	1	1	1	10	Very high gas retention characteristic of carbides, 3.6-g weight loss corresponding to practically entire Na inventory.
10/25/74	74A	X180	Mark-II metal fuel, Na-bonded 64% enriched.	9.5	55 270	13 60	10 50	10 50	8 40	6 30	7 40	
11/22/74	74F	X116B	Mixed-oxide experiment, 25% PuO_2-75% UO_2, U 93% enriched.	16.1	1,260	816	620	475	670	880	3,300	
12/27/74	75A	X213	Mixed-oxide experiment, 25% PuO_2-75% UO_2, U 93% enriched.	8.2	12,000	1,140	1,450	950	1,180	3,400?	16,000?	Unusually sudden release, entrained delayed-neutron precursors and large quantities of ^{135m}Xe to ^{138}Xe.

[a]NEA = (signal - background)/background.

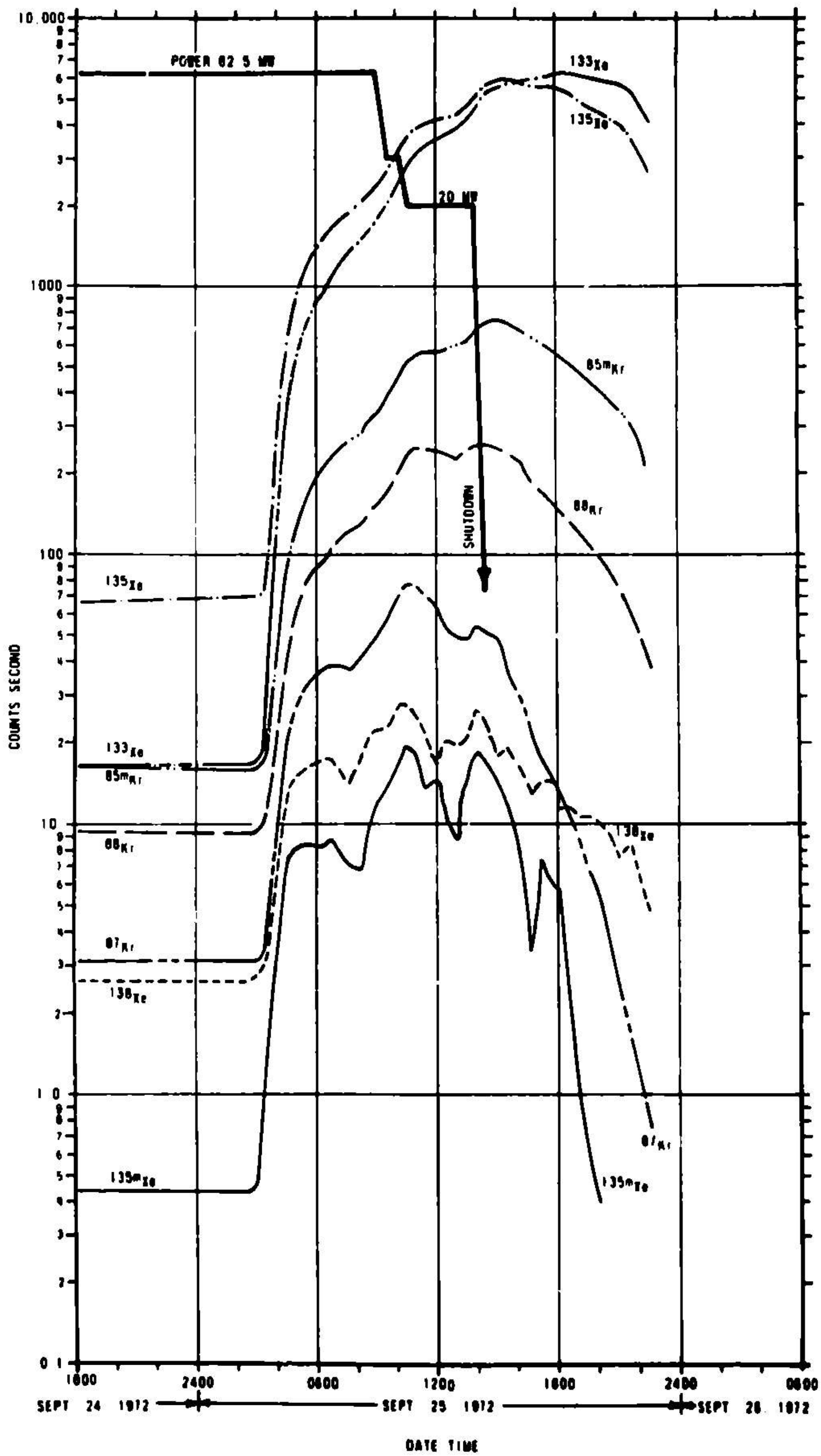

Fig. 20. GLASS Data for Run 58A (Leaker was Element 38 of Subassembly X083A). ANL Neg. No. 103-R5991.

The data shown for ^{138}Xe are poor and reflect the difficulty of detecting the weak 258.6-keV peak in the presence of a high concentration of ^{135}Xe (249.7 keV).

B. Subassembly X084A (March 14, 1973)[7]

This was the largest release so far encountered (Fig. 21). Subassembly X084A was a mixed-oxide helium-bonded experiment at ~18% burnup. In this case, the main release was preceded by a smaller one, as clearly indicated by the shorter-lived isotopes. The figure also indicated the difficulty of resolving ^{138}Xe (tramp count rate ≃ 1.6 s^{-1}) at 258.2 keV (see also Fig. 6). At 249.6 keV, ^{135}Xe has a tramp count rate of ~80 s^{-1} or about 50 times as great. During an excursion such as this, the ^{135}Xe exceeds the ^{138}Xe by two to three orders of magnitude. This overwhelming disparity, combined with reduced resolution due to high count rate, leads to poor results for ^{138}Xe. More recent experience suggests that our techniques have improved and that ^{138}Xe is now being analyzed better than shown here.

For some 18 hr after the reactor was shut down, the fuel element continued to leak. This is evident from the data for ^{133}Xe and ^{135}Xe. Note also that ^{135m}Xe continued to be evolved from the ^{135}I in the fuel. The sudden downturn in the data at 1800 hours on March 14 was due to initiation of purging with clean argon.

Subsequent radiochemical analysis for ^{137}Cs and ^{131}I found only normal levels of these two isotopes. This indicated that no fuel was in contact with the sodium coolant and that essentially all fission products escaped as gases. Postirradiation examination revealed the leaking element to be No. D-5 with a leak suspected ~51 mm below the top of the fuel column.

C. Subassembly X168A (September 6, 1973)[7]

Subassembly X168A was a run-to-failure test of Mark-IA metallic driver fuel. The plot of GLASS data is shown in Fig. 22. Compared with the preceding case, this is a relatively minor release, even less than from the similar X083A.

At about 0100 hours on September 6, all isotopes began to increase at similar rates, indicating a gas release. Some 3 hrs later, the rate of release quickly decreased, but gas continued to escape from the fuel element until the reactor was shut down shortly before 2400 hours. Note that the apparent ramp characteristic between 0500 and shutdown is deceptive. The data are presented on a semilogarithmic plot and actually represent an accelerating rate of increase. For the shorter-lived isotopes, this increase has to overcome the quantitatively increasing rate of decay as larger and larger concentrations exist in the primary system.

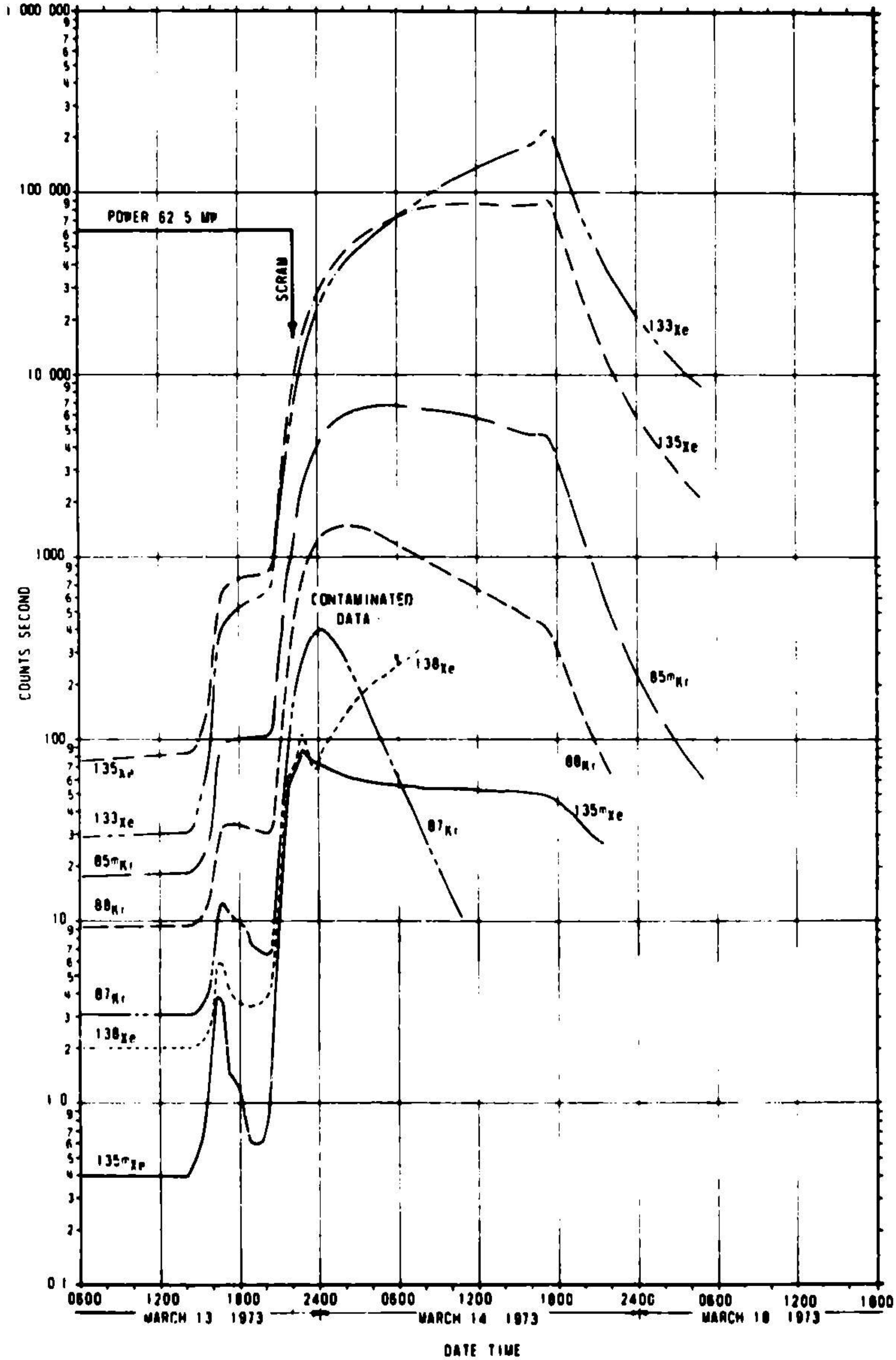

Fig. 21. GLASS Data for Run 62A (Leaker was Element D-5 of Subassembly X084A). ANL Neg. No. 103-S5868.

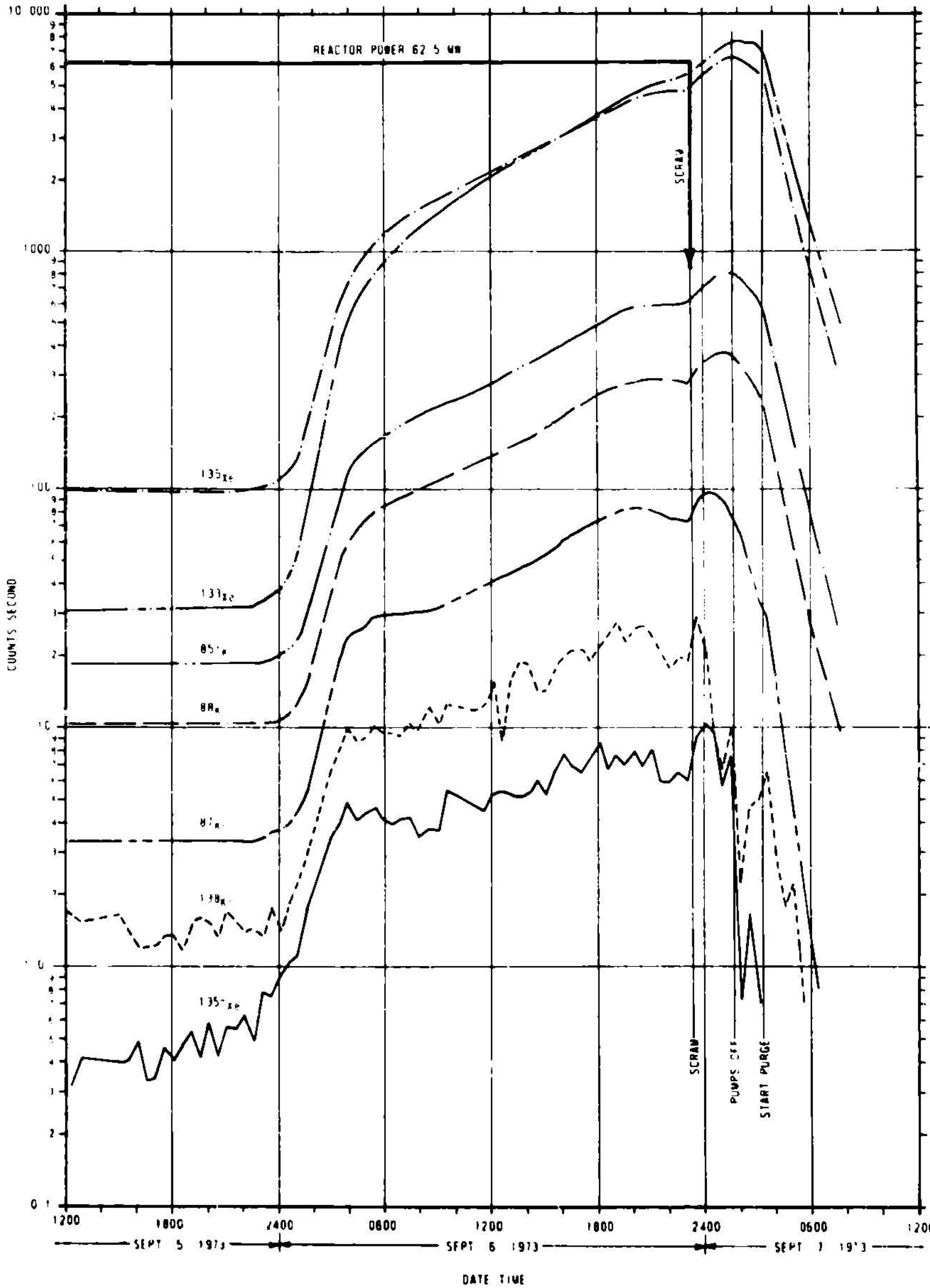

Fig. 22. GLASS Data for Run 65A (Leaker was Element 14 of Subassembly X108A). ANL Neg. No. 103-S5001.

Figure 20 shows that the activity level for ^{135m}Xe went up by a factor of ~2 before other isotopes showed any credible increase. This is a good indication that bond sodium is being extruded, carrying with it the precursor ^{135}I. Subsequent analysis showed that substantial ^{131}I was present in the sodium, confirming that bond sodium had been extruded. As a result of the short half-life of ^{135m}Xe (15.65 months), such bond leaks are signaled fairly quickly. Obviously, ^{135}Xe is also produced and in greater quantities, but its half-life (9.14 hr) prevents an earlier indication. Despite the very low background signal level (~0.3 counts/s) and resulting poor statistics, ^{135m}Xe is one of the most interesting of the detectable isotopes. It differs radically from the others in that its half-life is far shorter than that of its precursor.

Subassembly X168A was one of the four prime suspects that were removed from the reactor after the release of September 6, 1973. After four days of operation without any indication of a leaker, the reactor was shut down; and the other three suspects, among which was X114, were returned to the core. The reactor then operated for about three days before fission products were again detected in the cover gas. As was eventually determined, these came from X114, which unfortunately began leaking just about the time that X168A could have been confirmed as the September 6 leaker. Subassembly X114 completely confused the issue, and it was some weeks before both leakers were definitely identified and removed. Figure 23 is a schematic history of the search for these two leakers.

After X114 had been identified as the September 19 leaker as detailed in the following section, X168A was returned to the reactor with the results shown in Fig. 24. The reactor started up October 19 and operated at full power until October 23.

The activity levels on October 20, 21, and 22 were not considered significantly high, although in retrospect it can be seen that ^{135}Xe and ^{135m}Xe were rather stable at about twice normal levels. Other activities were slightly above normal, and the deviation appeared to be closely related to half-life. This situation could be interpreted as resulting from oozing sodium with ^{135}I entrained and to a lesser extent from krypton isotopes whose probabilities of escape were dependent on their relative half-lives.

On October 23, a small but significant release occurred. Apparently, it had taken this long for pressure to build up enough to start the leak, and the leak appeared to be gas rather than bond. Some control-rod juggling was undertaken (X168 was next to control rod No. 5), but the results were inconclusive. Subassembly X168A was removed from the reactor, and subsequent "clean" operation confirmed that it was the leaker sought.

D. Subassembly X114 (September 19, 1973)[8]

Subassembly X114 was a mixed-oxide-fuel experiment with ~14% peak burnup. The first release was a minor bubble at about 0030 hours on

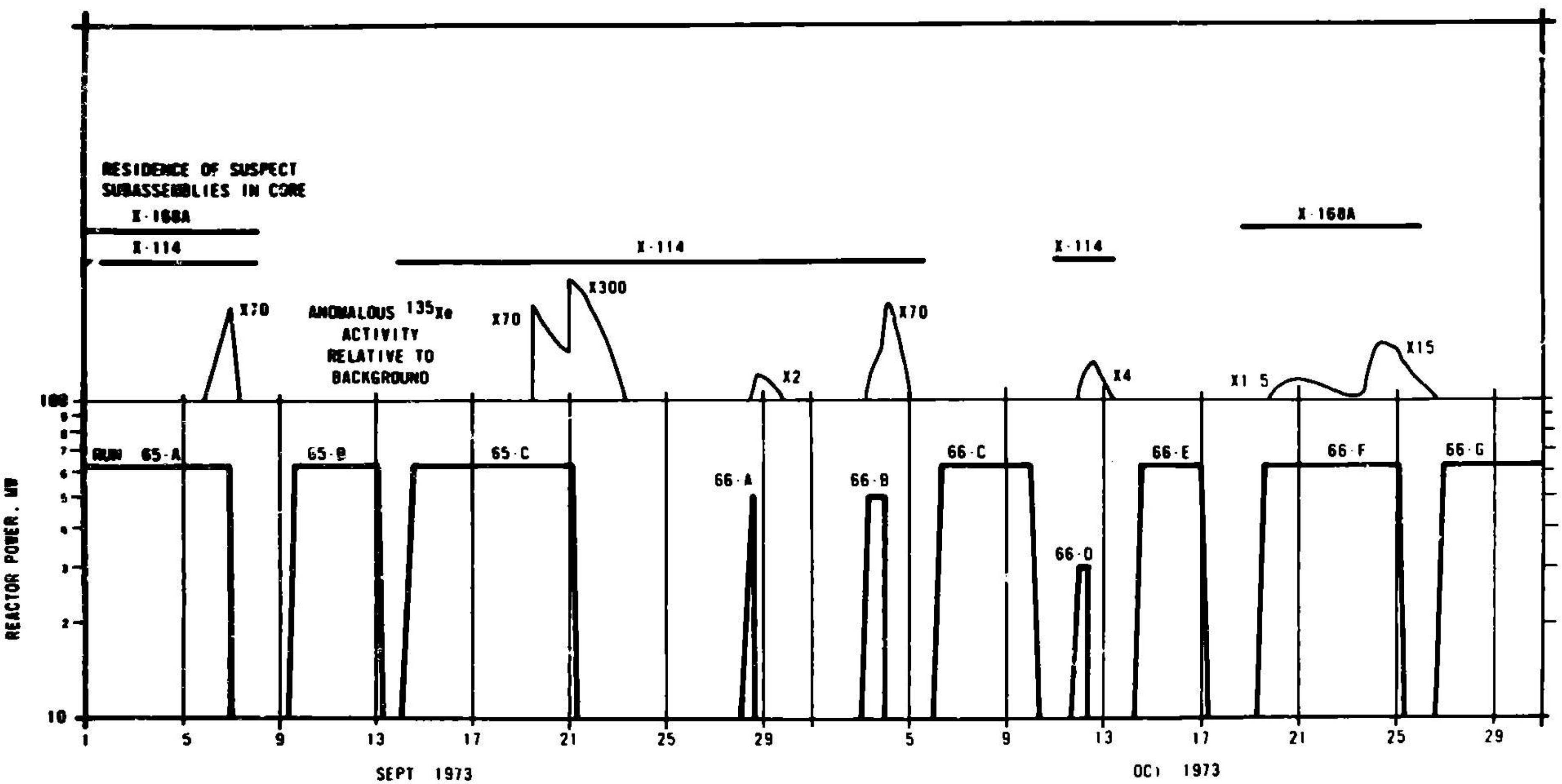

Fig. 23. Schematic History of Search for Leakers during September–October 1973. ANL Neg. No. 103-R5986.

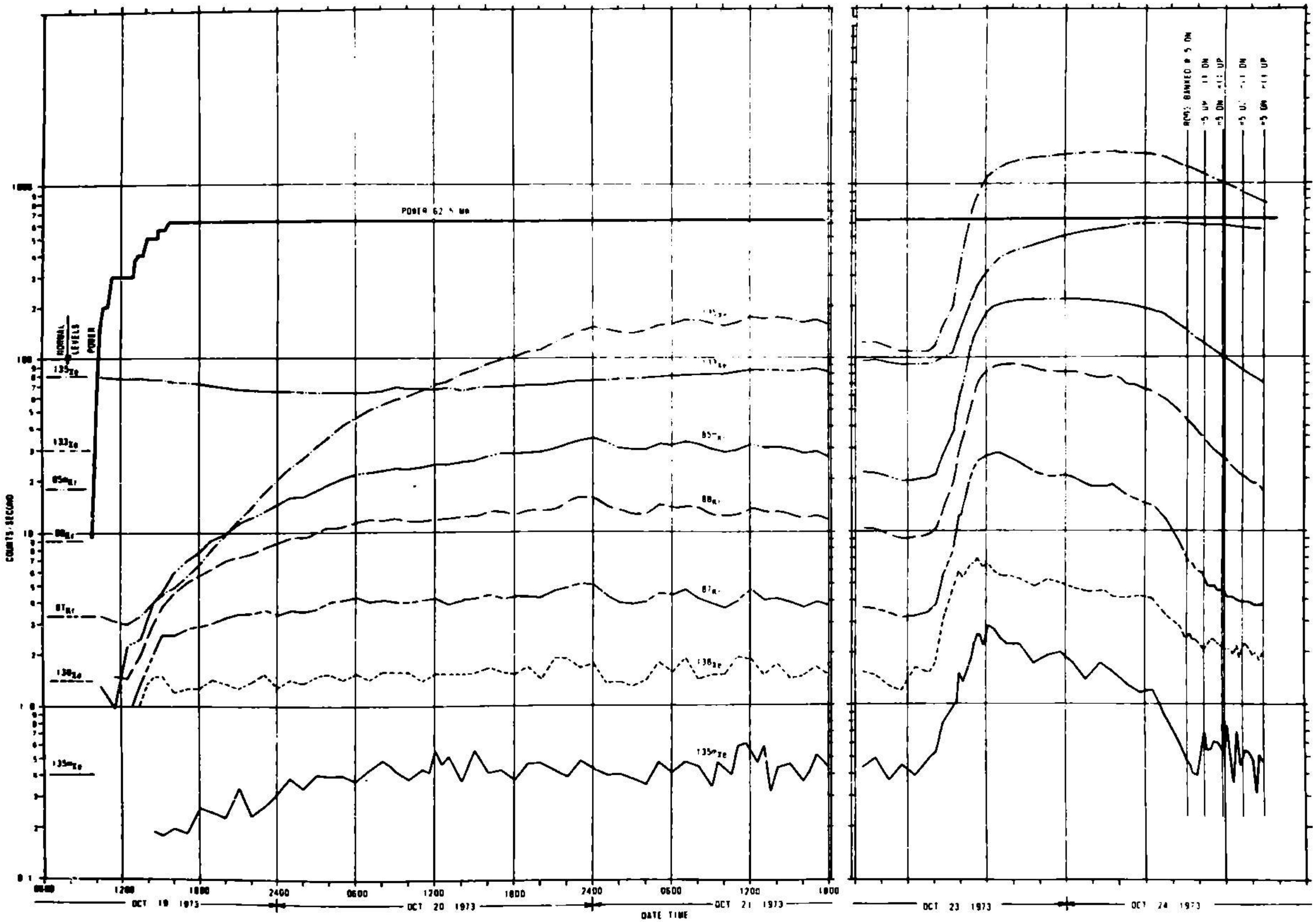

Fig. 24. GLASS Data for Run 66F (Leaker was Element 14 of Subassembly X168A). ANL Neg. No. 103-R5998.

September 18 with signal amplitude less than 10 times background. Beginning in the afternoon of September 19, there was a series of at least three bubble releases of decreasing amplitude, as shown in Fig. 25. Operations continued until early on September 21, when a much larger release caused the reactor to be shut down.

At 0425 hours, the primary pumps were turned off for about half an hour in an attempt to test for a bottom bond leaker, as mentioned earlier in connection with X083A. The ^{135m}Xe activity responded by dipping briefly as the concentration in the cover gas died out without replenishment by diffusion from the sodium. When the pumps came on again, the ^{135m}Xe concentration returned to about the original level. Beginning at about 0540 hours, the pumps were down for about 5 hrs, during which the ^{135m}Xe level decreased markedly (by a factor of ~50). When the pumps were again started, the count rate returned to about what it would have been if the effective decay half-life had been 6.6 hr (^{135}I) during the entire period.

Note that the observation of the 6.6-hr half-life does not necessarily indicate that ^{135}I has leaked into the sodium. It might merely mean that the fuel was still communicating with the primary sodium and leaking gaseous ^{135m}Xe as it evolved from the ^{135}I existing in the fuel. In this case, radiochemical analysis for ^{131}I in the sodium indicated that only a very small amount of iodine had escaped from the cladding. This is to be expected from helium-bonded oxide fuel. On the other hand, if ^{135m}Xe does not exhibit the 6.6-hr half-life (pumps being left on), it is conclusive evidence that no sodium bond or other nongaseous material has leaked from the fuel element.

The continuing leakage from the fuel element is confirmed by the generally upward trend of ^{133}Xe after the scram. The dip in ^{133}Xe activity between 0600 and 1100 hours can be disregarded. It was due to the pumps being shut down. At about 1230 hours, a purge at ~1.3 cfh (36.8 L/hr) was begun to reduce activity prior to fuel handling, and all activities responded. At 1815 hours, the purge rate was increased to 3 cfh (85 L/hr). Note that purging had little effect on ^{135m}Xe due to its short time constant, whereas other activities were markedly reduced by the purge.

Several suspects were removed, and the reactor was started on September 28. After a short time, it was apparent that the leaker was still in the core. The reactor was shut down for other reasons, and while it was down, five more suspects were removed.

Run 66B, loaded as shown in Fig. 26, began on October 3. Subassembly X114 was in position 6C5. The short-lived fission gases exceeded their normal background levels about the time the reactor reached 50 MW (see Fig. 27). The reactor was leveled at 50 MW, and an attempt was made to determine the general location of the leakers by juggling control rods. The difficulty with this technique is that two rods must be moved at one time to

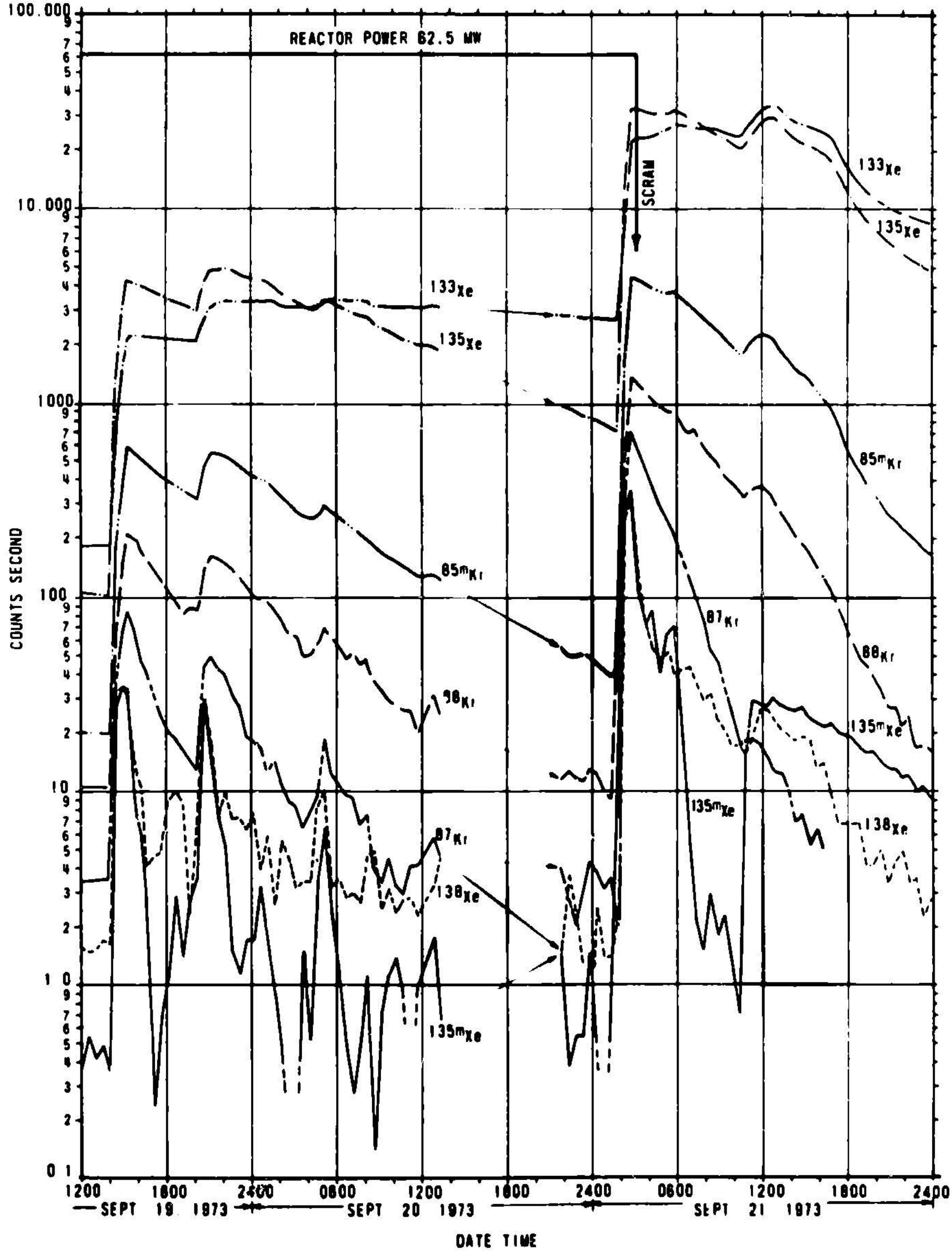

Fig. 25. GLASS Data for Run 65C (Leaker was Element S-1 of Subassembly X114). ANL Neg. No. 103-S5867.

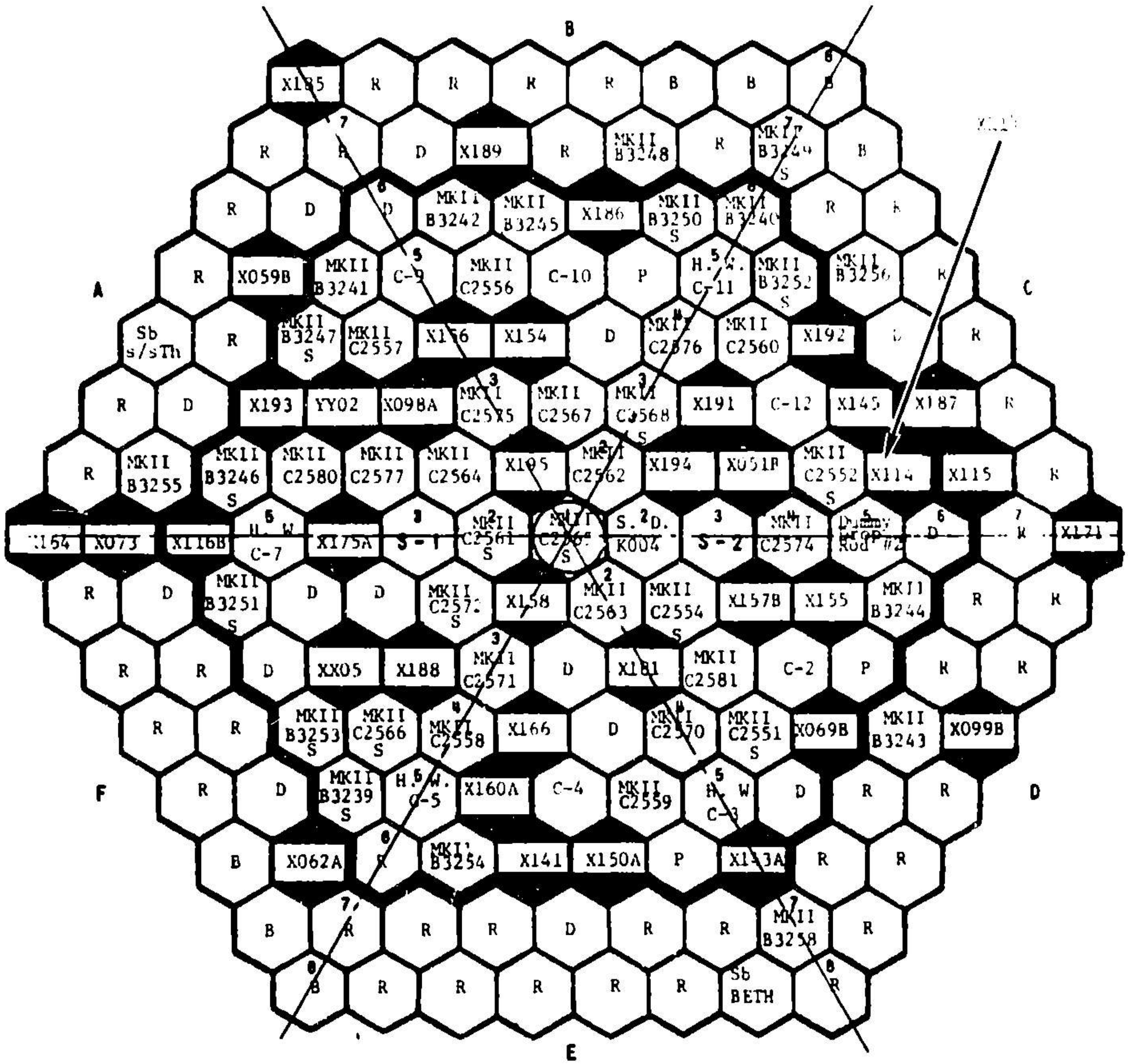

KEY:

D - STANDARD DRIVER
B - DEPLETED URANIUM
P - PARTIAL
MK-II - MK-II FUEL
R - SST REFLECTOR

H.W. - High Worth Control Rod
S.D. - Structural Dummy

Fig. 26. EBR-II Loading Diagram for Run 66B

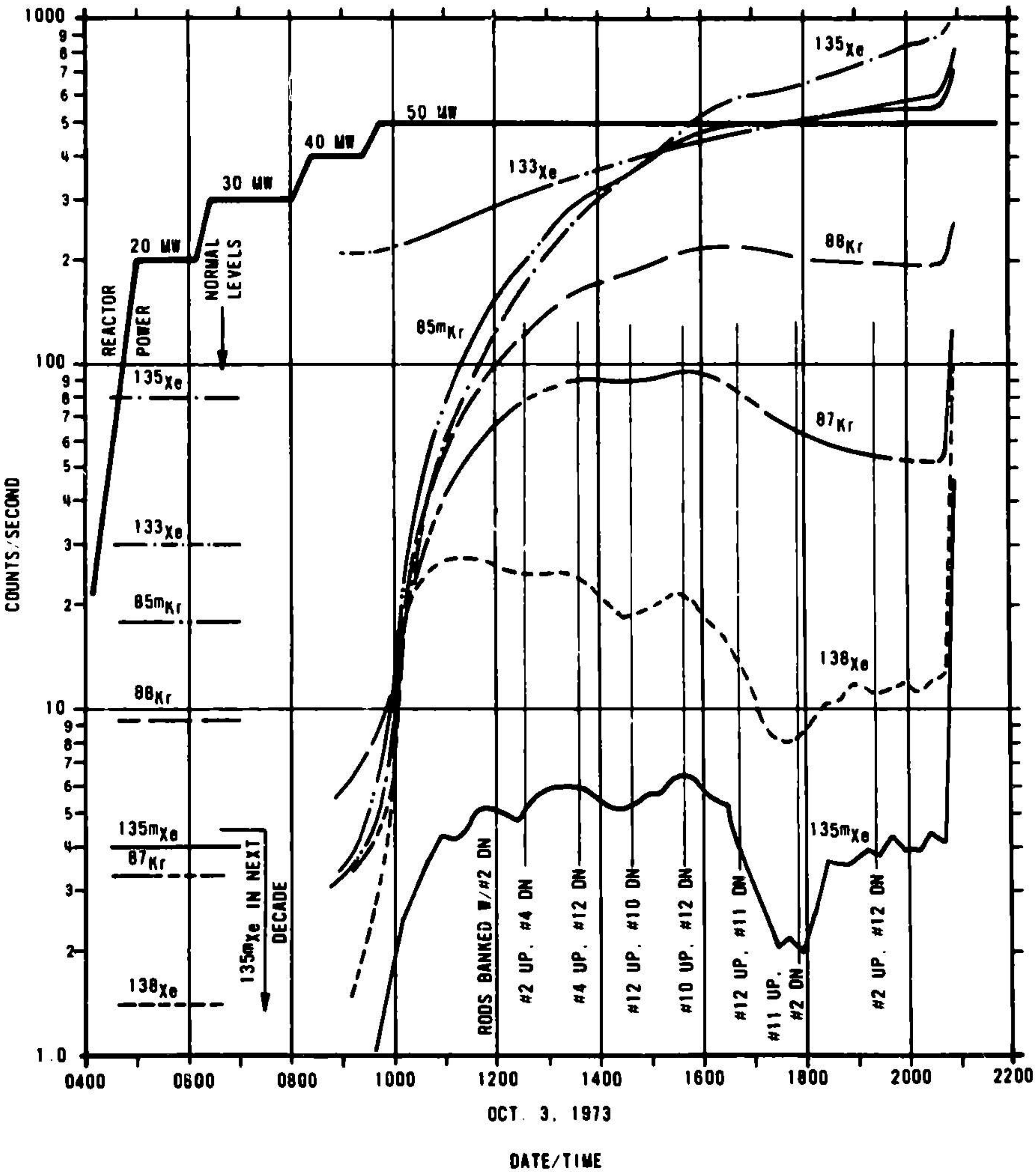

Fig. 27. GLASS Data for Run 66B during Search for Leaker (Element S-1 of Subassembly X114). ANL Neg. No. 103-R5999.

maintain reactivity (and stable power). The leak source must also remain reasonably constant. On this occasion the results were inconclusive, and the reactor was shut down when the activity "took off" at about 2100 hours.

In retrospect (after identification of X114 as the leaker), it is possible to find a weak correlation between the movements of control rod No. 12 (position 5C3) and the activity levels of ^{138}Xe and ^{135m}Xe. The effort was ended by an apparent plugging of the leak at about 1630 hours. From the loading diagram (Fig. 26), it is seen that X114 was a near but not immediate neighbor of control rod No. 12. Subassembly X114 was next to the control rod No. 1 position, which was occupied by a low-worth drop rod of no use in this respect.

For the following run, several suspects including X114 were removed from the core, and the reactor was operated at full power for ~4 days without any indication of a leaker. Thereupon, the reactor was shut down and the most likely suspects were loaded back in the core--insofar as possible, next to high-worth control rods (see Fig. 28). Because of their ^{10}B followers, these could be used to cause the maximum local perturbation. Subassembly X114 was immediately adjacent to control rod No. 7. The reactor was started up at about 2100 hours on October 11, and anomalous fission-product levels were apparent when the reactor reached 31 MW. Thereupon, the reactor was leveled at that power and control-rod juggling began (Fig. 29). Beginning at about 0400 hours, ^{138}Xe and ^{135m}Xe (to a lesser extent ^{87}Kr) followed control rod No. 7 through two updown cycles, and it was considered highly probable that X114 was the leaker. We intended to continue juggling with other control rods to test other suspects. However, the leak apparently plugged up at about 0730 hours, and there was no use continuing. The reactor was shut down, and only X114 was removed from the core. Subsequently, "clean" operation during run 66E confirmed that X114 was in fact the September 19 leaker. With X114 removed, X168A was returned to the reactor for confirmation as the September 6 leaker. This was discussed in the preceding section.

Although the rod juggling was successful in this case, it is evident that this was a fortuitous case in which the leaker happened to be checked during the few hours that the leak remained reasonably constant.

E. Subassembly X186 (November 26, 1973)[9]

Subassembly X186 was a helium-bonded mixed-oxide fuel experiment with 19 elements at ~4.1% peak burnup. There was a small "burp" at about 1400 hours on November 26 and another larger one at about 1600 hours, followed by a substantial release (see Fig. 30). The maximum excursion amplitude was about 1000 times in the case of ^{133}Xe. Subassembly X186 resembled X114 both in the amplitude of the release and in the relatively higher abundance of the shorter-lived isotopes in comparison with X084A. There was an indication of a small amount of ^{131}I in the primary sodium, the additional activity amounting to only about two times tramp.

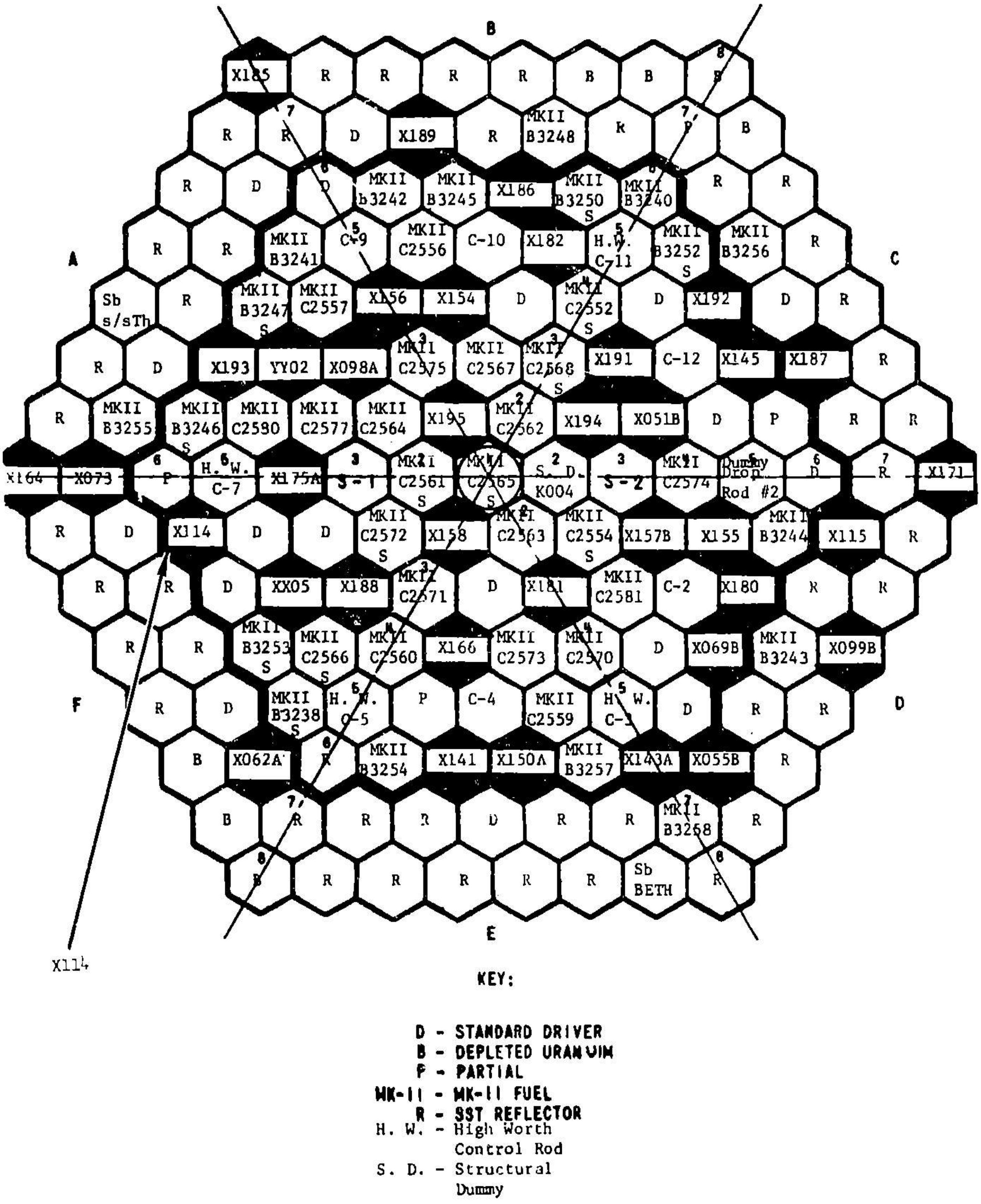

Fig. 28. Loading Diagram for Run 66D

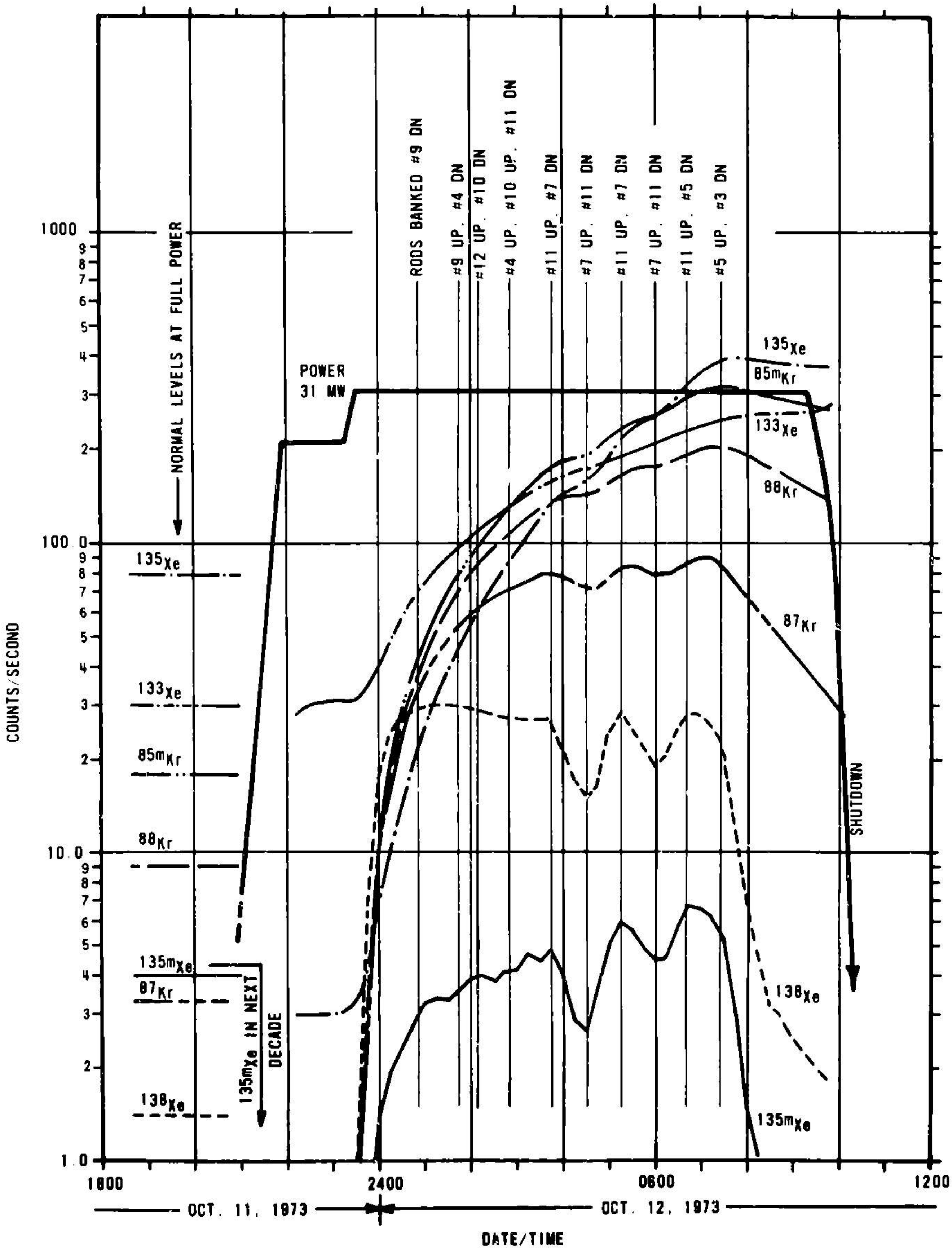

Fig. 29. GLASS Data for Run 66D during Search for Leaker (Element S-1 of Subassembly X114). ANL Neg. No. 103-R5988.

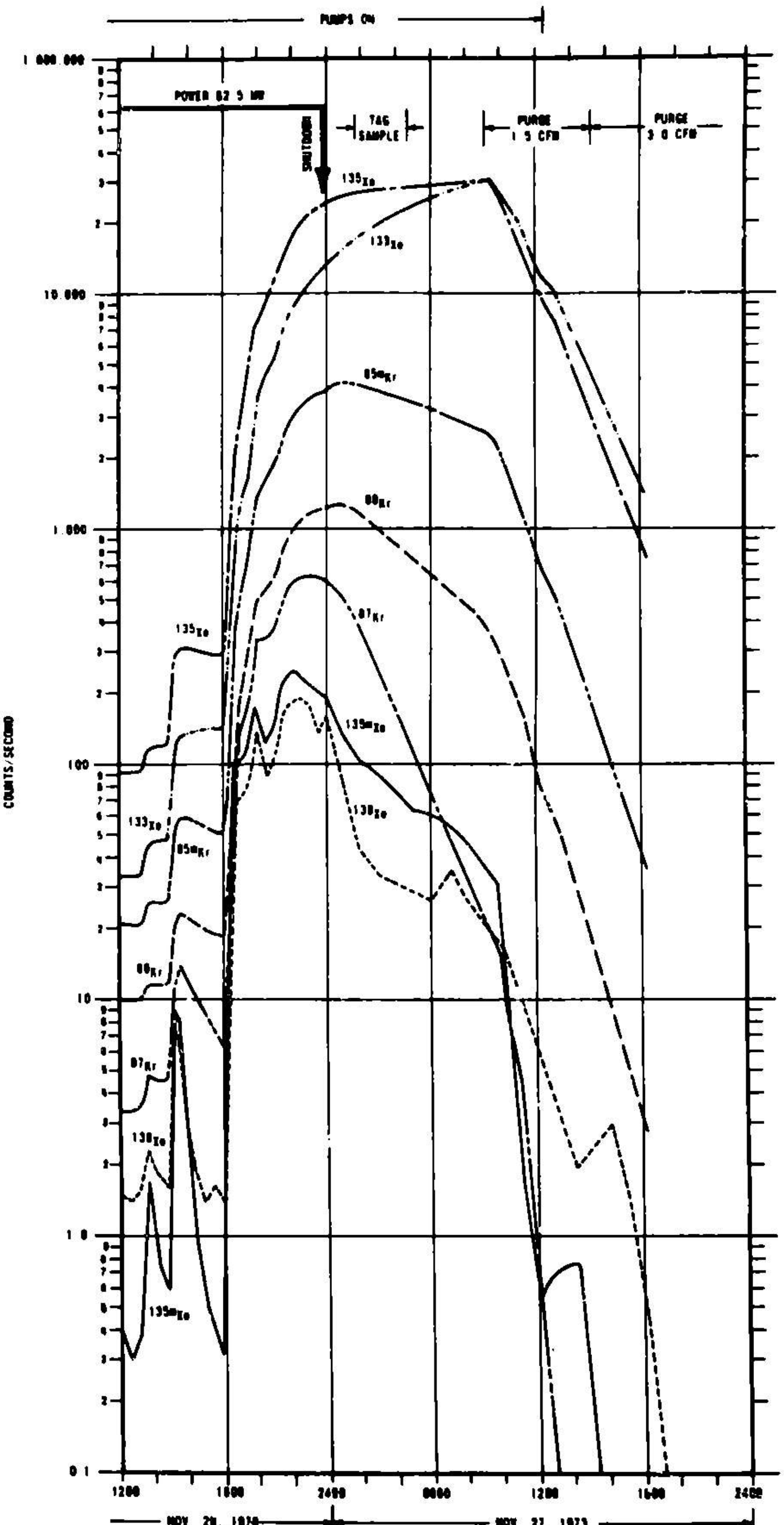

Fig. 30. GLASS Data for Run 67A (Leaker was Element P12A-63K of Subassembly X186). ANL Neg. No. 103-S5137.

After the reactor was shut down at about 2400 hours, gas continued to escape from the leaking element, as shown by increasing ^{133}Xe concentrations. This was supported by the slow decay of ^{135m}Xe, due to the in-growth from ^{135}I. Essentially all the ^{135}I remained inside the element, as indicated by the above result for ^{131}I.

Subassembly X186 was identified as the leaker by xenon tag and was removed immediately. Subsequently, examination revealed a probable leak about 51 mm below the top of the fuel column in element P12A-63K. The measured weight loss in this element was ~0.3 g.

F. Subassembly X191 (December 13, 1973)[10]

Subassembly X191 was similar to X186, and it leaked at a similar peak burnup (4.6%). It also "burped" before the major release occurred (Fig. 31). The burp was somewhat richer, relatively, in the short-lived isotopes than was the main release. This was also true of X186 and probably represents a real effect. The burp appears to carry material largely from near the site of the leak, but the main release represents channeling of high-pressure gas from the plenum, in which the longer-lived isotopes are enhanced by the time required for diffusion from the fuel. The amplitude of the release activity was similar to that of X186 and X114.

The leaking subassembly was identified by xenon-tag analysis and was removed without delay. The defective element N-122 had a weight loss of ~0.4 g.

G. Subassembly X193 (December 21, 1973)[10]

This leaker was a mixed-oxide subassembly, similar to the two preceding ones, except that it was at a somewhat higher burnup (6.8%). It resulted in similar excursion amplitudes for the various isotopes, but was not preceded by a burp (Fig. 32). After the reactor was scrammed at about 2000 hours on December 21, a tag sample was taken during the interval shown (~3 hr), and then a purge was begun so that the activity could be reduced to a level that would permit fuel handling. Note that the 1000-fold increase shown for X193 in Table V is based on the usual tramp background rather than the existing high level due to X191 which leaked a few days earlier. The ^{131}I level in the sodium increased to about five times normal background, although the mechanism of leakage is not clear.

At about 1000 hours on December 22, an interesting thing occurred. Assembly X191, which had been in the fuel storage basket since December 15, "burped," resulting in about a 20-fold increase in the already elevated ^{133}Xe activity. This bubble definitely came from X191, since it would have contained far more ^{135}Xe had it come from X193.

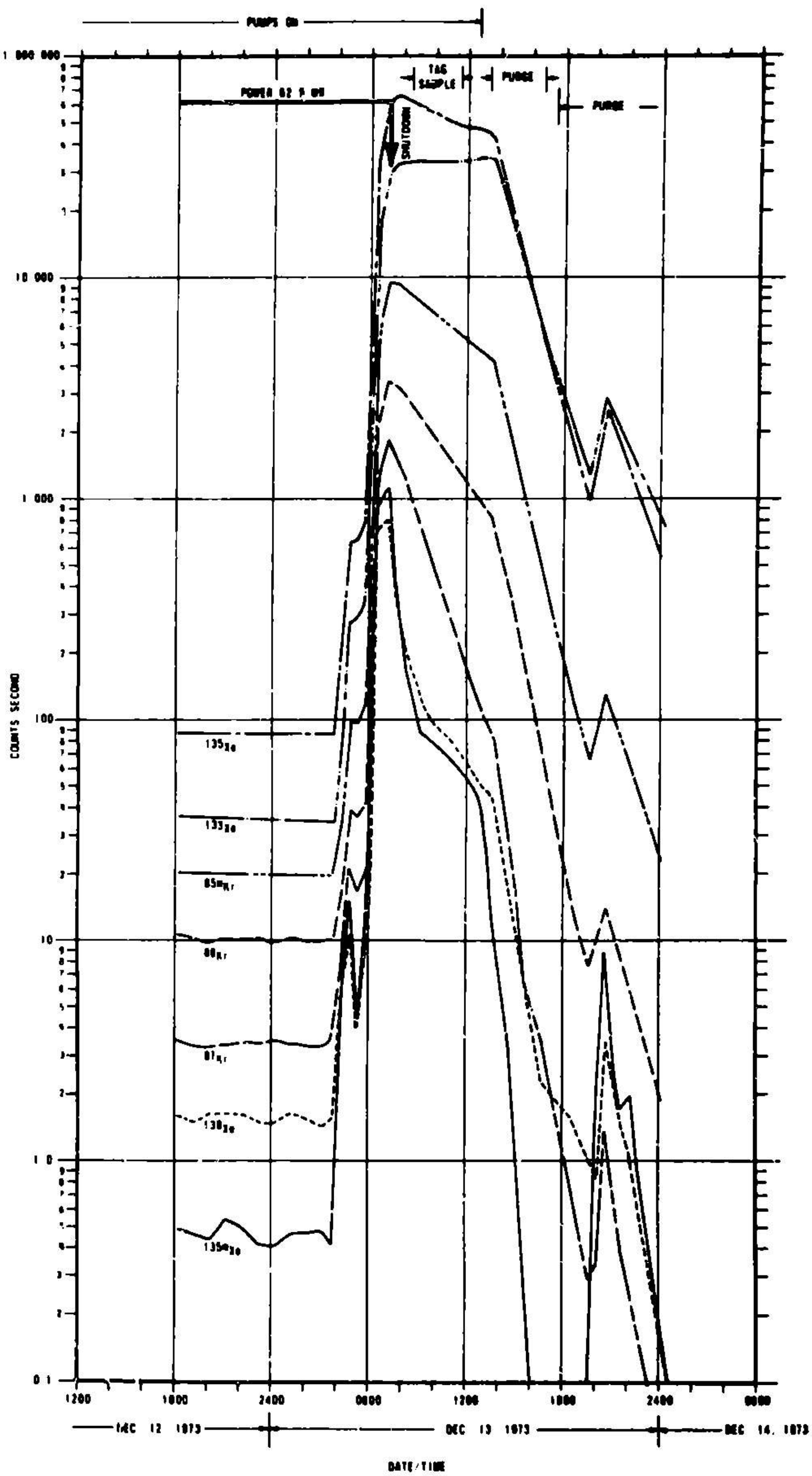

Fig. 31. GLASS Data for Run 67B (Leaker was Element N-122 of Subassembly X191). ANL Neg. No. 103-S5136.

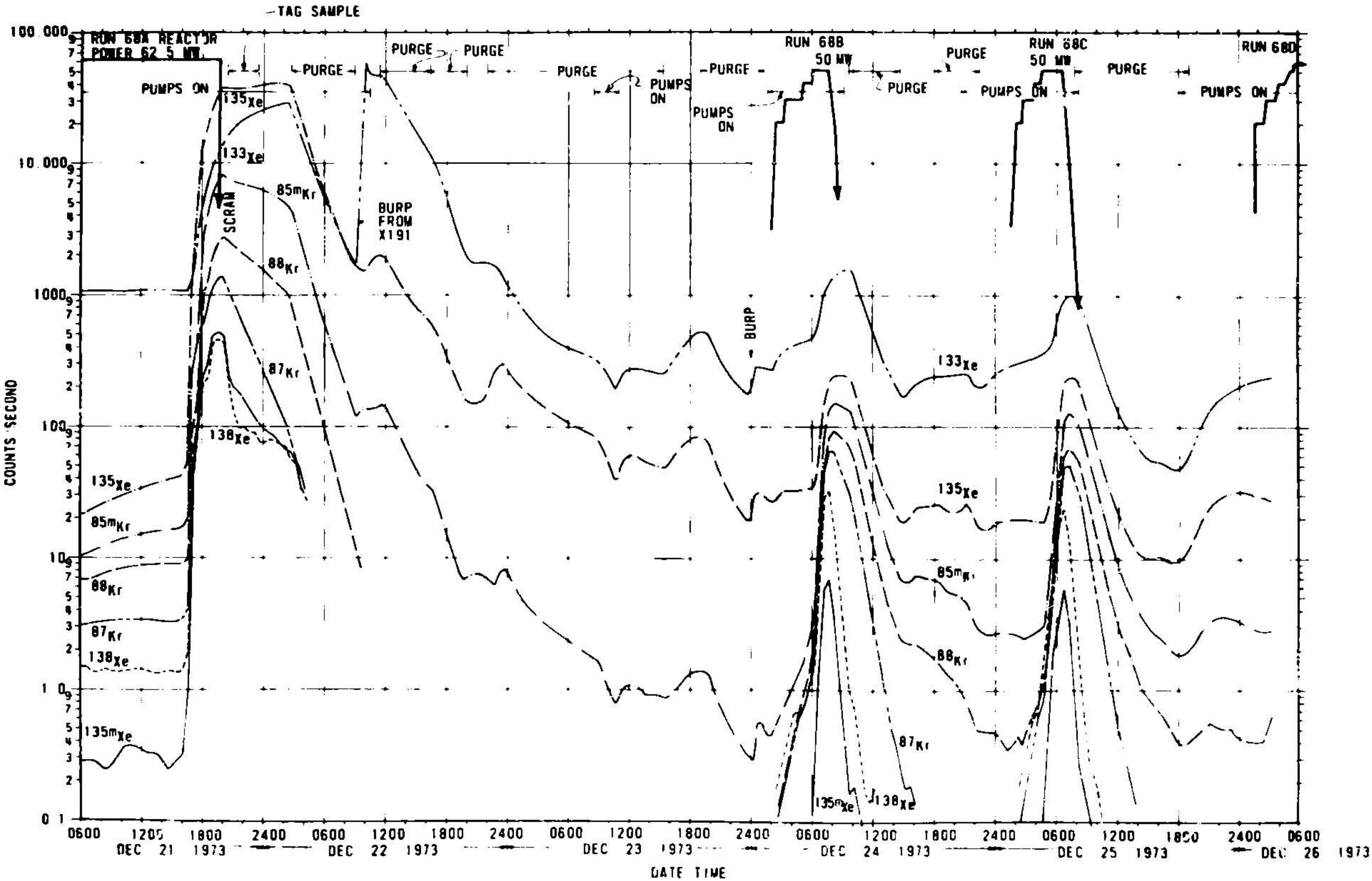

Fig. 32. GLASS Data for Runs 68A–68C (Leaker was Element PNL10-14 of Subassembly X193). ANL Neg. No. 103-S5869.

A xenon-tag sample was taken late on December 21, but in this case the tag indicated X069B as the most likely suspect. This subassembly was removed and the reactor was restarted early on December 24. Short-lived activities indicating the leaker was still in the core were apparent before the reactor reached 50 MW. The reactor was shut down to remove the next most likely suspect, X192, and return X069B to the core. Operations began early on December 25, and again it was apparent that the leaker was still in the core before the reactor reached 50 MW.

The reactor was shut down, and both X193 and X194 were removed. Subsequent "clean" operation indicated that one of these was the leaker. The lesser suspect X194 was returned to the core; further "clean" operation was considered convincing evidence that X193 was the leaker. It was transferred to HFEF on December 28, and analysis during cleanup demonstrated that it was, in fact, the leaker. The leaking element was PNL10-14.

In passing, it is interesting to note the great similarity between the two releases on December 24 and 25. No excursion amplitudes were estimated for these two events; transient operation so clouded the fission-product inventories in the leaker that excursion amplitudes could not be usefully compared with other cases.

H. Subassembly X156 (December 28, 1973)[10]

Subassembly X156 was a sodium-bonded mixed-carbide experiment, a fuel type with which there has not been much experience. This was the first and so far only carbide leaker. About midafternoon on December 28, it was noted (see Fig. 33) that the activity level of ^{135m}Xe was about four times as high as normal background; other activities were quite normal, except ^{133}Xe, which was high due to an inventory inherited from the preceding leaker (X193). This situation was interpreted as resulting from the extrusion of bond sodium; otherwise, gas activities would all have been higher. The ^{135m}Xe increase was followed, as was anticipated, by an increase in ^{135}Xe.

Sodium apparently was continuously extruded from the afternoon of December 28 until early on December 30. This conclusion comes from the fact that, during most of December 29, ^{135m}Xe was at a level about 10 times normal. Had there been a one-time extrusion on December 28, this level would have decayed with the 6.6-hr half-life of the precursor ^{135}I. The fact that other isotopes (except ^{135}Xe) were essentially unaffected is evidence that gases were not being leaked.

At about 0400 hours on December 30, there was a sudden emission of more sodium (indicated by a marked increase in ^{135m}Xe only), which contained fresh enough fission products to yield a signal increase of ~10% on all three channels of the delayed-neutron monitor (FERD). On seeing the increase on FERD, the Shift Supervisor manually scrammed the reactor. At 1000 hours,

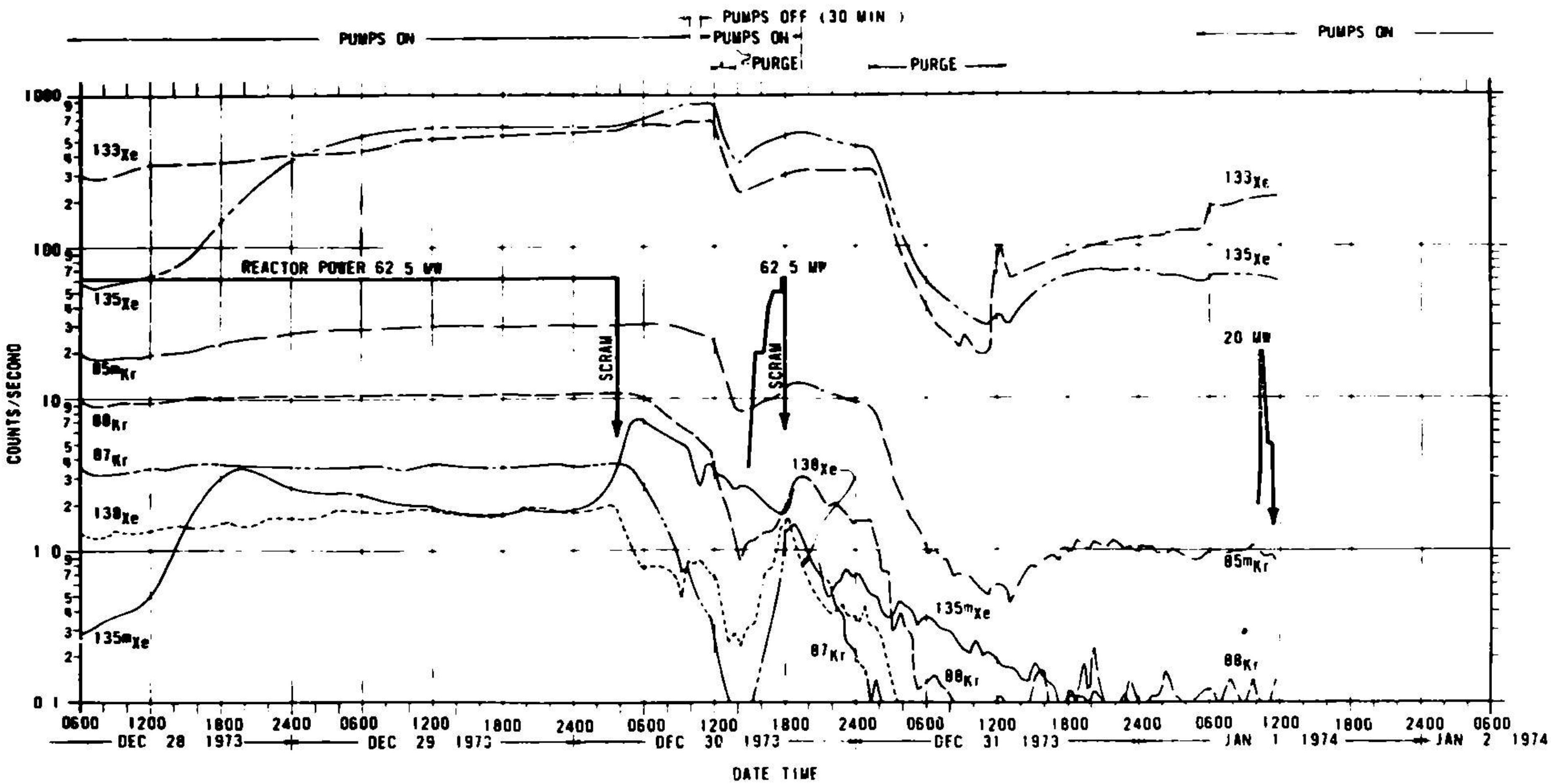

Fig. 33. GLASS Data for Run 68D (Leaker was Element U-248 of Subassembly X156). ANL Neg. No. 103-S5870.

the primary pumps were turned off for 30 min to see if further leakage could be stimulated. The ^{135m}Xe immediately decreased as replenishment by diffusion was halted; when the pumps were turned back on, the ^{135m}Xe returned to the level that would have been projected if the pumps had not been turned off. This indicated that no further sodium had been released as a result of turning the pumps off.

The reactor was cautiously restarted at about 1500 hours, and shortly after it reached 62.5 MW, there was a delayed-neutron signal large enough to satisfy the two-out-of-three scram criterion on FERD. A subsequent startup on January 1 was aborted for reasons not associated with the leak.

Analysis of the signals, especially that for ^{135m}Xe, strongly indicated a sodium-bonded element. A sodium sample was taken on December 31; the ^{131}I activity was about 40 times normal background. This is in qualitative agreement with the ^{135m}Xe signal which, although it only reached ~20 times background, did indicate sustained emission of sodium during December 29. Because of the disparity of half-lives, the ^{131}I would reach a relatively much higher level from a prolonged leak.

The two prime suspects were X180, a high-burnup metal-fuel experiment, and X156. Both were removed from the core, and the reactor was operated for about two days without any indication of a leaker. Subassembly X180 was returned to the core, and subsequent operation was clean. This strongly supported the conclusion that X156 was the leaker, and after some cooling, it was removed to HFEF for disassembly. Upon disassembly of the subassembly, it was found that element 248 had a weight loss of ~3.6 g. This is nearly the entire bond inventory.

Subsequent examination of the element at Los Alamos revealed a crack in the cladding only ~0.05 in. (~1 mm) long located 11.3 in. (287 mm) above the bottom of the fuel.

I. Subassembly X180 (October 26, 1974)

This was a Mark-II metal-fuel experiment with ~9.5% peak burnup. As shown in Fig. 34, there was a relatively mild release on October 26 (signal/background for ^{133}Xe was ~35) that was not serious enough to require shutdown. All seven isotopes monitored by GLASS participated in the excursion and subsided approximately according to half-life. This indicated a single bubble. Then on the following morning (October 27), there was a far larger release requiring reactor shutdown. Again, all isotopes exhibited similar increases in concentration and died away as though the release was the effect of a single bubble. This time the decay of ^{135m}Xe was slower than that indicated by its half-life. This was an indication that some ^{135}I had been expelled into the primary sodium; an abnormal concentration of ^{135}I in the sodium was found by subsequent analysis, which showed ^{131}I about five times tramp background.

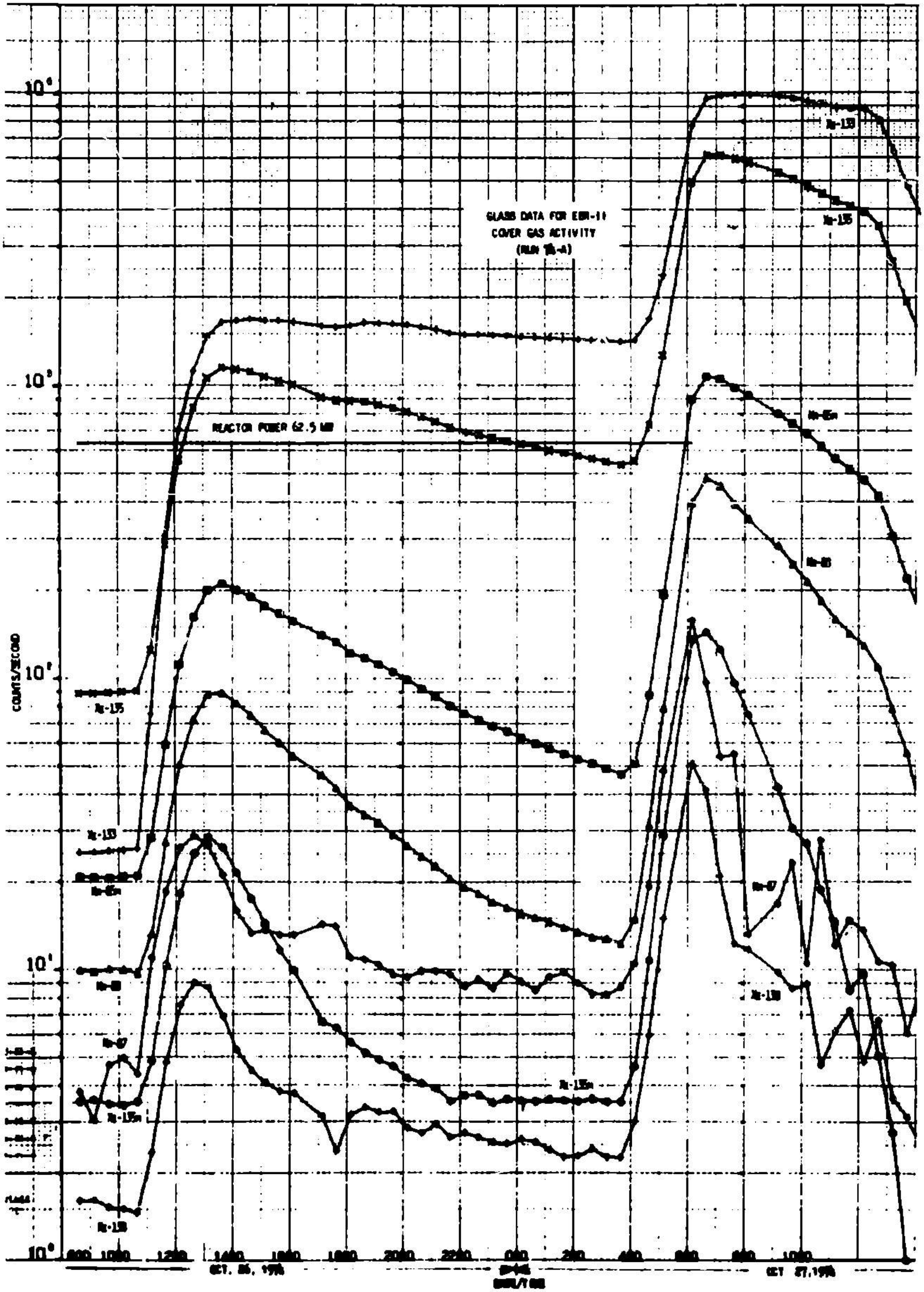

Fig. 34. GLASS Data for Run 74A (Leaker was Element 559 of Subassembly X180). ANL Neg. No. 103-S5989.

Two suspects, X116A and X143, were removed from the reactor and it was restarted on October 30 (see Fig. 35). As the reactor approached 20 MW at about 0730 hours, the concentration of ^{133}Xe, already above normal tramp level, began to increase noticeably. This indicated that the hole was open, but it was not until about 1015 hours that short-lived isotopes began to appear in significant quantities. The implication here is that the leak orifice communicated with the plenum region and that the short-lived isotopes were delayed by the path length for diffusion from their birthplace on the fuel surface to the plenum region.

Clearly the leaker was still in the core. The reactor was shut down, and X059B was removed. During the approach to power on October 31, the ^{133}Xe concentration, already ~10 times normal tramp level, began to increase when the reactor reached ~20 MW (~0930 hours). Again the short-lived isotopes did not reach abnormal levels until about 2 hrs later (~1130 hours). Shortly thereafter, the reactor was shut down and six subassemblies including X180 were removed from the core. Subassemblies X116A and X143 were returned to the core. Subsequent "clean" operation confirmed that the leaker was in the group removed. Then all suspects except X180 were returned to the core, and subsequent clean operation confirmed that X180 as the leaker. Some two weeks later, during removal from the reactor tank, X180 leaked very large quantities of ^{133}Xe and other fission products to the transfer coffin, thereby providing final proof that it was indeed the leaker.

It might seem that the small release of iodine to the bulk sodium was inconsistent with the moderate release of noble gases. This is not necessarily contradictory. In a metallic fuel element at this burnup, the fuel is swollen to the cladding wall and effectively all the sodium is forced from the annulus up to the plenum. Under these conditions, only the top-end surface of the fuel pin really injects iodine into the bond sodium. This means that the sodium carries a relatively much smaller quantity of fission products when it is leaked to the coolant. And in fact, the postmortem did show that practically all the bond sodium had been lost.

J. Subassembly X116B (November 22, 1974)

At about 1500 hours on November 22, all gamma activities started up sharply, as shown in Fig. 36. There was no detectable increase in delayed-neutron count rate. The reactor power was reduced to 50 kW at 1614 hours; complete shutdown was at 1730 hours. The high-speed purge (~85 L/min) was started at 1812 hours, causing a decrease of long-lived activities as shown in the figure.

The release was quickly diagnosed as originating from an unencapsulated oxide experiment on the basis of magnitude and relative abundance of isotopes. This was the first effective application of the identification criteria embodied in Figs. 37-40, all of which supported its identification as an oxide. No xenon tag was detected. The ^{131}I concentration was 26.2×10^{-5} $\mu Ci/g$, or roughly five times tramp level.

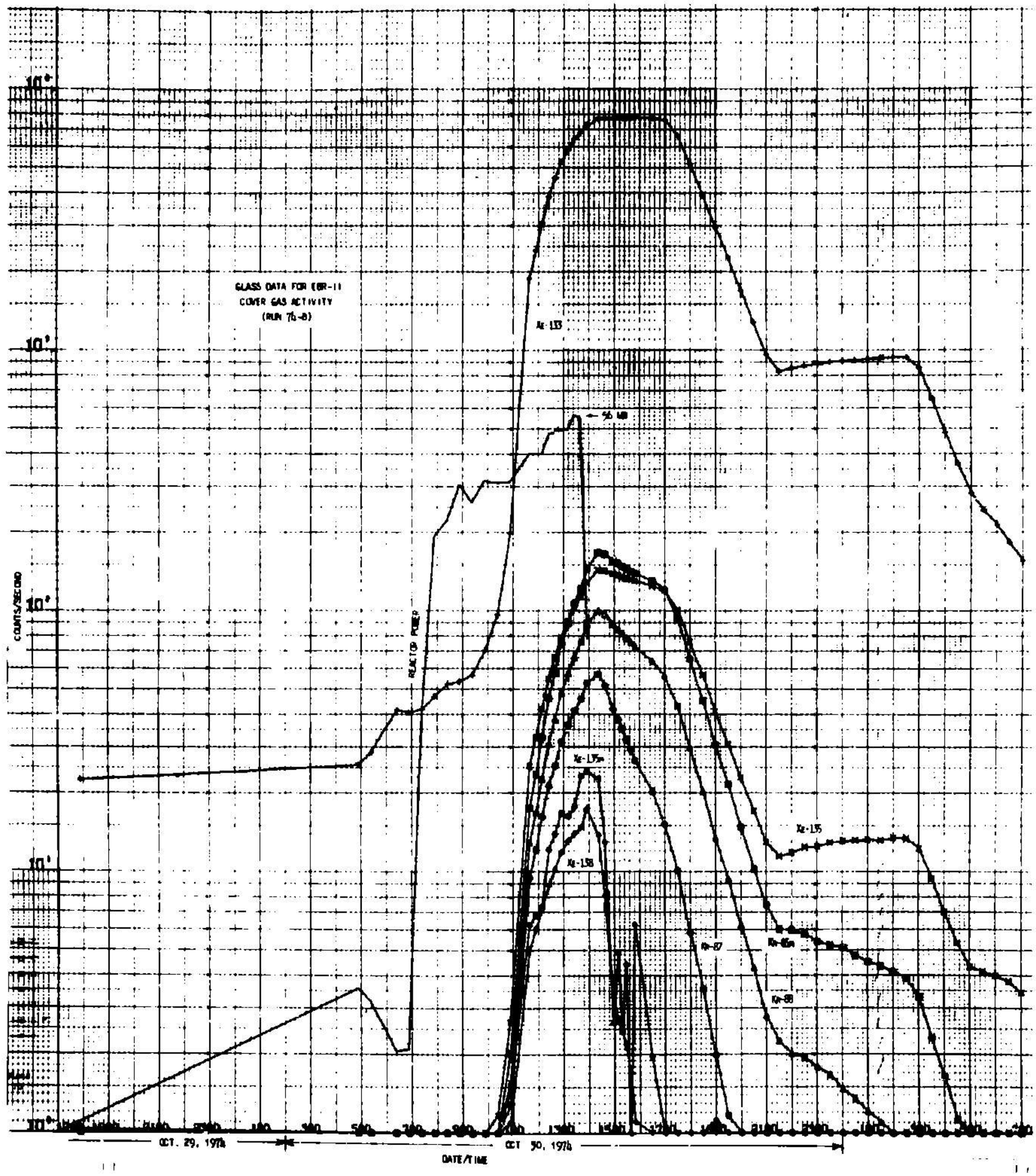

Fig. 35. GLASS Data for Run 74B (Same leaker as in preceding figure). ANL Neg. No. 103-S5990.

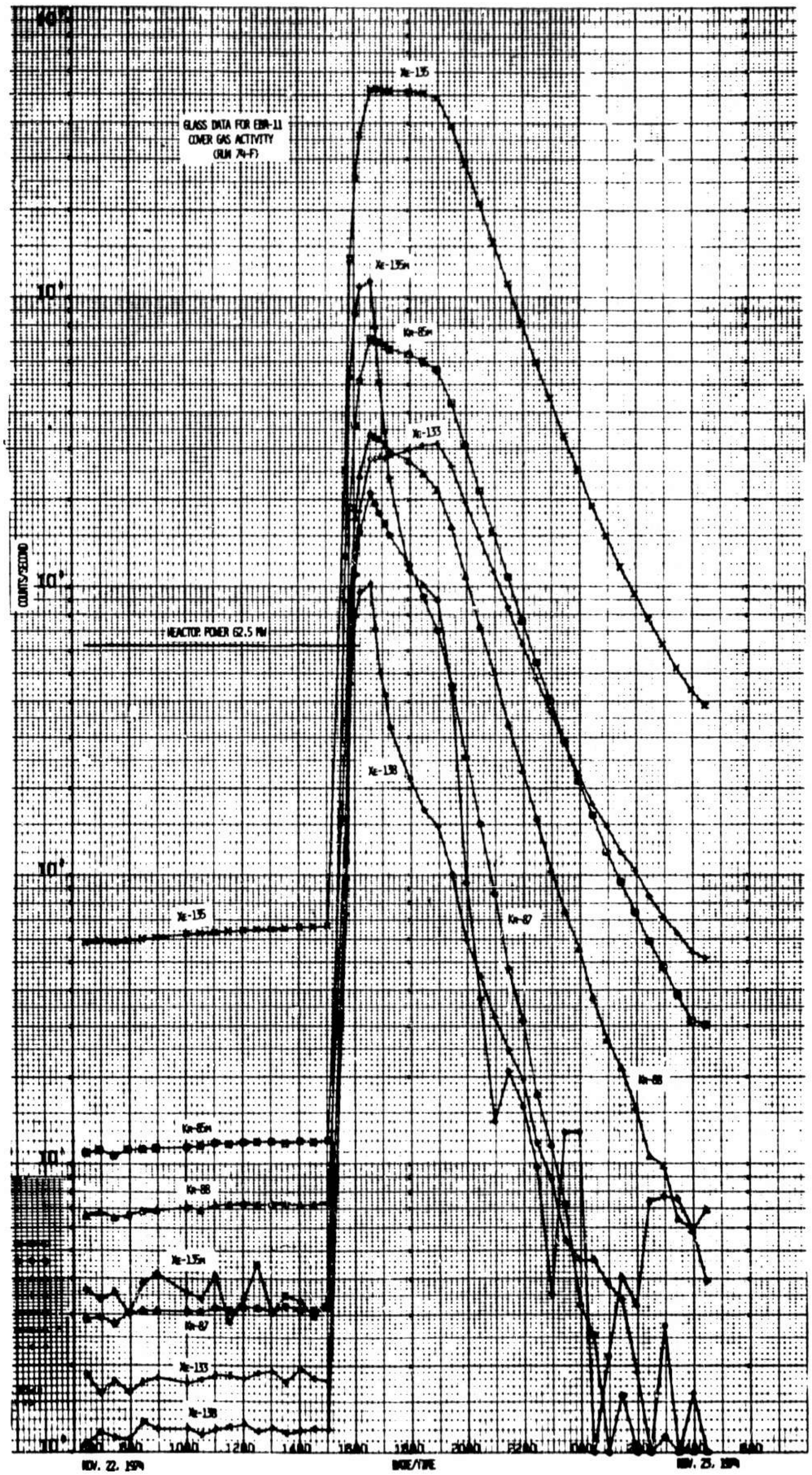

Fig. 36. GLASS Data for Run 74F (Leaker was Element PNL5-17 in Subassembly X116B). ANL Neg. No. 103-T5022.

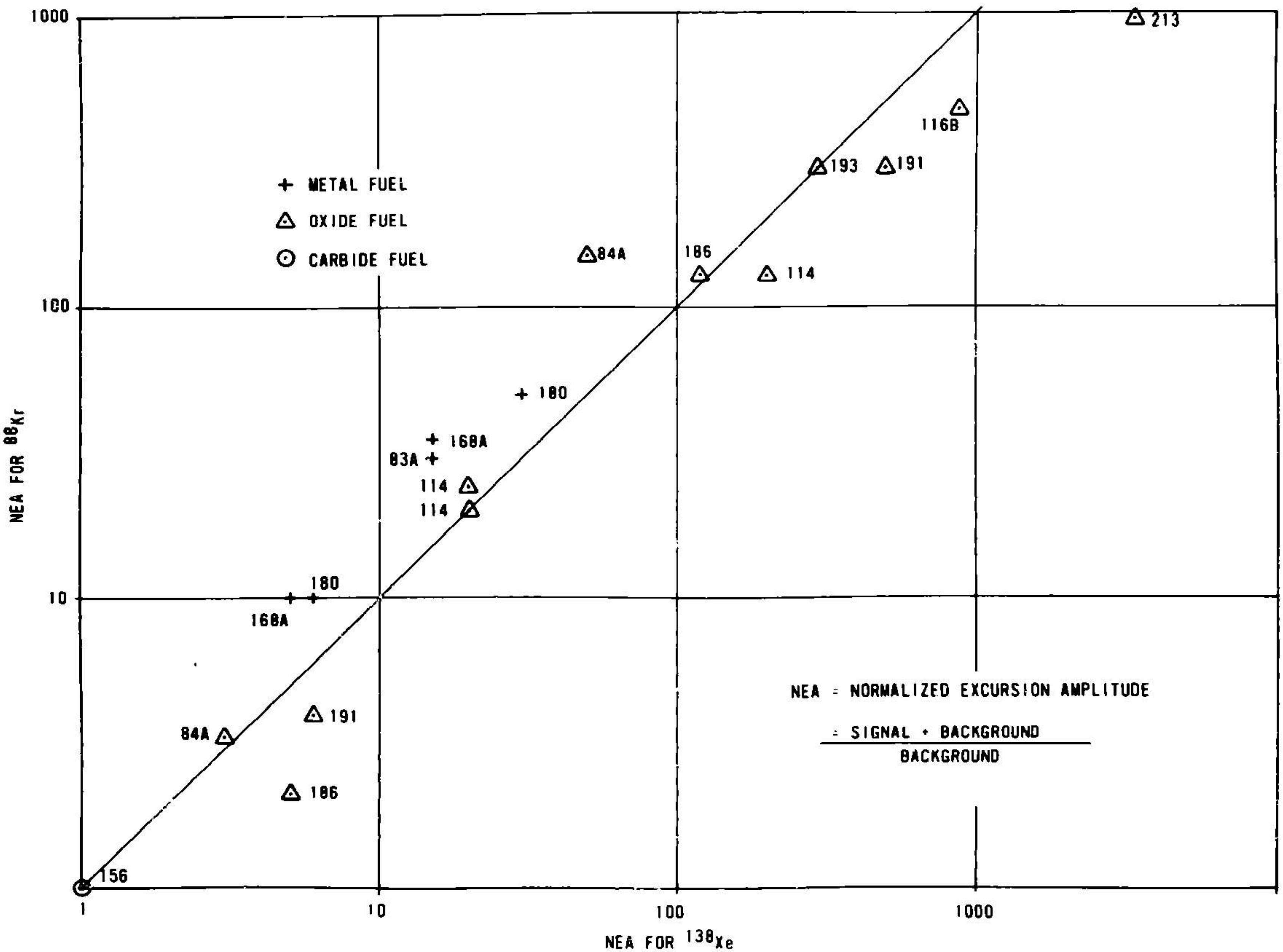

Fig. 37. Correlation of ^{88}Kr and ^{138}Xe Signals for Several Leakers in EBR-II. ANL Neg. No. 103-T5029.

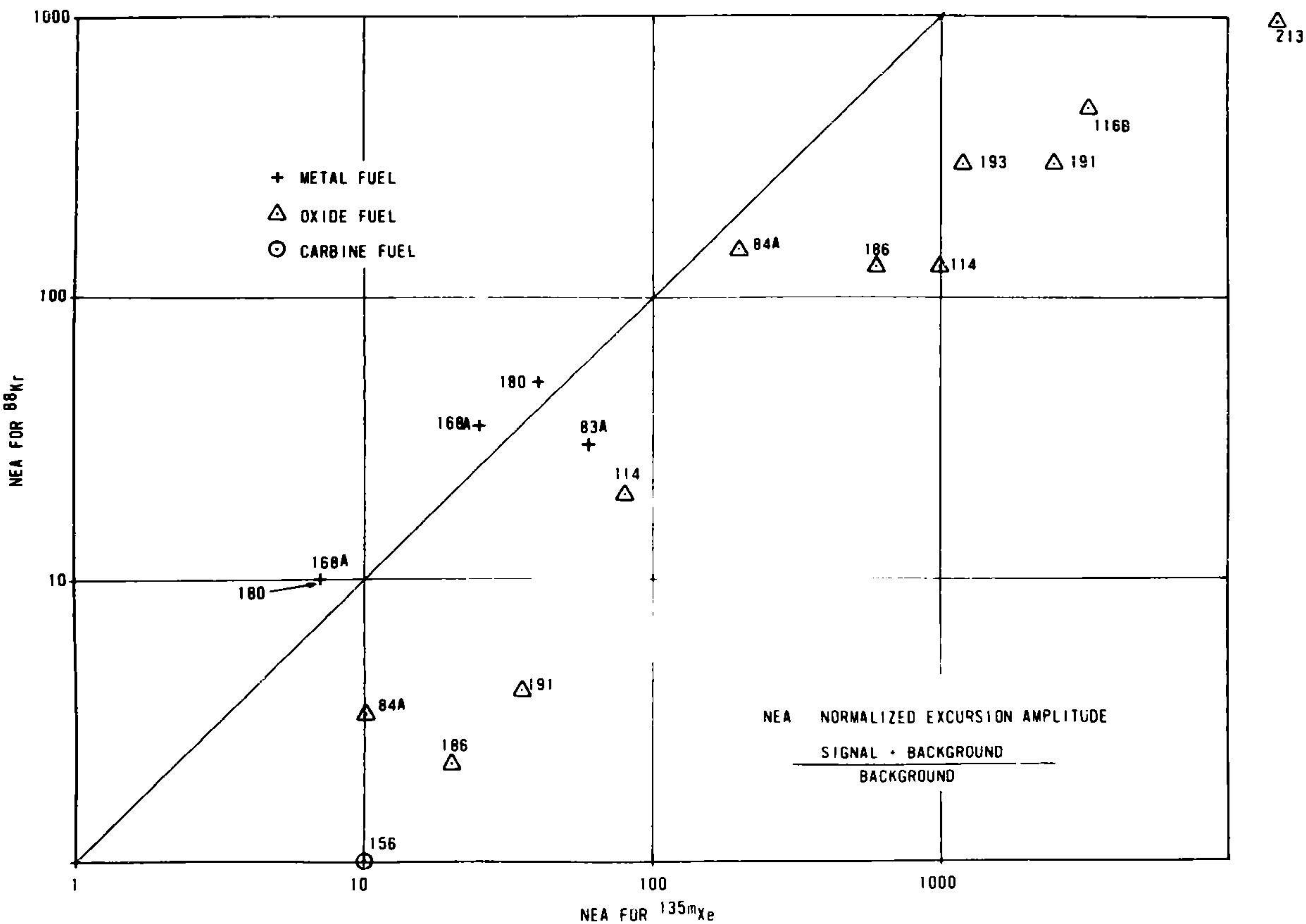

Fig. 38. Correlation of ^{88}Kr and ^{135}Xe Signals for Several Leakers in EBR-II. ANL Neg. No. 103-T5028.

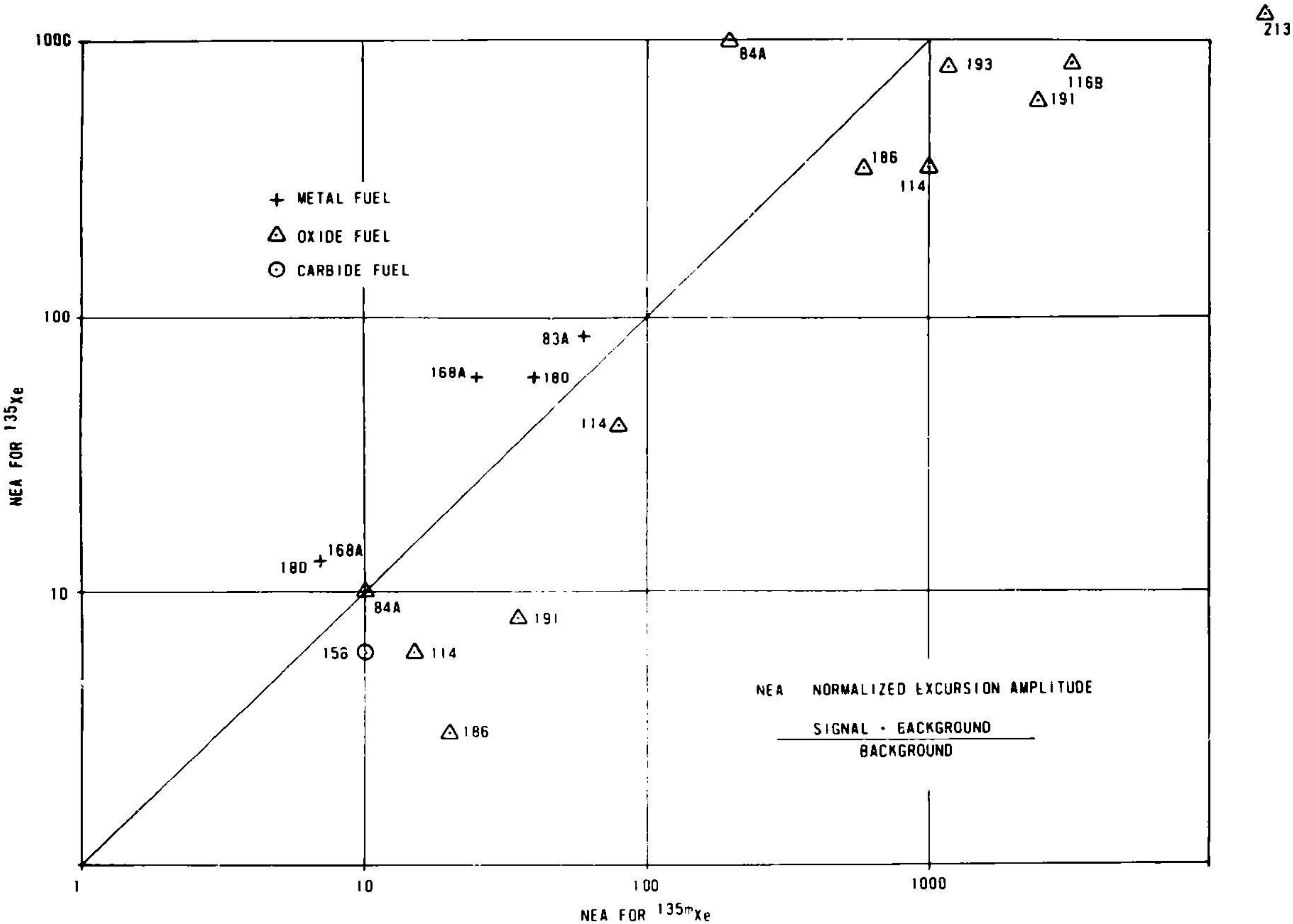

Fig. 39. Correlation of ^{135}Xe and ^{135m}Xe Signals for Several Leakers in EBR-II. ANL Neg. No. 103-T5027.

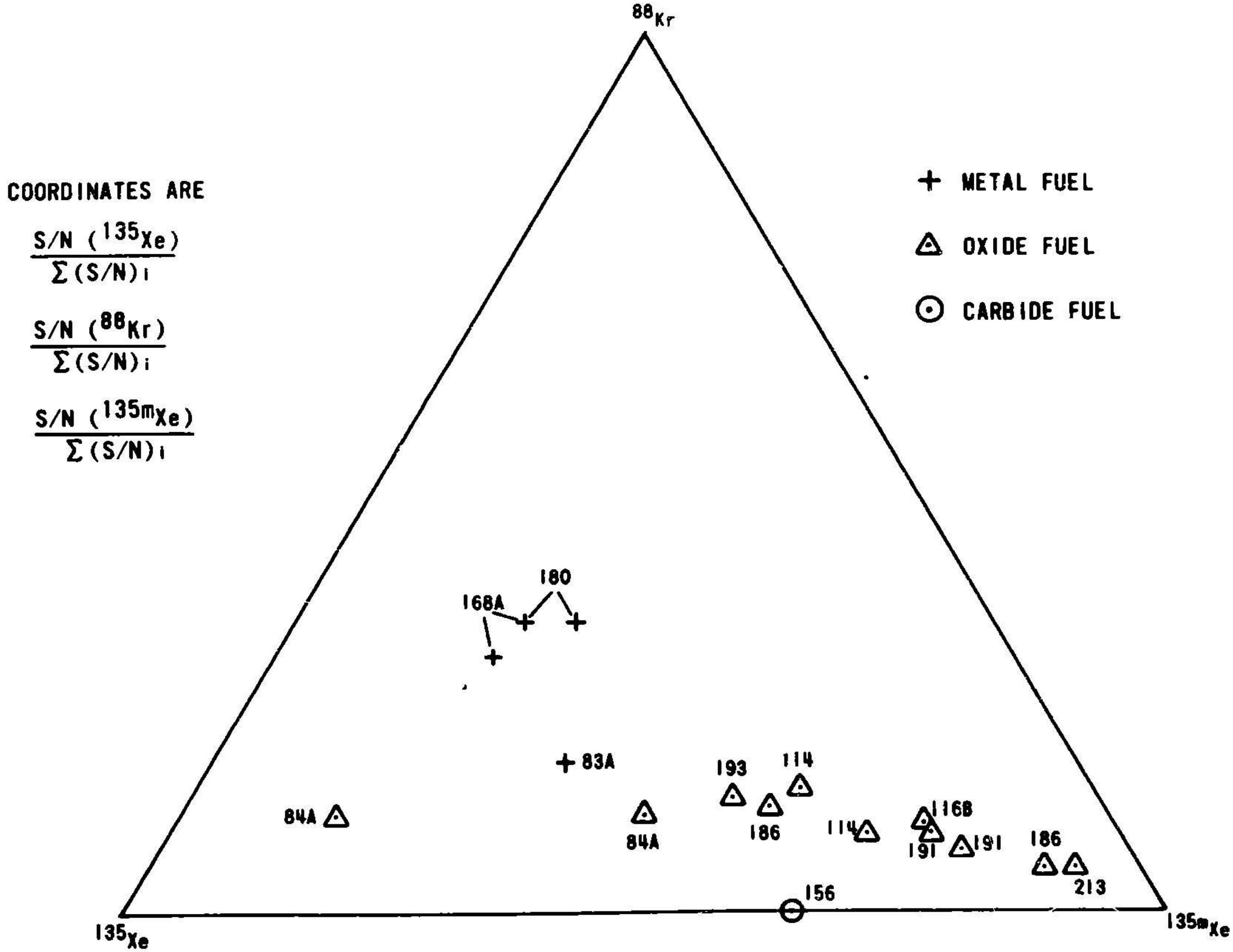

Fig. 40. Ternary Fingerprint of Leakers. ANL Neg. No. 103–T5026.

The two most suspect, untagged, unencapsulated oxides--X116B and X143A--were removed from the core. The reactor was restarted and returned to full power at about 0030 hours on November 25. Although there was a large quantity of ^{133}Xe in the cover gas, there were no unusual levels among the short-lived isotopes, and it was concluded that the leaking element must be in one of the two subassemblies removed.

Subassembly X116B was identified as the leaker on December 3 and 4 by observing that the level of ^{133}Xe activity in the cover gas remained constant while the suspect was isolated in the fuel-unloading machine. A convincing increase in the ^{133}Xe level was observed when X116B was in the basket and X143A was in the FUM. Due to the low leak rate from the suspect and the high leak rate from the argon cooling system, discrete gas samples drawn from the FUM were generally unconvincing. However, two FUM samples taken on December 2 did, in retrospect, support the identification of X116B as the leaker.

This was the first leak to occur after the cadmium filter (see Sec. VI.E above) was installed. Although this was a relatively large release characteristic of high-burnup oxide fuel, the high-count-rate overload problem was much reduced as compared with earlier releases of similar magnitude.

K. Subassembly X213 (December 27, 1974)

The reactor scrammed automatically from a two-out-of-three FERD signal at 2213 hours on December 27. The concentration of all fission products in the cover gas rose rapidly and to an unusually high level. The increase was so rapid that some GLASS data were lost before it was realized that the amplifier channel was saturated. In magnitude, the release was of the order of X084 (judged by the increase in ^{133}Xe). However, the release must have been very much more rapid, since it carried along not only much larger quantities of ^{135m}Xe and ^{138}Xe but also detectable quantities of delayed-neutron precursors, which were not seen at all in the case of X084.

The data are included in Table V and plotted in Figs. 37-40. The data on ^{135m}Xe and ^{138}Xe have a large uncertainty, but this is clearly the largest excursion seen so far for those two isotopes. However, their unusually large increases are entirely consistent with the equally unusual detection of a delayed-neutron signal.

The size of the excursion and the generally high level of short-lived activities immediately identified the leaker as an oxide. A xenon-tag sample was collected and analyzed as quickly as possible. Of the subassemblies known to be tagged, X202 had the tag most closely resembling the tag collected. Subassembly X202 was removed from the core, and the reactor was restarted early on December 29. At about 0515, while the reactor was still at ~30 MW, it became apparent that the leaker was still in the core; the reactor was shut down at 0600 hours.

A review of the data on the xenon tags revealed that X213, not previously identified as having a tag, actually carried a tag much closer to the one recovered than X202. Subassembly X213 was removed from the core, and subsequent "clean" operation confirmed that it was the leaker. Examination determined that the leaking element was No. 11B.

VIII. CONSOLIDATION OF RESULTS

We have attempted to systematize the results in a useful form. In Fig. 41, the normalized excursion amplitudes (NEA's)* are plotted for eight leakers (two instances for X114). Along the horizontal axis are scaled the decay constants of the various isotopes. The most obvious point to be drawn from the figure is the gross way in which the curve for X156, the one mixed-carbide leaker, is distinguishable both by amplitude and shape from the others.

However, closer examination suggest definite qualitative differences between metals and oxides. The oxides, even including the minor preliminary release from X114, tend to have a pronounced dip in the region of ^{88}Kr, whereas the metals (X083A and X168A) have little if any. Figure 37 uses some of the same data to make the distinction clearer. The NEA for ^{88}Kr is plotted against the NEA for ^{138}Xe. Except for X084A, for which the data are known to be defective, all oxides fall essentially on, or to the right of, the line representing the 1:1 ratio between the two numbers. The three metal leakers are well to the left of the line, including a small release from X168A on October 23, 1973, while it was being reirradiated, and the small preliminary release from X180 on October 26, 1974.

The difference between metals and oxides in this respect is due in part to the different yield ratios for ^{235}U and plutonium. It is apparent from Fig. 19 that while the yield for ^{138}Xe does not differ much between fissile species, the yield for ^{88}Kr varies widely. Assume that the fission rate for plutonium is 1.15 times the fission rate for ^{235}U; this implies in a 25% Pu-75% (93%-enriched uranium) mixed oxide that

$$\frac{1.15 \times 0.25}{(1.15 \times 0.25) + (1.0 \times 0.75 \times 0.93)} = \frac{0.2875}{0.2875 + 0.6975} = 0.29 = 29\%$$

of the fissions occur in plutonium. Thus, with the data from Table II, the ratio of yield is

$$\frac{^{88}\text{Kr}}{^{138}\text{Xe}} = \frac{(0.29 \times 1.44) + (0.71 \times 3.63)}{(0.29 \times 5.9) + (0.71 \times 6.71)} = \frac{3.00}{6.47} = 0.46.$$

For uranium alone, the ratio is 0.54.

Obviously, this small difference in yield ratios does not account for the difference in ratios seen in Fig. 37. Another factor operating in this case is the disparity between the half-lives of ^{138}Xe (14.2 min) and ^{88}Kr (2.8 hr). The apparent yield of ^{88}Kr is probably enhanced in sodium-bonded metal elements by the fact that a larger percentage of the nuclei survive diffusion through the bond to the leak.

*NEA = (signal + background)/background.

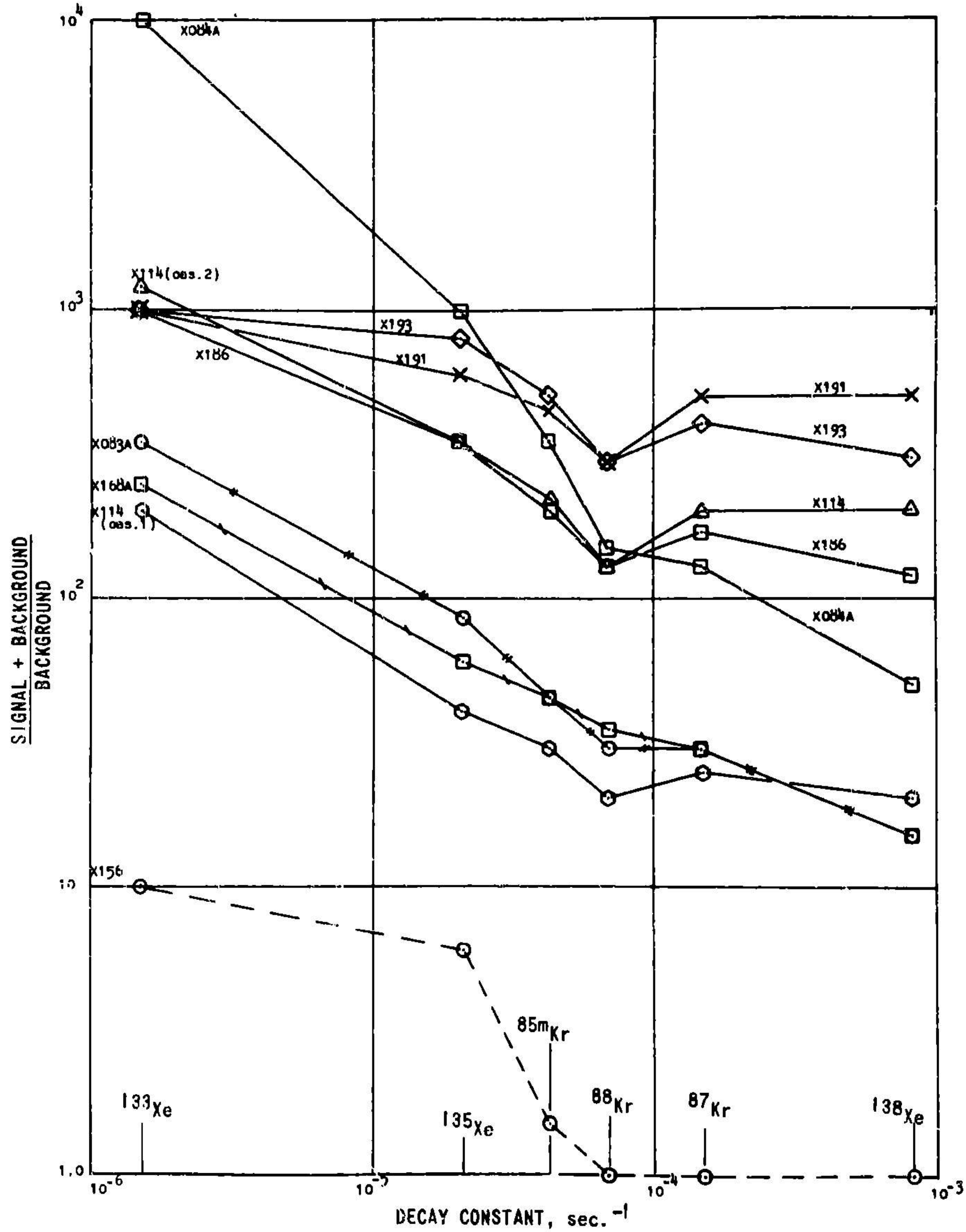

Fig. 41. Amplitude of Leaker Signals in EBR-II Cover Gas as a Function of Decay Constant. ANL Neg. No. 103-S5320.

The data in Table V can be treated in other ways to seek differences in the fingerprints of the various types of leakers. For example, Fig. 38 displays the results of correlating the excursions in ^{88}Kr and ^{135m}Xe activities. Here, there is a definite grouping of metal leaks, burps included, away from oxide burps, and even farther away from main oxide releases. Figure 39 gives the same type of plot for ^{135}Xe versus ^{135m}Xe, and so far seems to provide clearest separation between the various types of leakers.

Finally, Fig. 40 is a novel plot of the ^{135}Xe, ^{135m}Xe, and ^{88}Kr data in a ternary form. The numbers actually used are the signal-to-noise ratios or S/N's (S/N = NEA - 1) normalized to unity; i.e.,

$$P(^{135}\mathrm{Xe}) = \frac{S/N(^{135}\mathrm{Xe})}{S/N(^{135}\mathrm{Xe}) + S/N(^{135m}\mathrm{Xe}) + S/N(^{88}\mathrm{Kr})} = \frac{S/N(^{135}\mathrm{Xe})}{\sum_i S/N};$$

$$P(^{135m}\mathrm{Xe}) = \frac{S/N(^{135m}\mathrm{Xe})}{\sum_i S/N}; \quad P(^{88}\mathrm{Kr}) = \frac{S/N(^{88}\mathrm{Kr})}{\sum_i S/N}.$$

Here again is a fairly wide qualitative difference between oxide and metal fuels. Note that the one carbide leaker X156 gave no ^{88}Kr signal at all.

With regard to Figs. 37-40, it should be remarked that the data for X084 are defective. This was due to severe overloading from the very high count rate and was especially harmful to the results for the short-lived, relatively low-count-rate isotopes ^{135m}Xe and ^{138}Xe. The points for these isotopes are considered "wild," but have been included for completeness. The data for X083 may be questioned; those were the first presentable data taken with the equipment, and they may have suffered from our inexperience.

In time, one or some combination of these relations may turn out to be the most useful in distinguishing leakers. For the foreseeable future, the approach is to plot each new leaker on each of these graphs to see which group it most resembles. Since burps show identifiable characteristics, a leaker may even be classified on that basis before a major release occurs.

IX. CONCLUSION

A moderate amount of information can be extracted from the cover-gas gamma spectrum. Factors that tend to detract from the measurement are:

1. The relatively low photopeak efficiency of the germanium-lithium detector; this reduces the dynamic range of the channel and requires provision for at least two changes of sensitivity in order to encompass releases from high-burnup oxide elements.

2. The interference of the activation products ^{23}Ne and ^{41}A, which are expected to interfere much more in the Fast Flux Test Facility (FFTF) and the demonstration LMFBR.

3. The holdup effect of the bulk sodium; this holdup effect obscures analysis of relative yields. This effect will probably be much less troublesome in the FFTF and the LMFBR because in those systems the primary flow rate relative to total primary-system coolant volume is nearly an order of magnitude greater than in EBR-II.

On the other hand, it should be possible in EBR-II to identify a carbide leaker unambiguously. Furthermore, it is encouraging to believe that an oxide leaker can be distinguished from a metal one by the characteristics of a preliminary burp, possibly a few hours before the main release occurs.

APPENDIX A

GLASS Operating Instructions

1. Monitor Stations

a. Cover-gas Monitor in Depressed Area

Note: All electrical supply to GLASS equipment in the depressed area is through breaker No. 8 on the FERD distribution panel R-7. Both control and instrumentation systems can be serviced safely if this one breaker is opened.

(1) Sample-gas System

(a) Normal Settings. This system is shown schematically in Figs. 10-12. Under normal operation, the switch settings (see Fig. 42) are BYPASS OFF, PURGE OFF, and BLEED OFF. The sample-chamber OPEN light should be on. The flow indication should be 45 mm on the right-hand flowmeter on the GLASS shielding table and 0 on the left-hand flowmeter. (The flowmeters are visible in Fig. 1.) The 45-mm indication is obtained by adjusting the throttle valve on the sample input line (see Fig. 42). The valves V-322A and -322R on the supply and return manifolds (see Fig. 5) must be fully open. The needle valve on the right-hand flowmeter must always be fully open. Figure 43 is the calibration curve for this flowmeter.

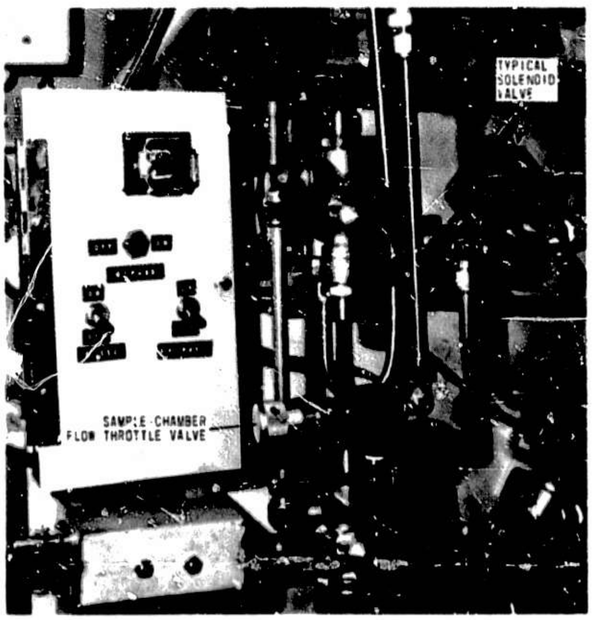

Fig. 42. GLASS Sample-gas Controls in Depressed Area. ANL Neg. No. 103-R5931.

(b) Adjustments for Off-normal Operation. Two other valves must be adjusted so that calibrated dilution can be obtained under conditions of high cover-gas activity. These adjustments are obtained as follows:

1. Turn the BYPASS and PURGE switches ON (Fig. 42). Now adjust valve V-25 on the clean argon supply line so that a flow indication of 45 mm is obtained on right-hand flowmeter. The needle valve on right-hand flowmeter must always be open.

2. Leaving the BYPASS and PURGE switches ON, turn the BLEED switch ON and adjust the sample-gas bleed input indication to 100 mm by means of the needle valve on the left-hand flowmeter. Figure 44 is the calibration curve for this flowmeter.

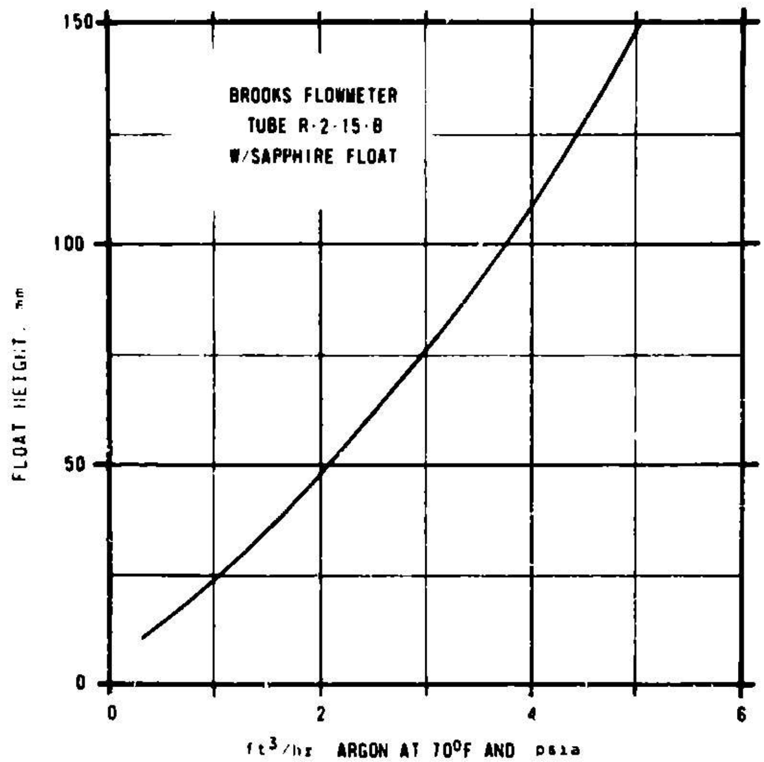

Fig. 43. Calibration Curve for Flowmeter Measuring Gas Flow through GLASS. ANL Neg. No. 103-R5989.

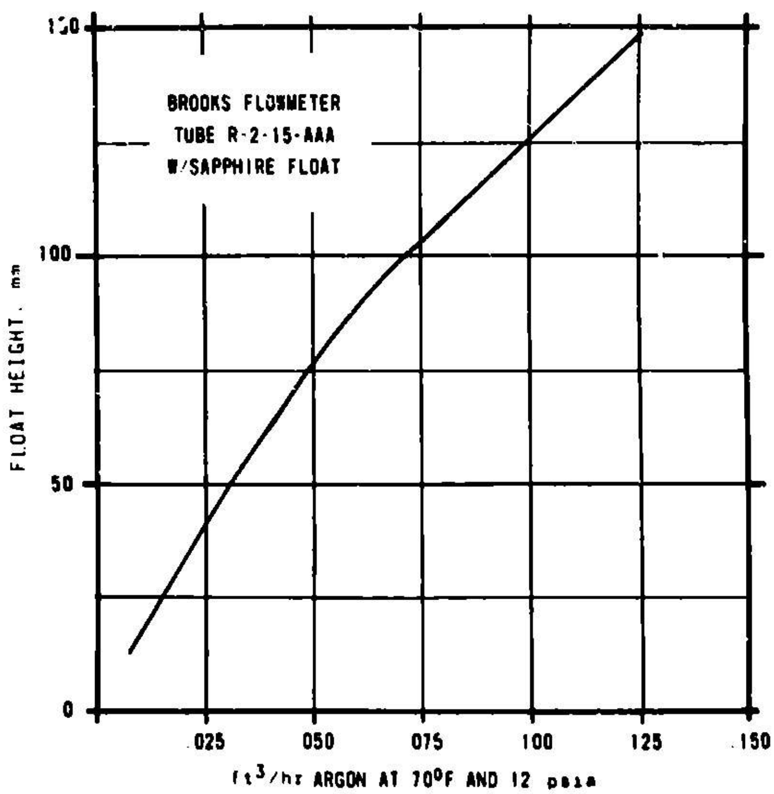

Fig. 44. Calibration Curve for Flowmeter Measuring Sample-gas Aliquot during Dilution in GLASS. ANL Neg. No. 103-R5981.

(c) Always leave the BYPASS, PURGE, and BLEED switches OFF in the depressed area. Actual operation is obtained by means of controls in the EEL.

(2) Detector and Associated Electronics. The following remarks, unless otherwise stated, refer to the Nuclear Diodes Detector No. L685.)

(a) The preamplifier is attached directly to the detector, and no adjustment is required. Three cables are connected to the preamplifier at clearly labeled receptacles:

1. High-voltage detector bias from the high-voltage supply.

2. Signal cable to the amplifier.

3. Power cable to drive the preamplifier. This power cable must be connected to the preamplifier socket of a Canberra amplifier.

(b) The high-voltage power supply is a Hewlett-Packard Model 6516A. For the Nuclear Diodes detector, the bias is +2900 V. This is obtained by putting the grounding plug on the NEG receptacle and connecting the cable to the POS connector; voltage is set with thumbwheel switches and unit is turned on with pushbutton switch. The unit draws power from the 115 V receptacle on the GLASS control panel.

(c) The NIM bin draws power from the 115 V receptacle on the GLASS control panel and provides standard NIM voltage to the amplifier and preamplifier. The only control is an OFF-ON power switch with an ON indicator light.

(d) The amplifier is a Canberra Model 1417B (ANL No. 164295). The settings in Table VI are for this amplifier and are very nearly exact. If another 1417B is substituted, the settings will be very close. Although the control setting would be different, a Canberra Model 1413 amplifier can be substituted if need be. It is essential that the amplifier have sufficient cable-driving capacity for this application.

Further, note that exact and painstaking adjustments of the amplifier are necessary for this application. Before the gain is adjusted, the amplifier must be matched to the preamplifier by using the screwdriver-adjustable pole-zero potentiometer (marked P/Z) on the amplifier panel. This must be done by using an oscilloscope and following the detailed instructions for the model. (Manuals for all GLASS components are stored in the metal cabinet in the EEL.) The P/Z adjustment must be made with the base-line restorer turned off and the shaping time constant set at 2 μs. At the same time, the dc level of the output should be adjusted to zero by means of the screwdriver-adjustable potentiometer adjacent to the output receptacle. Gain settings must be made from the same side each time, since the backlash in the fine-gain potentiometer is perceptible to the multichannel analyzer.

TABLE VI. Settings and Connections for Amplifiers of GLASS Cover-gas and Air Monitors

Function	Cover-gas Monitor (Canberra Model 1417B)	Air Monitor (Canberra Model 1413)
	Connections	
Power	Plugged into NIM Bin	Plugged into NIM Bin
Input	BNC Receptacle NEG INPUT POS INPUT capped	BNC Receptacle INPUT
Output	BNC Receptacle RESTORED-DELAYED OUT	BNC Receptacle OUTPUT-UNIPOLAR
	Settings[a]	
Course gain	8	300
Fine gain	810	036
Shaping time constant	1 μs	2 μs
Input polarity	NEG (by above connection)	NEG
Input impedance	1 kΩ	-
Output polarity	POS	POS
Output range	-	10 V
Restore	Low	Low
Detector High voltage	+2900 V	+2900 V

[a]Exact settings for Canberra Model 1417B; approximate settings for Canberra Model 1413.

b. Air Monitor on Main Reactor Floor

(1) Air-sampling System. The air sample consists of just that air contained within the lead shield (~0.40 x 0.40 x 0.45 m, internal dimensions). A blower (no controls except ON-OFF switch) is used to draw representative air through the counting volume.

(2) Detector and Associated Electronics

(a) The preamplifier is attached directly to the detector (normally Princeton Gamma Tech No. 779), and no adjustment is required. Three cables are connected to the preamplifier at clearly labeled receptacles:

1. High voltage from the high-voltage supply.

2. Signal cable to the amplifier.

3. Power cable to drive the preamplifier.

For the Princeton Gamma Tech detector, the cable must be connected to the PREAMP receptacle on the back of the Canberra (1417B or 1413) amplifier.

(b) The high-voltage power supply is a Hewlett-Packard Model 6516A. For the Princeton Gamma Tech detector No. 779 the bias is -2500 V. This is obtained by putting the grounding plug on the POS receptacle and connecting the cable to the NEG receptacle; voltage is set with the thumbwheel switches, and the unit is turned on and off with a pushbutton switch. Power for the high-voltage supply is 115 V from an ordinary ac outlet switch near the detector.

(c) The NIM bin draws power from a 115-V ac outlet near the detector and provides standard NIM voltages to the amplifier and preamplifier.

(d) The amplifier is a Canberra Model 1413, although Model 1417B can be substituted freely if proper gain adjustment is made. The amplifier must have adequate cable-driving capacity. The proper setting for this amplifier is given in Table VI. See Sec. 1.a(1)(d) above on the GLASS amplifier for operating instructions.

c. General Remarks on Servicing Germanium-Lithium Detectors

There are three germanium-lithium detectors; they are normally located as follows:

(1) Nuclear Diode No. L685--installed in cover-gas monitor in depressed area. The bias voltage is +2900 V, and the preamplifier must be powered from the receptacle on a Canberra amplifier.

(2) Princeton Gamma Tech No. 1131--installed in the air monitor on the main reactor floor. The bias voltage is +3000 V, and the preamplifier must be powered from a Canberra receptacle.

(3) Princeton Gamma Tech No. 779--normally held as a ready spare (for other two) in the EEL. The bias voltage is -2500 V, and the preamplifier must be powered from a Canberra receptacle.

All three detectors are cooled by 31-L Dewars of liquid nitrogen. Although there is a considerable safety margin, these Dewars should be filled to the top once a week. Liquid is obtained from the stockroom and delivered in 15-L transfer Dewars. A liquid-nitrogen transfer assembly is used to transfer the liquid into the detector Dewar. The transfer assembly is plugged into the top of the transfer Dewar, and the center tube is connected by a rubber hose to the fitting spout of the detector Dewar. The other tube is connected to a compressed-air supply by means of which the nitrogen is "blown" into detector Dewar. Care is needed to avoid applying too much air pressure. The air-supply connection and valve are located at the right of the detector assembly.

As an added precaution, the detector Dewar rests on the platform of an improvised scale, which reads out on the large dial at the left of the detector assembly (see Fig. 1). The actual quantity (pounds) of nitrogen in the Dewar is obtained by multiplying the scale reading by 10. (Other weights have been tared out.) The scale reads 5 when the Dewar is full, indicating 50 lb (23 kg) of nitrogen, and would read 0 if all the nitrogen were gone. As a matter of practice, the reading should never be allowed to drop below 2.

On the main floor, the air-supply connection and valve for the Dewar of the air monitor are located at the right side of the detector table. This Dewar has no scale and is simply filled until it runs over.

The Dewar for the spare detector is filled by simply raising the detector and neck plug about 125 mm so as to permit pouring directly into the Dewar until it overflows.

At each detector is a card on which the time and date of replenishment are logged. Note also that gloves and face shield are required while handling liquid nitrogen.

2. Analytical and Data-recording Equipment

The analytical and data-recording equipment is located in the experimental engineering laboratory on the ground floor of the power plant. Power is supplied from a separate stepdown transformer.

a. Single-channel-analyzer Array

The signal from the cover-gas monitor in the depressed area comes in on the cable marked GLASS No. 3. The cable is connected through a 93-Ω Tektronix terminator to a bus, which furnishes the signal to 12 single-channel analyzers (SCA's) as well as to an analog-to-digital converter for the multichannel analyzer. As shown in the schematic (Fig. 3), the SCA's are connected in pairs to determine the peak count rate and background of specific gamma peaks. The SCA's are identified with embossed tape as to the isotope and whether signal or background. The settings for the SCA's are shown in Table VII.

Each pair of SCA's feeds an on-line digital subtract unit (ODSU), which subtracts the background and supplies a logarithmic signal both to the

EBR-II Data-aquisition System (DAS) and to recorders in the control room. The isotopic identification and time setting for each ODSU are marked on the front of the unit. Note that each ODSU has two outputs, 0-1 mA and 0.10 V. The 0-1 mA is designed to drive small three-pen L & N recorders. Either signal can go to the DAS, provided that the DAS staff has been told what the scale factor is.

TABLE VII. Settings for Single-channel Analyzers

Isotope	Signal Threshold,[a] V	Background Threshold,[a] V	Sample and Hold Time, s
	For Cover-gas Monitor		
^{135}Xe	1.80	2.00	1
^{133}Xe	0.47	0.61	1
^{85m}Kr	1.07	1.30	2
^{88}Kr	1.43	1.60	6
^{87}Kr	3.05	3.18	10
^{23}Ne	3.30	3.54	50
	For Air Monitor		
^{133}Xe	0.55	0.70	60

[a]All windows (ΔE) are set at 0.10 V.

The SCA's and ODSU's are plugged into and derive their power from standard NIM bins. The ODSU's require a +6-V supply, which is not available in the standard bins. For this reason, two auxiliary +6-V supplies have been connected to bins containing ODSU's to provide that voltage through the assigned pin in the multipin connector. In starting the equipment, one must press the START button on each ODSU; the other controls can be ignored since they provide options not used in this application.

b. Analyzer-Computer System

The analyzer and computer are shown in Figs. 45 and 46, respectively. The analog-to-digital converter (ADC) for the cover-gas monitor is shown in Fig. 47. The control settings for the analyzer and the ADC's are shown in the photographs. (Both ADC's use the same settings.)

The loading and operation of the computer require careful explanation.

Loading the computer requires three steps:

(1) Load the BOOTSTRAP program by hand.

(2) Load the BINARY program with the teletype tape reader.

(3) Load the data-acquisition program with the teletype tape reader.

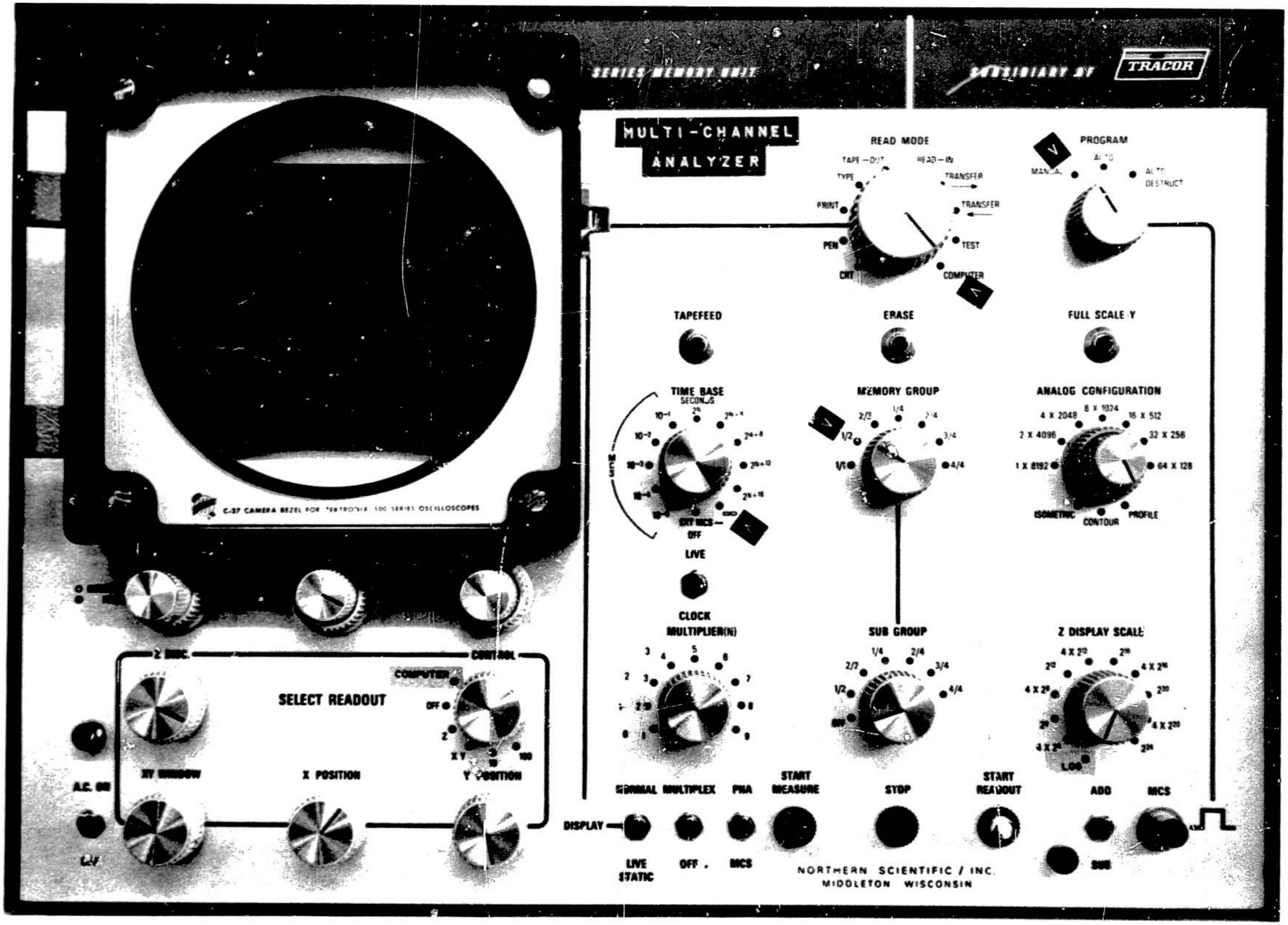

Fig. 45. Multichannel Analyzer, Showing Control Settings for Routine GLASS Operation. ANL Neg. No. 103-R5720.

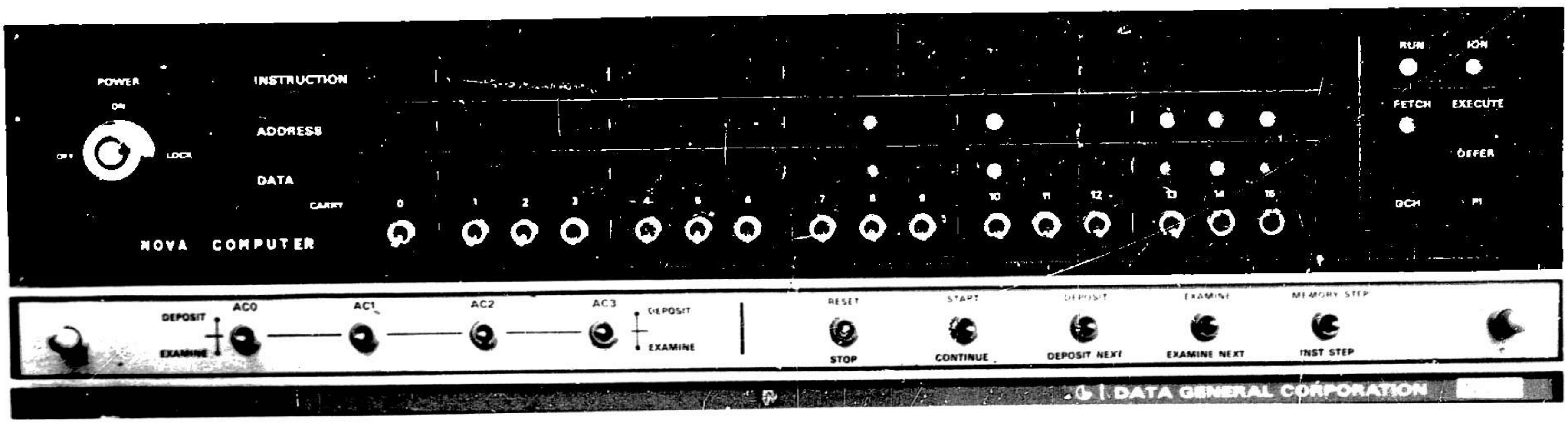

Fig. 46. NOVA Minicomputer Used to Control Data Taking and to Process Data (Switches are shown in operating position). ANL Neg. No. 103-R5723.

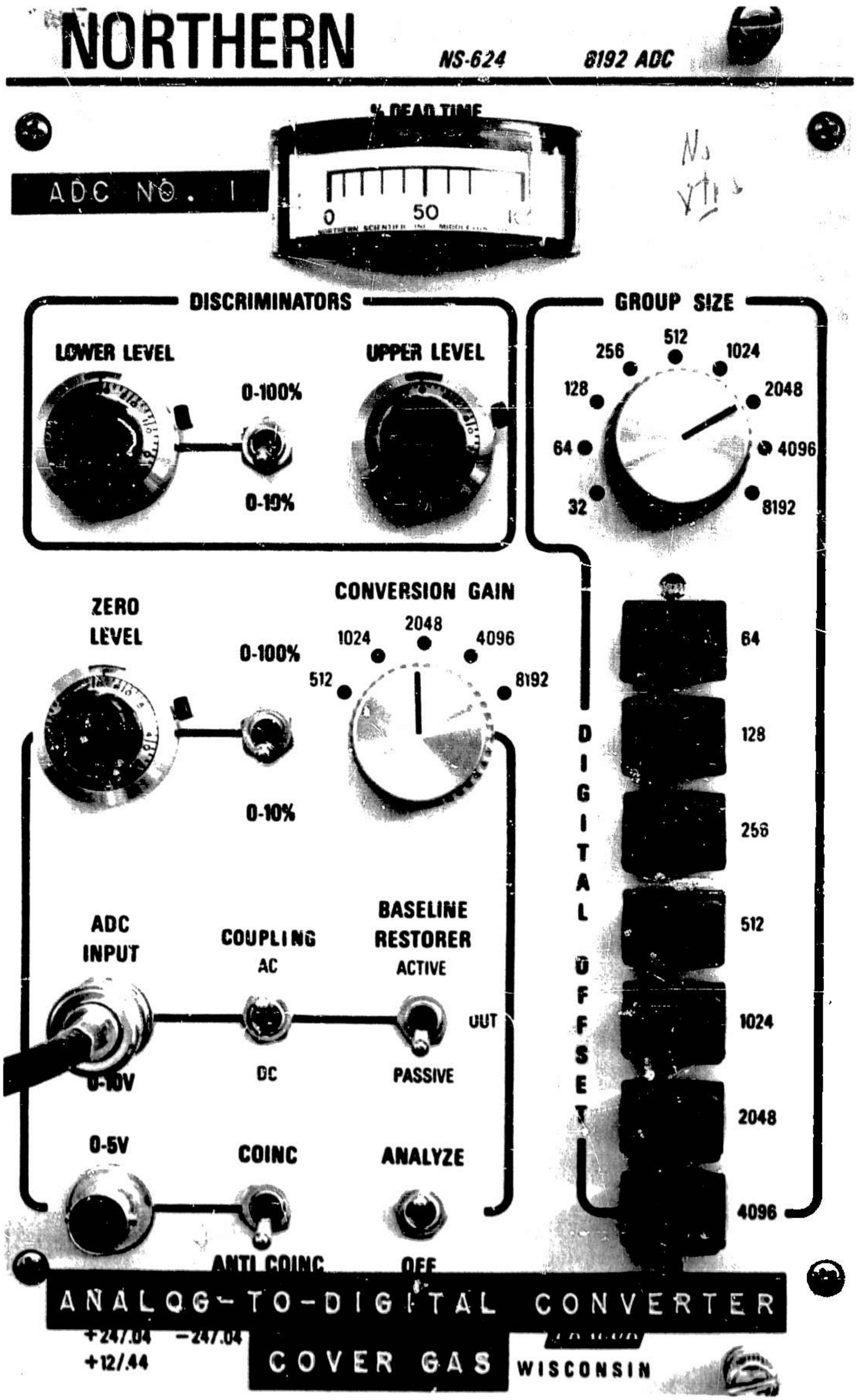

Fig. 47. Analog-to-Digital Converter for GLASS, Showing Operating Position of Controls (ADC for air monitor uses same settings). ANL Neg. No. 103-R5722.

In the photograph of the computer (Fig. 46) is a row of 16 data switches numbered 0-15. These switches are marked off in groups of three from the right. In each group of three, the left-hand place has a value of 4, the center place a value of 2, and the right-hand place a value of 1. Taken together, the three switches can be used to represent any octal digit. If a switch is up it represents 1, down 0. For example:

	LH	CEN	RH
3_8 =	0	1	1
	($0 \times 4 + 1 \times 2 + 1 \times 1 = 3$)		
5_8 =	1	0	1
	($1 \times 4 + 0 \times 2 + 1 \times 1 = 5$)		
7_8 =	1	1	1
	($1 \times 4 + 1 \times 2 + 1 \times 1 = 7$)		

(1) Loading the BOOTSTRAP program requires keying in by hand one address and 13 commands. The detailed operation follows.

(a) Place the computer power-key switch in the ON position.

(b) Set the data switches to the initial address 017757, which will look like this on the console:

Switch No.	0	1	2	3	4	5	6	7	8	9	10	11	12	13	14	15
Setting	0	0	0	1	1	1	1	1	1	1	1	0	1	1	1	1
Octal value	0		1			7			7			5			7	

(c) Press RESET and release. This brings the computer to the proper location for the first command.

(d) Set the data switches to the first command 126440, which will look like this:

Switch No.	0	1	2	3	4	5	6	7	8	9	10	11	12	13	14	15
Setting	1	0	1	0	1	1	0	1	0	0	1	0	0	0	0	0
Octal value	1		2			6			4			4			0	

(e) Press DEPOSIT and release. This places the first command at the previously designated address.

(f) Set the data switches to the second command 063610, and press DEPOSIT NEXT. This stores the second command at the next address.

It will not be necessary to key in any more addresses, since the DEPOSIT NEXT switch takes care of that. The rest of the program is loaded one command at a time exactly as in steps d and e above. For clarity, all the steps are listed below in concise form.

Power Switch ON

017757	RESET
126440 (1st command)	DEPOSIT
063610 (2nd command)	DEPOSIT NEXT
000777	DEPOSIT NEXT
060510	DEPOSIT NEXT
127100	DEPOSIT NEXT
127100	DEPOSIT NEXT
107003	DEPOSIT NEXT
000772	DEPOSIT NEXT
001400	DEPOSIT NEXT
060110	DEPOSIT NEXT
004766	DEPOSIT NEXT
044402	DEPOSIT NEXT
004764	DEPOSIT NEXT

At this point, the BOOTSTRAP program has been loaded.

(g) Now key in 017770 and press RESET. This brings the computer to the proper address so that the BOOTSTRAP program can read in the BINARY program from the teletype.

(2) This subsection covers the loading of the BINARY program. Two views of the teletype are shown in Figs. 48 and 49.

Fig. 48. Teletype (ASR 35) Used to Input Commands and Print Out Data. ANL Neg. No. 103-R5719.

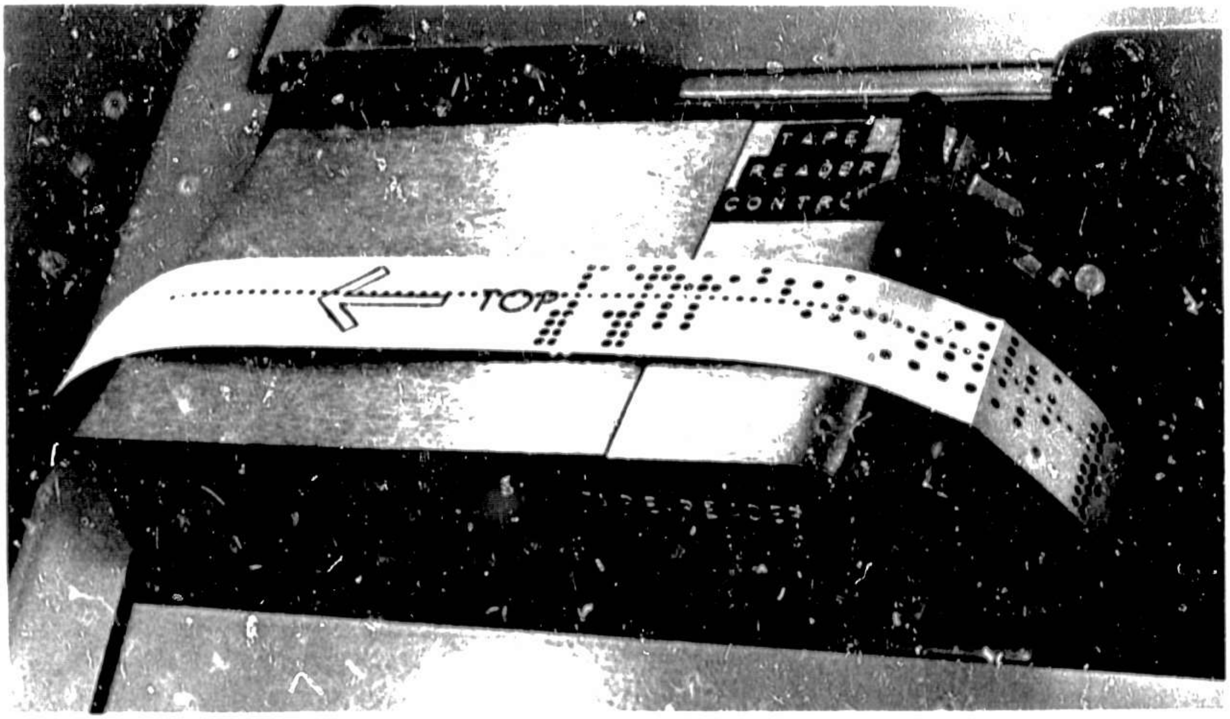

Fig. 49. Teletype Tape Reader, Showing Gate Open and Program Tape on Feed Sprocket. ANL Neg. No. 103-R5718.

(a) Referring to Fig. 48, the power switch must be turned to ON LINE and the Mode Switch to KT.

(b) Referring to Fig. 49, use the square button to open the tape-feed gate.

(c) Lay the front end of the BINARY program tape (No. 091-000004-08) in the tape reader, being sure that the directional arrow is on top and pointed to the left. The tape feeds from right to left.

(d) Carefully align the tape, close the gate, and put the tape-reader control in RUN.

(e) On the computer, press START. At this point, the teletype should begin reading the tape. If this does not happen, review all the foregoing steps, beginning with loading the BOOTSTRAP program.

(f) Reading this short tape requires less than a minute. When it has been read, open the gate and remove the tape.

(g) At this point, the BINARY program is loaded.

(h) On the computer, key in 017777 (the BINARY program starting address) and press RESET. This readies the system to read the main program tape.

(3) The subsection covers loading of the main program.

(a) Secure the main program tape (latest version of A1-711 program) and load it into the tape reader as described in the previous subsection, being sure that tape-reader control is in RUN. Alternatively, the A1-711 program can be loaded from a mag tape through the Sigma V computer (see 4 below).

(b) On the computer, press START. The teletype should begin reading tape. If not, review the preceding steps. This tape requires about 25 min to read in. If, as rarely happens, the tape reader stops, it is not necessary to start again from the beginning. Place the tape-reader control in FREE and gently pull the tape backward until there is an interblock gap at the reading position. Figure 50 shows how to locate an interblock gap. Return the tape-reader control to RUN, and press CONTINUE on the computer control panel.

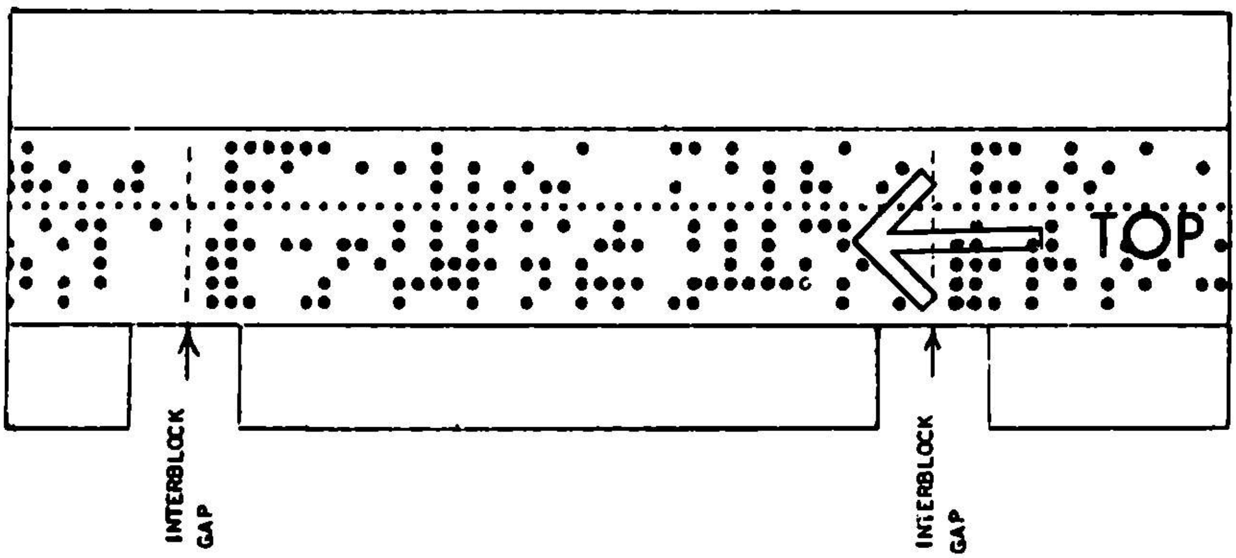

Fig. 50. Section of Program Tape, Showing How to Locate Interblock Gaps

(c) When the tape has been read, remove it from the reader and close the gate.

(d) Turn the teletype mode control to K.

(e) Key into the computer the program starting address 000003 and press RESET, then START. If loading has been satisfactory, the teletype will execute a carriage return and line space.

(f) At this point, program loading is complete, and all further operations are controlled from the teletype keyboard.

(g) Turn the computer power switch to LOCK to disable the computer control panel.

(4) The data-acquisition program can also be loaded from mag tape through the Sigma V computer.

(a) At the NOVA do the following:

1. Ready the tape labeled "Program to Receive Data from the Sigma V."

2. Set the tape-reader switch to RUN.

3. Turn the teletype dial to KT.

4. Turn the teletype to ON LINE.

5. Set the NOVA switches to 017777.

6. Press the NOVA RESET, then the START switches.

7. When the tape is read, set the NOVA switches to 017102.

8. Before the program is run on the Sigma V, press the RESET, then the START switches.

9. When program has been completely read in, the NOVA will stop at location 017121 with 063077 in the data lights.

10. Start the program normally.

(b) At the Sigma V, do the following:

1. Mount the current tape on unit 0. (The current tape is presently labeled "Glenn Brunson AL711 July 11, 1974," and is stored on the lower shelf in the tape cabinet behind the printer in the DAS room.)

2. Ready the tape.

3. After NOVA is running, hit the INTERRUPT switch on the Sigma V teletype.

4. Type RUN TAPTON.

5. Hit NEW LINE.

6. At the program end the tape will be rewound.

(5) Initiation of the data-acquisition program is almost completely covered in Fig. 51, an example of operator interaction with the computer.

(a) Set the overall parameters (time, memory space) to be used in acquiring the data. Normally used parameters are shown in the example.

(b) Set in the data for the specific isotopes to be monitored. The program can handle up to 10. The numbers relating to each isotope are listed in Table VIII.

S$ MO 4$ DA 20$ HR 10$ MI 44$ SE 50$	*This block sets clock at April 20 10:44::50 and it starts running at final spacebar operation.*
R$ APR 20 10:45::23.0	*Reads clock to see if it is running.*
FA 30$ FB 4096$	*Sets data cycle = 30 minutes* *Sets data storage field = 4096 channels*
FGS 1 XE133$ LIMITS 158 166$ START OF BACKGROUND? 170$	*Indicates by a 5-character symbol which isotope will be analyzed first, where in the analyzer memory its peak and background will be found.*
FGS 2 KR85M$ LIMITS 298 307$ START OF BACKGROUND? 350$	*Ditto for second isotope and continue for as many isotopes as are to be analyzed up to a limit of ten.*
FGS 8 #	*End of isotope list is indicated to computer by numbering first unused position and typing "CTRL" "D". This is not necessary if all ten positions are used.*
A$	*"A$" initiates data acquisition.*
NEW POWER= "SIGMA 5 DID NOT ACKNOWLEDGE" APR 20 11:08::20.7	*Sigma 5 not on line in this example.*
START APR 20 11:08::23.7	*Data acquisition begins.*

This teletype printout represents the operator's interaction with the computer in introducing the instructions and parameters necessary for data acquisition; it is necessary to do this each time the program is reloaded. The underlined characters are the keys actually struck by the operator. "$" indicates operation of the spacebar at the end of an input. It will not actually show on the real input. "#" indicates simultaneous operation of "CTRL" and "D" keys. It will not print either.

Fig. 51. Summary Example of Steps for Preparing Computer for Data Acquisition

TABLE VIII. Channel Identification of Isotopes To Be Monitored by Multichannel Analyzer

Isotope	Lower-limit Signal Window (Channel No.)	Upper-limit Signal Window (Channel No.)	Lower-limit Background Window (Channel No.)
^{85m}Kr	297	307	369
^{87}Kr	799	811	830
^{88}Kr	387	398	407
^{133}Xe	157	167	177
^{135}Xe	494	505	532
^{135m}Xe	1046	1060	1066
^{138}Xe	512	522	532
^{137}Cs[a]	1315	1322	1324
^{133}Xe[b]	2205	2215	2222
^{135}Xe[b]	2542	2552	2567

[a]This is a permanent calibration source. The "signal" window is set on the left shoulder of the peak, and the "background" window is on the right shoulder. If the peak does not drift, the two symmetrically placed windows essentially cancel and produce a count near zero. The deviation from 0 is a sensitive measure of the magnitude and direction of the drift.

[b]These isotope inputs are from the air monitor and are stored in the second quadrant of the analyzer memory.

(c) Initiate the program by typing the command A, SPACE.

(6) The data program can be interrupted for other keyboard commands.

(a) The data-taking program (or any other program) can be interrupted by pressing CTRL and D simultaneously on the teletype keyboard.

(b) Having thereby assumed control for the keyboard, the operator can now perform many useful operations by keyboard command:

1. Type M, P, A, SPACE in sequence to simply accumulate data.

2. Type V, SPACE to halt accumulation and view data.

3. Type K, SPACE to erase memory.

4. Type I, SPACE, S, SPACE, (Channel No.), SPACE, (Channel No.), SPACE to intensify on the oscilloscope display channels from the first through second channel numbers. (Normally, those regions that are specified for analysis of peaks in Table VIII are left intensified.)

5. Type I, SPACE, D, SPACE, (Channel No.), SPACE to delete the intensified region beginning at the specified channel.

6. Type I, SPACE, K, SPACE to delete all intensification. [Note: Erasing the analyzer memory with the ERASE button will also delete intensification. It is always preferable to erase the analyzer memory by the keyboard command (K, SPACE) in order to avoid inadvertently losing intensification.]

(c) Appendix B contains a full listing of available keyboard commands.

c. Methods of Calibration

(1) The multichannel analyzer is used to calibrate the amplifier.

(a) Erase the analyzer memory by (K, SPACE).

(b) Mount the following two low-intensity sources in the shield near the detector:

^{109}Cd 88.0 keV

^{137}Cs 661.6 keV

(c) Erase all earlier intensification, and intensify the following two regions to correspond with the above two sources:

Channels 171-181 (2 x 88 ± 5)

Channels 1318-1328 (2 x 661.6 ± 5)

(d) Accomplish calibration by using the amplifier gain control and the ADC ZERO LEVEL control (see Fig. 47) to bring both peaks to the exact center of their respective intensified regions. This establishes a strict 2:1 relationship of channel number to keV.

(e) Repeat a-d above for the air monitor, except that the channel numbers are augmented by 2048 to put the spectrum in the second quadrant.

(2) The multichannel analyzer is used to calibrate single-channel analyzers after amplifier gain has been established as outlined in the preceding subsection.

(a) Erase the intensification used in the preceding subsection, and intensify the regions specified by the first two columns of Table VIII for the isotopes to be monitored.

(b) Install a ^{60}Co source in the detector at such a distance as to give several percent dead time as indicated on the DEAD TIME meter of the ADC. Note that two single-channel analyzers, "signal" and "background" are associated with each isotope. Note also that all SCA windows are set at 0.10 V.

(c) Connect a coaxial cable from the output of the ^{87}Kr-signal SCA to the COINC ANTICOINC connector of the ADC (see Fig. 47). This connection inhibits storage of those pulses accepted by the SCA. Take a count by using the keyboard commands, and display it on the analyzer scope. The display will show a nearly uniform Compton background, except that the channels corresponding in energy to the window of the SCA will be depressed. The adjustment of the SCA consists of varying the signal threshold E so that the depressed region of the spectrum corresponds to the intensified region specified for ^{87}Kr. This can be done by taking repeated short counts with the analyzer and observing that the depressed region moves left (lower E) or right (higher E) with the adjustment of the threshold potentiometer on the SCA.

(d) The background SCA for ^{87}Kr is then set with E equal to the above-determined E for the signal SCA + 0.13 V.

(e) Leave the ^{60}Co source in place, and connect the ^{88}Kr signal SCA to the ADC. Repeat the above to cause the depressed region of the spectrum to fall in the intensified region designated for ^{88}Kr. Set the ^{88}Kr background SCA 0.17 V higher than the E obtained for the signal SCA.

(f) Leave the ^{60}Co source in place, and connect the ^{85m}Kr signal SCA to the ADC. Repeat the above to get the depressed region in the region intensified for ^{85m}Kr. Set the ^{85m}Kr background SCA 0.23 V higher than the signal SCA.

(g) Leave the ^{60}Co source in place, and repeat for ^{135}Xe. Set the ^{135}Xe background SCA 0.20 V higher than the signal SCA.

(h) Leave the ^{60}Co source in place, and repeat for ^{23}Ne. Set the ^{23}Ne background SCA 0.24 V higher than the signal SCA. (Note: ^{23}Ne is not a fission product; it is monitored by the recorder in the EEL as an indication that the gas-sample system is working properly. If flow is shut off or significantly restricted, the ^{23}Ne count rate will immediately fall off.)

(i) The ^{133}Xe SCA's cannot be calibrated this way. Remove the ^{60}Co source and install the ^{133}Ba source. Set the ^{133}Xe signal SCA as shown in Table VII. Temporarily connect the SCA output to the count-rate meter, and adjust the E potentiometer of the SCA to get a peak count-rate indication on the count-rate meter. Unless there has been a serious malfunction in the SCA, the new setting will differ from the old (see Table VII) by only a few hundredths of a volt. Set the E of background SCA 0.14 V above that of the signal SCA.

(j) The SCA's for the air monitor are calibrated as described above for ^{133}Xe, except that the ^{133}Ba source is installed in the air monitor, the signal SCA is connected to the count-rate meter, and the E potentiometer is set for maximum count rate. Set the background SCA 0.15 V above the signal SCA.

(k) Each pair of SCA's feeds an on-line digital-subtract unit (ODSU). Set the sample and hold time for each isotope with the ODSU thumbwheel switches as shown in Table VII. Press the RESET and START buttons on each ODSU.

3. Operation during Release Conditions

When a fission-product release occurs in the reactor it is normally observed first on the RCGM and FGM. Similar data are also available from GLASS on the two three-pen recorders in the control room. Actually, only two things are necessary to be sure that the GLASS data adequately represent what is happening.

a. It is desirable, when a release occurs, to decrease the data-cycle time so that finer time resolution is available and changes in the activity levels can be better correlated with the console log. Assume that the system is running on the normal 30-min cycle when a fission-gas release is observed to be starting. If it is less than 15 min to the end of the cycle, allow that cycle to type out so that data will not be lost unnecessarily. Then interrupt the program by depressing CTRL and D simultaneously. Change to a 10-min cycle by typing F, A, SPACE, 10, SPACE, and restart the data cycle by typing A, SPACE. If more than 15 min remain in the data cycle, interrupt the program immediately and change the cycle time as described above.

b. When release conditions prevail, observe closely that the count rate does not become excessive and overload the amplifier channel. This is determined by the gross count rate displayed by the blue pen of the recorder located with the analyzer. Reduce the sensitivity when the count rate exceeds ~30,000 counts/s. (The recorder scale for the blue pen is from 100 to 100,000 counts/s.) If the decision to reduce sensitivity is made near the end of a count cycle, delay changing until the end of the cycle so that data are not lost. If the decision to change sensitivity is made early in the count cycle, interrupt the program as described above and restart it after sensitivity is reduced. This avoids mixing data that have been taken under two different conditions.

c. Assuming that the system has been operating at normal sensitivity, make the first reduction in sensitivity by reducing chamber volume. This is accomplished by the CHAMBER switch on the gas-system control box (see Fig. 52). Hold the switch in the CLOSE position until the CLOSED light comes on. This requires about 20 s.

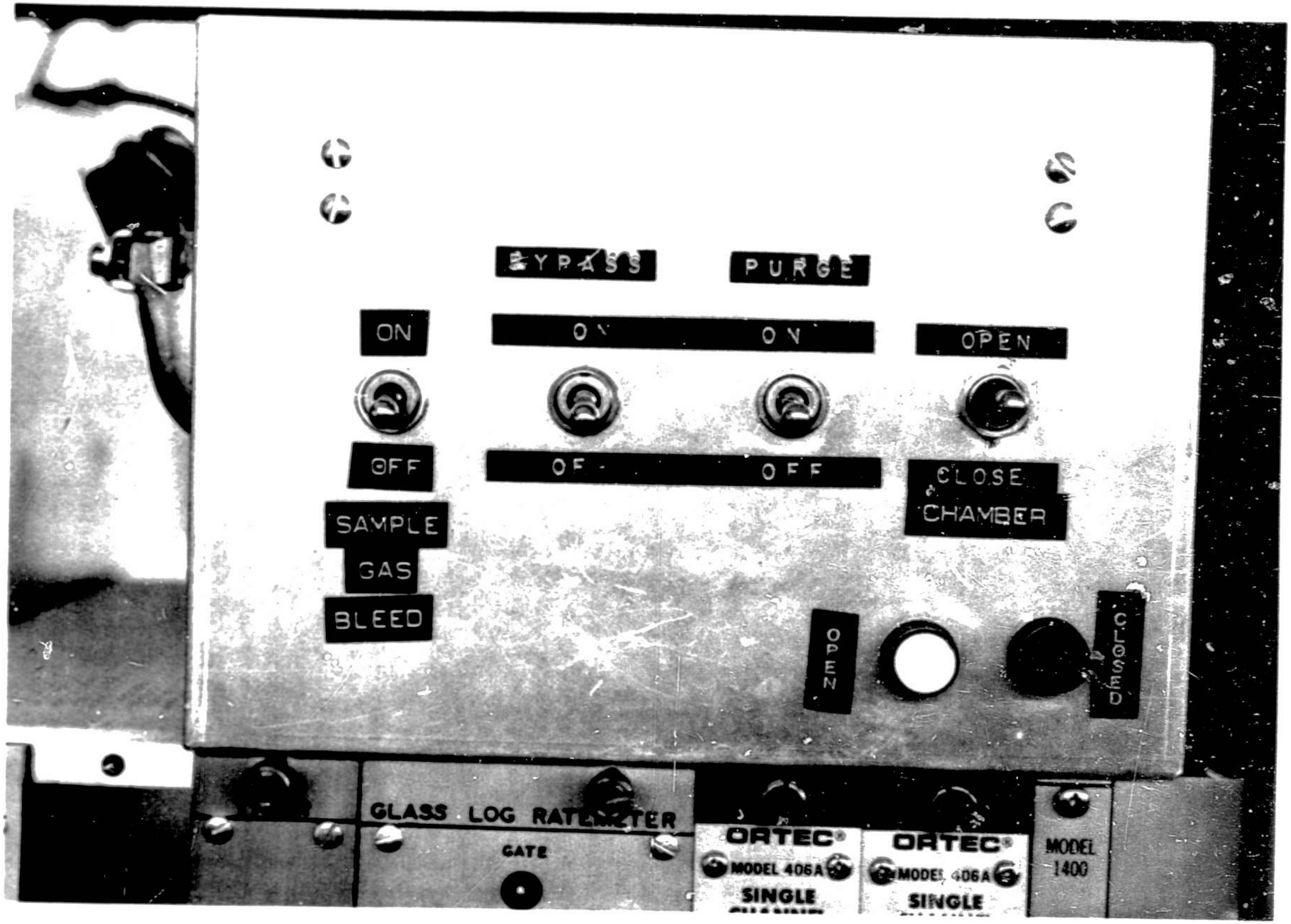

Fig. 52. Gas-sample Control Box in the Experimental Engineering Laboratory. ANL Neg. No. 103-[illegible]5882.

d. For a very large release, the count rate may again exceed ~30,000 counts/s, even after the chamber volume has been reduced. This calls for the second stage of sensitivity reduction, which is accomplished by dilution. Turn the following switches to ON: BYPASS, PURGE, and SAMPLE GAS BLEED (Fig. 52). The order of switching is not important. Again the sensitivity change should be coordinated with the data cycle as described above in order to avoid losing or garbling data.

e. After a release, as the cover-gas activity goes down either through decay or purging, return GLASS to normal operation by taking the above steps in reverse order. When the gross count rate falls below ~1000 counts/s, turn off the three switches in the preceding paragraph to discontinue dilution. When the gross count rate again becomes less than ~1000 counts/s, hold the CHAMBER switch in the OPEN position for ~20 s until the OPEN light comes on. Finally, return the system to the normal 30-min data cycle by interrupting the program (CTRL, D), typing F, A, SPACE, 30, SPACE to change the cycle time, and typing A, SPACE to restart the program. These changes also should be made in coordination with the data cycle to avoid losing or garbling data.

APPENDIX B

Computer Keyboard Commands

72-5311-0S

KEYBOARD COMMANDS FOR NS-660 COMPUTER AIDED MEMORY SYSTEM

FORMAT EXACTLY AS WRITTEN

NOTE: @=SPACE CHARACTER
TO TERMINATE ANY OPERATION OR COMMAND STRING PREMATURELY, DEPRESS THE "CTRL" KEY AND STRIKE THE LETTER "D".

A@

ENTRY TO AUTOMATIC DATA ACQUISITION PROGRAM WHEREBY AT THE INTERVALS PREVIOUSLY SPECIFIED AND IN RATIOS PREVIOUSLY SET, BOTH POWER UPDATE AND DATA COUNTING CYCLES WILL BE EXECUTED. THE START TIME AND STOP TIME FOR EACH CYCLE IS PRINTED OUT BY THE TELETYPE.

C@B@

ENTRY TO THE CALIBRATE TABLE. THE PRESENT TABLE (IF ANY) WILL BE PRINTED FOLLOWED BY THREE ASTERISKS (***). IF THE PRESENT TABLE IS SATISFACTORY, TYPE THE LETTER "K" MEANING 'KEEP'; BUT IF A NEW TABLE IS DESIRED, TYPE THE LETTER "N". THE COMPUTER WILL THEN ASK FOR CHANNEL NUMBER AND THE CORRESPONDING ENERGY.
NOTE: THE CHANNEL NUMBERS MUST BE IN ASCENDING ORDER. UP TO TEN CHANNELS AND ENERGIES MAY BE ENTERED.

D@

ENTRY TO THE "DATA GENERAL" "DEBUG I" OCTAL DEBUG ROUTINE. IN ADDITION TO THE STOCK COMMANDS LISTED IN THE "DEBUG I" MANUAL, ONE MAY TYPE AN OCTAL ADDRESS FOLLOWED BY THE LETTER "D" WHICH WILL INTRODUCE A DISPLACEMENT INTO THE ADDRESS CALCULATIONS. THIS FEATURE ALLOWS ONE TO WORK IN RELOCATABLE PROGRAMS WITH EASE.
NOTE: THE "R" (RUN) COMMAND ALWAYS ASSUMES ZERO DISPLACEMENT.

E@C@(ADDRESS)@

GIVES THE ENERGY OF THE DESIGNATED ADDRESS AS CALCULATED FROM THE ABOVE TABLE.

E@PA@

GIVES THE ENERGY OF THE INTENSIFIED PEAKS IN MEMORY AS CALCULATED FROM THE ABOVE TABLE.

E@PO@

FIRST PLACES THE MEMORY IN THE "CRT" MODE SO THAT INTENSIFICATION MAY BE PLACED AS DESIRED. PRESSING THE SPACE BAR WILL TYPE THE ENERGY OF THAT PEAK AND PLACE THE MEMORY BACK IN "CRT" MODE SO THAT THE INTENSIFICATION MAY BE REPOSITIONED. ONE MAY THUS STEP FROM PEAK TO PEAK FROM ONE END OF THE MEMORY TO THE OTHER.

FA@

ENTRY TO ROUTINE WHICH SETS DATA COLLECTION INTERVAL.
NOTE: ENTRY IS IN MINUTES--LIMITED TO 100.

FB@

SET DATA FIELD SIZE. THIS NUMBER MUST THEN BE IN BINARY INCREMENTS FROM 1024 TO 8192.

FGR@(NUMBER)@

ENTRY TO [illegible] IDENTIFICATION TABLE. THIS COMMAND ALLOWS ONE [illegible] THE ISOTOPE WHOSE TABULAR NUMBER IS IDENTIFIED [illegible] SOTOPE NAME AND ITS REGION WILL BE TYPED.

FGS@(NUMBER)@

ENTRY TO SET THE ISOTOPE TABLE. AFTER IDENTIFYING THE TABULAR POSITION ONE MUST TYPE EITHER A FIVE CHARACTER IDENTIFICATION CODE OR "CTRL" "D". IF A CODE IS TYPED THE COMPUTER WILL ASK FOR THIS ISOTOPE'S LIMITS WITHIN THE NS-636 MEMORY. THIS INFORMATION ALONG WITH THE NAME WILL BE ENTERED IN THE TABLE AT THAT PARTICULAR SLOT. IN THE ACQUISITION PROGRAM THE REGIONS WILL BE CALCULATED IN THE ORDER WHICH THEY OCCUPY IN THE TABLE. UNLESS THE LAST ISOTOPE USED IS #10, THE POSITION FOLLOWING THE LAST USED LOCATION MUST BE IDENTIFIED USING THE "FGS" COMMAND FOR THAT SPACE, FOLLOWED BY THE "CTRL""D" ESCAPE.

G@FA@

FINDS THE CENTROID OF THE INTENSIFIED PEAKS IN MEMORY.

G@PO@

FIND THE CENTROID OF THE INTENSIFIED PEAKS ONE BY ONE EVERY TIME THE SPACE BAR IS DEPRESSED.

H@

HALTS THE MEMORY UNIT FROM ANY UNASSISTED OPERATION.

I@NC@(START)@(STOP)@

GIVES THE SUM OF THE CONTENTS OF ADDRESSES START THROUGH STOP.

I@NI@

GIVES THE ADDRESS BOUNDARIES AND THE SUM OF THE CONTENTS OF THE DISPLAYED INTENSIFIED REGIONS.

I@D@(ADDRESS)@

DELETES THE COMPUTER SET INTENSIFICATION FROM THE NAMED ADDRESS TO THE END OF THAT INTENSIFIED GROUP.

I@DI

DELETES COMPUTER INTENSIFICATION FROM ALL REGIONS PRESENTLY INTENSIFIED BY ANY MEANS.

I@K@

REMOVES ALL COMPUTER SET INTENSIFICATION.

I@M@(PRESENT)@(FUTURE)@
MOVES THE INTENSIFIED GROUP STARTING AT "PRESENT" TO THE LOCATION STARTING AT "FUTURE".

I@S@(START)@(STOP)@
INTENSIFIES THE CHANNELS FROM START THROUGH STOP.

I@SA
SETS COMPUTER INTENSIFICATION AT THOSE REGIONS PRESENTLY INTENSIFIED BY ANY MEANS.

K@
KILLS THE DATA IN ALL CHANNELS. DOES NOT AFFECT INTENSIFICATION.

MMA@
PLACES MEMORY IN MULTI-CHANNEL-SCALING MODE.

MMS@
PLACES MEMORY IN MCS SUBTRACT MODE.

MPA@
PLACES MEMORY IN PHA AID ACQUISITORY MODE.

MPS@
PLACES MEMORY IN PHA SUBTRACT MODE.

N@(START)@(STOP)@(FUNCTION)(CONSTANT)@
NORMALIZES THE GROUP OF CHANNELS FROM START TO STOP BY THE GIVEN FUNCTION AND CONSTANT. THE CONSTANT NEED NOT BE A WHOLE NUMBER. ACCEPTABLE FUNCTIONS ARE:
+ = ADD: - SUBTRACT: * = MULTIPLY: / = DIVIDE.

O@R@(ADDRESS)@
GIVES THE CONTENTS OF THE ADDRESS IN DECIMAL.

O@W@(ADDRESS)@(NUMBER)@
PLACES THE GIVEN DECIMAL NUMBER AT THE ADDRESS.

P@A@
PRINTS THE ADDRESSES OF THE BOUNDARIES OF THE INTENSIFIED REGIONS.

P@G@(START)@(STOP)@
PRINTS THE CONTENTS OF THE ADDRESSES FROM START THROUGH STOP.

P@I@
PRINTS THE CONTENTS OF THE INTENSIFIED REGIONS.

QP@
PLACES THE NS-636 IN THE PLOT MODE TO OUTPUT EITHER THE CONTENTS OF MEMORY OR THE INTENSIFIED REGIONS.

R@
READS THE TIME-OF-DAY CLOCK.

S@

ENTRY TO THE ROUTINE WHICH SETS THE TIME-OF-DAY CLOCK.
SETTING OF THE CLOCK IS ACCOMPLISHED BY TYPING THE CORRECT
NUMBERS IN RESPONSE TO THE COMPUTER'S QUERIES.
THE TIME IS FIXED AT THE END OF THE LAST RESPONSE.

T@R@(START)@(STOP)@(NEW START)@

TRANSFERS THE GROUP BOUNDED BY START AND STOP TO
THE REGION DEFINED BY "NEW START".

UT@

ROUTINE TO TRANSMIT NS-636 ANALYZER DATA TO SIGMA 5.

V@

PLACES THE MEMORY IN VISUAL (CRT) DISPLAY MODE.

Z@(START)@(STOP)@

ZEROS (ERASES) THE GROUP OF ADDRESSES FROM START TO STOP.

APPENDIX C

Reference Data on Isotopes Detected by or Related to GLASS Operation

These data were taken primarily from two articles in the Nuclear Technology Division Annual Program Report for Period Ending June 30, 1972, ANCR-1088, Aerojet Nuclear Company:

a. "Evaluation of Decay Schemes for Fission Gas Monitoring," R. C. Greenwood, R. G. Helmer, C. W. Reich, J. E. Cline, and R. J. Gehrke, pp. 53-55.

b. "Measurement of Gamma-Ray Energies and Relative Intensities of Fission Product Gases and their Daughters," L. D. McIsaac, R. J. Gehrke, J. E. Cline, and R. L. Heath, pp. 387-390.

Some known gamma lines have been omitted as being too low in yield and/or too short in half-life to have any conceivable effect in GLASS. In the tabulation below, the gamma peaks normally analyzed are underlined for identification.

Isotope	Half-life	Decay Constant, s^{-1}	Gamma Peak Energy, keV	Peak Abundance, %	Precursor	Precursor Half-life	Daughter	Daughter Half-life	Gamma Peak Energy, keV	Peak Abundance, %
^{85}Kr	10.76 yr	2.04×10^{-9}	514.0	0.41	^{85m}Kr	4.4 hr	^{85}Rb	Stable		
^{85m}Kr	4.48 hr	4.30×10^{-5}	151.2	75	^{85}Br	3.0 mo	^{85}Kr	Data listed above		
			304.9	14						
^{87}Kr	76.4 mo	1.51×10^{-4}	402.6	53	^{87}Br	55 s	^{87}Rb	5×10^{10} yr		
			674.0	2.3						
			845.4	8						
			1174.7	2.2						
			1740.5	2.5						
			2011.8	3.7						
^{88}Kr	2.80 hr	6.87×10^{-5}	165.9[a]	3.8	^{88}Br	16 s	^{88}Rb	Data listed below		
			196.3	30.4						
			240.6	0.4						
			362.3	2.6						
			390.6	0.8						
			471.9	0.8						
			788.5	0.8						
			834.8	13.3						
			862.3	0.8						
			985.9	1.4						
			1141.4	1.5						
			1529.7	11.8						
			2029.8	5.4						
			2035.4	4.0						
			2195.8	14.8						
			2392.0	39.0						
^{89}Kr	3.16 mo	3.65×10^{-3}	220.8	25	^{89}Br	4.5 s	^{89}Rb	15.2 mo	657.8	11.0
			356.3	6.5					947.8	10.3
			497.9	11.0					1031.9	65.4
			577.2	8.0					1248.2	46.5
			585.9	21					2195.9	15.5
			737.6	4.0					2570.0	10.5
			867.5	6.0						
			904.6	7.5						
			1472.1	9.5						
			1533.4	11.0						

Isotope	Half-life	Decay Constant, s^{-1}	Gamma Peak Energy, keV	Peak Abundance, %	Precursor	Precursor Half-life	Daughter	Daughter Half-life	Gamma Peak Energy, keV	Peak Abundance, %
^{88}Rb	17.8 mo	6.49×10^{-4}	898.0 1382.3 1836.0 2677.6	14.2 0.7 23.2 [illegible]	^{88}Kr	2.8 hr	^{88}Sr	Stable		
^{131m}Xe	12.0 days	6.68×10^{-7}	164.0[a]	1.9	^{131}I	8.05 days	^{131}Xe	Stable		
^{133m}Xe	2.22 days	3.6×10^{-6}	232.6	9.8	^{133}I	21 hr	^{133}Xe	Data listed below		
^{133}Xe	5.30 days	1.51×10^{-6}	79.55 81.0 160.7[a]	0.25 36.6 0.03	^{133m}Xe	2.22 days	^{133}Cs	Stable		
^{135m}Xe	15.65 mo	7.38×10^{-4}	526.6	80	^{135}I	6.7 hr	^{135}Xe	Listed below		
^{135}Xe	9.14 hr	2.11×10^{-5}	158.5[a] 249.7 358.6 408.2[b] 608.1	0.26 91 0.24 0.34 2.6	^{135}I	6.7 hr	^{135}Cs	3×10^{6} yr	No gamma	
^{137}Xe	3.85 mo	3.00×10^{-3}	455.4	33	^{137}I	23 s	^{137}Cs	30.0 yr	661.6	93.5
^{138}Xe	14.2 mo	8.13×10^{-4}	154.3[a] 243.1 258.6[c] 396.6 401.5[b] 434.2 1768.0 2002.0 2014.0	11 7.5 40 8 3 24 22 8 11.2	^{138}I	5.9 s	^{138}Cs	Data listed below		
^{137}Cs	30.0 yr	7.32×10^{-10}	661.6	93.5	^{137}Xe	3.85 mo	^{137}Ba	Stable		
^{138}Cs	32.2 mo	3.59×10^{-4}	408.8 462.7 546.9 871.7 1009.6 1435.8 2217.7 2639.1	4.5 30 10.5 5.0 30 76 15.7 7.8	^{138}Xe	14.2 mo	^{138}Ba	Stable		
					Activation Products					
^{23}Ne	37.6 s	1.84×10^{-2}	440.0 1630.0 2079.0	33 1.0 0.1	None		^{23}Na	Stable		
^{24}Na	15.0 hr	1.28×10^{-5}	1369.0 2754.0	100 100	None		^{24}Mg	Stable		
^{41}A	1.83 hr	1.05×10^{-4}	1293.6 1660.0	99 0.05	None		^{41}K	Stable		

[a]These gamma lines interfere to some extent with the measurement of the ^{85m}Kr gamma at 151.2 keV and the associated background.
[b]These gamma lines interfere to some extent with the measurement of the ^{87}Kr gamma at 402.6 keV and the associated background.
[c]The determination of the weak ^{138}Xe peak at 258.6 keV is made difficult by the proximity of the very strong ^{135}Xe peak at 249.7 keV.

REFERENCES

1. F. S. Kirn, *EBR-2 as a Fast Reactor Irradiation Facility*, Nucl. News *13*(3), 62-68 (1970).

2. G. S. Brunson, *On-line Noble Gas Fission Product Monitoring in Experimental Breeder Reactor II*, Nucl. Technol. *10*(1), 33-43 (Jan 1971).

3. G. S. Brunson, R. N. Curran, and F. H. Just, *Two Circuits for On-line Monitoring of Specific Lines in a Gamma Spectrum*, Nucl. Instrum. Methods *106*, 21-27 (1973).

4. I. G. Dillon and Leslie Burris, Jr., *Estimation of Fission Product Spectra in Fuel Elements Discharged from the Power Breeder Reactor and the Experimental Breeder Reactor No. 2*, ANL-5334 (Oct 1954).

5. *Code of Federal Regulations, Title 10--Atomic Energy, Part 20--Standards for Protection Against Radiation*, U. S. Atomic Energy Commission (Revision of Dec 10, 1969).

6. R. M. Fryer and G. S. Brunson, "Release of Activity to the Primary System from Subassembly X083A during Run 58," *Reactor Development Program Progress Report: October 1972*, ANL-RDP-10, p. 1.13 (Nov 30, 1972).

7. T. D. Claar and R. Villarreal, "March 13-14 Fission-product Release to the Primary System," *Reactor Development Program Progress Report: April-May 1973*, ANL-RDP-16, p. 1.32 (July 9, 1973).

8. T. D. Claar and G. S. Brunson, "Release of Fission Products to the Primary System, September-October 1973," *Reactor Development Program Progress Report: October 1973*, ANL-RDP-21, p. 1.6 (Nov 30, 1973).

9. T. D. Claar, G. S. Brunson, and E. R. Ebersole, "Identification of Defected Fuel Element in Run 67A," *Reactor Development Program Progress Report: December 1973*, ANL-RDP-23, p. 1.4 (Jan 29, 1974).

10. T. D. Claar and G. S. Brunson, "Identification of Defected Fuel Elements in Runs 67B-68C," *Reactor Development Program Progress Report: February 1974*, ANL-RDP-25, p. 1.8 (Mar 29, 1974).